

**Functional Analysis of a Gene Cluster of Two Aliphatic-Aromatic Polyester
Type Plastic Degrading Enzymes from *Roseateles depolymerans* strain**

TB-87

July 2019

Azura Ahmad

**Functional Analysis of a Gene Cluster of Two Aliphatic-Aromatic Polyester
Type Plastic Degrading Enzymes from *Roseateles depolymerans* strain**

TB-87

A Dissertation Submitted to
the Graduate School of Life and Environmental Sciences,
the University of Tsukuba
in Partial Fulfillment of
the Requirements for the Degree of Doctor of Philosophy in Biotechnology
(Doctoral Program in Bioindustrial Sciences)

Azura Ahmad

Abstract

Plastic waste pollution is one of the major environmental concerns in recent years caused by the rapid growth of plastic utilizing industries. To overcome many problems associated with plastics waste, the development of biodegradable plastics for use especially in packaging have been gaining attention since these plastics can be degraded into low molecular weight monomer generating carbon dioxide, methane, and water by suitable microorganisms. However, in recent years, concerns regarding the fate of biodegradable plastics have arisen; the production of micro- and nanoplastics as a result of the breakdown of the plastics. The development of biodegradable plastics comprise of recyclable monomers is, therefore, more economical and environmentally benign approach to the problems. To achieve this final aim, the biodegradation mechanism by microorganisms first needs to be clarified.

Previously in this laboratory, the isolation and characterization of polyester-degrading enzymes, designated as Est-H and Est-L from freshwater bacterium, *Roseateles depolymerans* strain TB-87, capable to degrade various polyester-based biodegradable plastics such as poly(butylene succinate) (PBS), poly(butylene succinate-co-adipate) (PBSA) and poly(ϵ -caprolactone) (PCL), have been reported. Although both Est-H and Est-L have similar substrate specificity and degradation activity as well as nearly identical molecular masses, studies suggested that both proteins are of different proteins. While many other similar studies reported on the single enzyme responsible for the degradation, strain TB-87 possesses two identical enzymes with similar functions. This study aims to elucidate the functions of the genes encoding for the enzymes.

Two open reading frames (ORFs) consisting of 1083 bp and 870 bp nucleotides, corresponding to *est-H* and *est-L*, encoding enzymes of 360 and 289 amino acids, respectively, were predicted. In addition, another ORF consisting of 735 bp encoding a chaperone-like protein (Est-Ch) of 244 amino acids was identified in the intergenic region of *est-H* and *est-L*. The presence of a promoter region upstream of *est-H* and the absence of a terminator region downstream of the ORF and vice versa for *est-Ch*, suggests that *est-H* and *est-Ch* are polycistronically expressed. Est-H and Est-L showed homology with plastic degrading enzymes, such as esterase and cutinase while Est-Ch showed homology with bacterial lipase chaperone. The presence of consensus lipase sequences (-Gly-His-Ser-Met-Gly-) was observed in these enzymes, thus Est-H and Est-L were hypothesized to be hydrolases with serine (Ser) in their active center.

Following gene annotation, Est-H and Est-L were overexpressed in *E. coli* BL21 (DE3) to obtain purified protein for further biochemical characterization studies. Results of overexpression in *E. coli* BL21 (DE3) suggested possible gene toxicity, therefore overexpression in another strain, *E. coli* Lemo21 (DE3) was attempted. Analysis by sodium dodecyl-polyacrylamide gel electrophoresis (SDS-PAGE) revealed the insoluble expression of both proteins. The refolding of both proteins was performed *in vitro* using immobilized metal affinity column chromatography (IMAC). The proteins could not be retrieved even after changing many buffers and refolding conditions, suggesting aggregation of the proteins in the column during simultaneous refolding and purification.

The entire gene cluster was disrupted using a kanamycin antibiotic cassette to elucidate the functions of esterase-encoding genes previously annotated. The mutant strain lost the ability to form a clear zone on PBSA emulsion-overlaid NB agar plates, suggesting that the annotated esterase-encoding genes are indeed the genes responsible for the PBSA degradation ability of *R. depolymerans* strain TB-87. However, the exact mechanism of PBSA-degradation at the molecular level remains unclear. Further, gene annotation data showed the presence of a chaperon-encoding gene in the intergenic region of *est-H* and *est-L*, which functions remains unclear, therefore, gene disruption was performed to elucidate the functions of the gene. The deletion of only *est-Ch* produced mutants unable to form halo zone on PBSA emulsion-nutrient agar plate, similar to that observed after the deletion of the entire esterase gene cluster. Unpublished preliminary results obtained suggested that the *est-Ch* is possibly existed as a subunit or as a part of a protein complex with Est-H and Est-L.

Understanding of function of genes encoding for plastic-degrading enzymes could lead to the elucidation of the decomposition activity and substrate specificity exclusive to the biodegradable plastic enzymes. This will allow manipulation and modification of the genes to obtain enzymes having more specific properties particularly for the development of enzyme-based monomer recycling system in the future.

Contents

Abstract		i
Contents		iii
Abbreviations		vii
Chapter 1	General Introduction	1
	1.1 Concerns related to plastic production and disposal	1
	1.2 Macro-, micro- and nanoplastics	2
	1.3 Biodegradable polymers	2
	1.3.1 Polybutylene succinate (PBS) and poly[(butylene succinate)- <i>co</i> -adipate] (PBSA)	4
	1.4 Degradability of biodegradable plastics	4
	1.5 Polyester-based biodegradable plastics degrading enzyme	7
	1.6 Biochemical monomer recycling	9
	1.7 Review of literature	12
	1.7.1 Microbial degradation of PBS/PBSA	12
	1.7.2 Characterization of gene encoding for biodegradable plastic-degrading enzymes	13
	1.7.3 Recombinant production of biodegradable plastic-degrading enzymes	14
	1.7.4 Targeted gene disruption for the elucidation of gene function	15
	1.8 Background of research	15
	1.9 Objectives of the study	16
Chapter 2	Analysis of Gene-encoding Region of Esterase from <i>Roseateles depolymerans</i> strain TB-87	17
	2.1 Introduction	17
	2.2 Materials and method	17

2.2.1	Total genome analysis of TB-87 strain	17
2.2.2	Determination of ORF of <i>est-H</i> and <i>est-L</i>	18
2.2.3	Signal peptide analysis	18
2.2.4	Homology search based on the deduced amino acid sequence	18
2.2.5	Multiple sequence alignment	18
2.2.6	Phylogenetic tree construction	18
2.3	Results and discussion	
2.3.1	Annotation of <i>est-H</i> , <i>est-L</i> and chaperone-like gene region	18
2.3.2	Homology analysis of esterase with other highly homologous enzymes	24
2.3.3	Multiple sequence alignment of esterase and other homologous enzymes	24
2.3.4	Dendrogram of Est-H, Est-L, and Est-Ch	26
2.3.5	Prediction of the tertiary protein structure of Est-H and Est-L	26
2.4	Conclusion	30
Chapter 3	Recombinant Expression of Esterase Genes in <i>E. coli</i>	32
3.1	Introduction	32
3.2	Materials and method	32
3.2.1	Bacterial strains, plasmids, and chemical reagents	32
3.2.2	Construction of expression plasmid	33
3.2.3	Transformation of pET21b plasmid bearing esterase genes into host cells	33
3.2.4	Overexpression of recombinant esterase in <i>E. coli</i>	33
3.2.5	Molecular weight estimation of esterase	35
3.2.6	On-column protein refolding	36
3.2.7	Spectrophotometric enzyme assay	36
3.3	Results and discussion	36
3.3.1	Recombinant expression of esterase by deleting the	36

	N-terminal tag of pET21b	
	3.3.2 Recombinant expression of esterase in <i>E. coli</i> Lemo21 (DE3)	43
	3.3.3 On-column refolding of insoluble esterase	49
	3.3.4 Measurement of active esterase activity	51
	3.4 Conclusion	51
Chapter 4	Disruption of Esterase-encoding Genes of <i>R. depolymerans</i> Strain TB-87	53
	4.1 Introduction	53
	4.2 Materials and method	53
	4.2.1 Bacterial strains, plasmids, and chemical reagents	53
	4.2.2 Growth medium and culture conditions	54
	4.2.3 Template DNA preparation, primers, and PCR conditions	54
	4.2.4 Gene deletion of the entire esterase gene region	56
	4.2.5 Bacterial conjugation between <i>E. coli</i> S17-1 with wild type strain TB-87	56
	4.3 Results and discussion	57
	4.3.1 Construction of plasmids for the conjugation with wild type strain TB-87	57
	4.3.2 Screening of <i>Δest</i> -TB-87 mutants bearing knocked-out esterase genes	60
	4.3.3 Verification of gene deletion of the <i>Δest</i> -TB-87 mutants	64
	4.3.4 Assessment of the degradation ability of <i>Δest</i> -TB-87 mutants	66
	4.4 Conclusion	69
Chapter 5	Functional Analysis of Chaperone	70
	5.1 Introduction	70
	5.2 Materials and method	70
	5.2.1 Bacterial strains, plasmids, and chemical reagents	70
	5.2.2 Growth medium and culture conditions	70

5.2.3	Template DNA preparation, primers, and PCR conditions	70
5.2.4	Construction of plasmid bearing knocked-out <i>est-Ch</i>	72
5.2.5	Bacterial conjugation between <i>E. coli</i> S17-1 with wild type strain TB-87	72
5.3	Results and discussion	72
5.3.1	Deletion of the putative Est-Ch-encoding gene by homologous recombination	72
5.4	Conclusion	79
Chapter 6	General Conclusion and Suggestions for Future Work	80
6.1	Conclusion	80
6.2	Suggestions and recommendations for future work	83
References		84
Addendum		99
Acknowledgements		100

Abbreviations

PBS	Polybutylene succinate
PBSA	Poly[(butylene succinate)-co-adipate]
PCL	Poly(ϵ -caprolactone)
PES	Poly(ethylene succinate)
PLA	Poly(L-lactic acid)
PHB	Poly(3-hydroxybutyrate)
PET	Poly(ethylene terephthalate)
PBAT	Poly(butylene adipate- <i>co</i> -terephthalate)
PBST	Poly(butylene succinate- <i>co</i> -terephthalate)
PBSTIL	Poly(butylene succinate/terephthalate/isophthalate- <i>co</i> -lactate)
NCBI	National Center for Biotechnology Information
ORF	Open reading frame
IPTG	Isopropyl- β -D-thiogalactoside
PCR	Polymerase chain reaction
TD PCR	Touchdown polymerase chain reaction
LB	Luria-Bertani medium
OD ₆₀₀	Optical density at 600 nm
SDS-PAGE	Sodium dodecyl sulfate-polyacrylamide gel electrophoresis
bp	Base pair
MW	Molecular weight
kDa	Kilodalton
CBB	Coomassie brilliant blue
SDS	Sodium dodecyl sulfate
IMAC	Immobilized metal affinity column chromatography
pI	Isoelectric point
KmC	Kanamycin cassette
X-Gal	5-bromo-4-chloro-3-indolyl- β -D-galactopyranoside
pNP	<i>para</i> -nitrophenol

CHAPTER 1

General Introduction

1.1 Concerns related to plastic production and disposal

The first synthetic plastics was synthesized in 1907 and have become widely used since then due to its low cost, durability, safeness, and processability (Sardon and Dove, 2018). Plastic is a polymer to which additives have been added to yield products with physical properties needed for commercial purposes (Gigault *et al.*, 2018). Due to its many advantages, plastics have found their broad range of application in packaging films, wrapping materials, shopping and garbage bags, fluid containers, clothing, toys, household, and industrial products, and building materials (Singh *et al.*, 2017). Since the large-scale production of synthetic materials began in early 1950, the usage of plastics has escalated, amounted to 8.3 billion metric tons in 2015. From this amount, 6.3 billion tons ended up as waste and from this waste total, only 9 percent was recycled, 12 percent was incinerated, and 79 percent end up accumulated in the natural environment. It was predicted that if the current trends are to continue, approximately 12 billion metric tons of plastic waste will end up in landfills or the natural environment by 2050 (Geyer *et al.*, 2017).

Improper disposal of plastic wastes imposed many problems to the environment. Landfills available for plastic disposal are fast depleting which could cause disposal without consent in an inappropriate location. As approximately 80 percent of ocean plastics come from land-based sources (Ritchie and Roser, 2019), a large amount of this improperly disposed plastics could end up in oceans causing threats to marine organisms. In addition, most plastic debris persist in the environment for centuries due to its resistance to degradation (Li *et al.*, 2016).

To overcome many problems associated with plastic waste, the development of biodegradable plastics for use especially in packaging have been gaining attention since they can be degraded into low molecular weight monomer generating carbon dioxide, methane and water (Roohi *et al.*, 2017) by suitable microorganisms. However, the replacement of traditional petroleum-based plastics with biodegradable plastics could not fully alleviate the problems of plastics pollution. As the monomers of biodegradable plastics are commonly blended together to achieve commercially functional properties, some polymers and their blends have shown to

unable to be biodegraded (Narancic *et al.*, 2018). The copolymers of blended biodegradable and non-biodegradable monomers may cause serious pollution since only the biodegradable components will be degraded in the environment, while non-biodegradable components that have broken up into smaller particles diffuse into the environment (Iwata, 2015).

1.2 Macro-, micro- and nanoplastics

Large plastic debris, known as macroplastic (items >5 mm in diameters) (Bouwmeester *et al.*, 2015), has been the focus of major environmental concern for many years. However, in recent years, the focus has been shifted to the production of small particles; down to micro and nanometer in scale, produced partly as a result of the breakdown of macroplastics. Microplastics are dominated by plastic particles smaller than 1 cm in diameter (Hidalgo-Ruz *et al.*, 2012) or ~20 μm diameter fibrous materials (Thompson *et al.*, 2004), and these millimeter-sized particles can be nanofragmented to even smaller particles, termed nanoplastics (Cozar *et al.*, 2014). Marine pollution of these micro- and nanoplastic are deemed more harmful as they can be easily ingested by the marine organisms due to their small size and may, therefore, be introducing toxins to the base of the food chain (Teuten *et al.*, 2009).

1.3 Biodegradable polymers

Biodegradable polymers defined as polymers that degrade as a result of the action of microorganisms, such as bacteria, fungi, and algae (Leja and Lewandowicz, 2010), and/or enzymes (Karlsson and Albertsson, 1998). The rate of biodegradation depends on the type of repetitive unit, morphology (e.g. crystallinity, size of spherulites), hydrophilicity, surface area and additives (Karlsson and Albertsson, 1998). Biodegradable plastics and polymers were first introduced in the 1980s and can be classified into two classes; natural or synthetic (Vroman and Tighzert, 2009). Natural polymers are obtained from natural resources while synthetic polymers are produced from oil/petroleum (Babak and Hadi, 2013). Figure 1-1 illustrates the schematic diagram of the classification of biodegradable polymers.

Petroleum-derived polymers are notoriously difficult to degrade; however, polymers having hydrolyzable backbones are more susceptible to biodegradation under particular conditions, thus, polymers with these properties have been developed. Examples of such polymers including polyesters, polyamides, polyurethanes and polyureas, poly(amide-enamine)s, polyanhydrides (Chandra and Rustgi, 1998; Nair and Laurencin, 2007).

Polybutylene succinate (PBS) and its copolymer, poly[(butylene succinate)-co-adipate] (PBSA) are the examples of biodegradable aliphatic polyesters studied predominantly in this

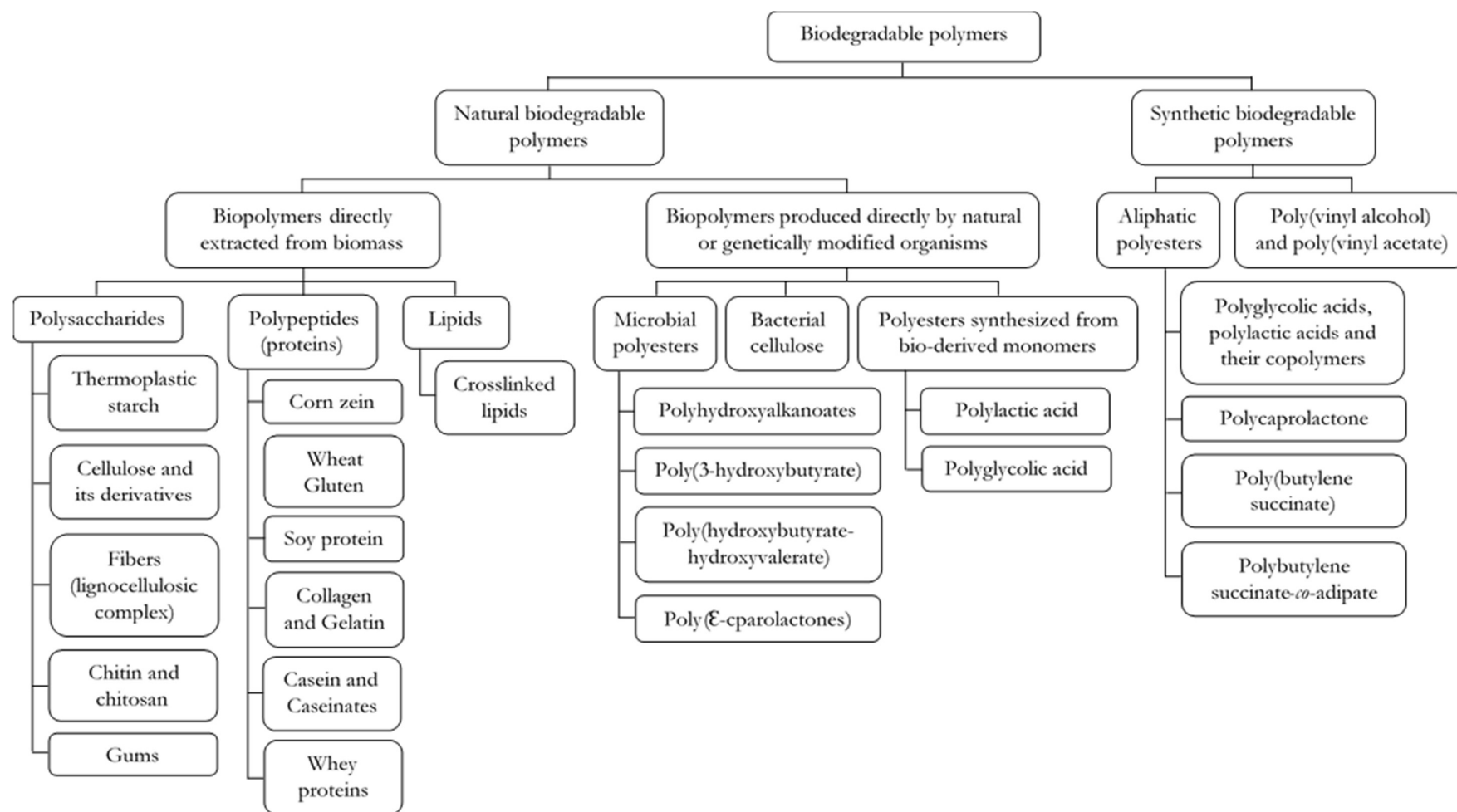


Figure 1-1 Schematic diagram of the classification of biodegradable polymers (Adapted from Babak and Hadi, 2013).

laboratory. Aliphatic polyesters, having hydrolyzable ester bonds, are the most extensively studied class of biodegradable polymers because of their important diversity and synthetic versatility. Another important class of polyesters including aromatic and aliphatic-aromatic co-polyesters. The former is insensitive to hydrolytic degradation and to enzymatic or microbial attack, therefore the latter, consisting of a mixture of aliphatic and aromatic monomers, were developed to improve the biodegradation of the aromatic polyesters (Vroman and Tighzert, 2009). Chemical structures of some of aliphatic, aromatic, and aliphatic-aromatic co-polyester biodegradable plastics are summarized in Table 1-1.

1.3.1 Polybutylene succinate (PBS) and poly[(butylene succinate)-*co*-adipate] (PBSA)

PBS is a biodegradable aliphatic polyester synthesized by the polycondensation of succinate and 1,4-butanediol (Jacquel *et al.*, 2011). They are produced by Showa Denko (Japan) and Mitsubishi Chemical under trade name Bionolle® and GsPLA, respectively (Tserki *et al.*, 2006). PBS is a white crystalline thermoplastic with a high melting point of 115°C, low production cost, and good mechanical properties similar to polypropylene or polyethylene (Ishioka *et al.*, 2002).

PBSA is a copolymer of PBS, produced on a semi-commercial scale through the transesterification and polycondensation of 1,4-butanediol, succinate, and adipate. Due to the introduction of secondary component (adipate), a polyester tensile strength of the PBS decreases (Nikolic and Djonlagic, 2001), lowering its crystallinity resulting in higher degradability by enzymatic processes compared with other materials.

PBS and PBSA are primarily used in the food and cosmetic packaging, and in disposable products such as tableware or medical articles (Tserki *et al.*, 2006). Other fields which PBS and PBSA applications finds interest in including agriculture (for fabrication of mulching films or delayed-release materials for pesticide and fertilizer), fishery (for fishing nets), forestry, and civil engineering (Nikolic and Djonlagic, 2001), and medical (as biodegradable drug encapsulation systems (Fujimaki, 2002). The chemical structures of PBS and PBSA are shown in Table 1-1.

1.4 Degradability of biodegradable plastics

To date, the term biodegradation has not been applied consistently, resulting in confusion among scientists (Palmisano and Pettigrew, 1992). Biodegradation comprises of three stages; biodeterioration, biofragmentation, and assimilation (Lucas *et al.*, 2008). The biodeterioration

Table 1-1 Chemical structures of aliphatic, aromatic, and aliphatic-aromatic co-polyester biodegradable plastics (Adapted from Nakajima-Kambe *et al.*, 2009a, 2009b; Shah *et al.*, 2013a, 2013b).

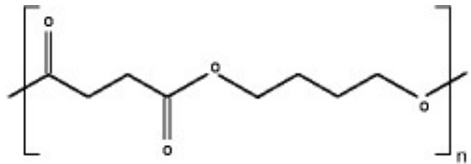
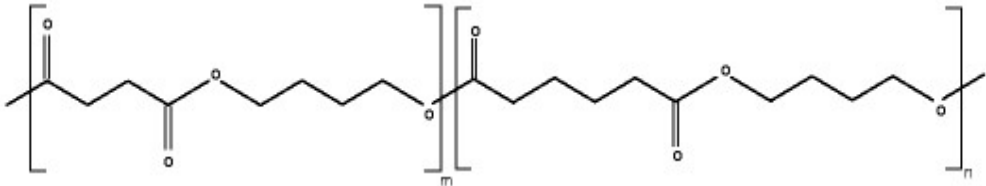
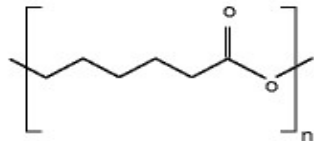
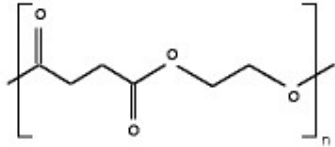
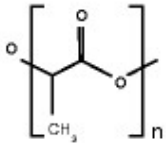
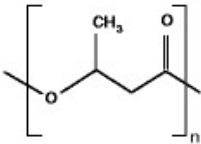
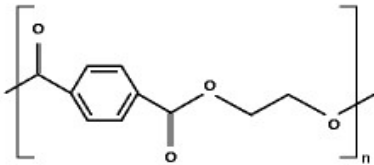
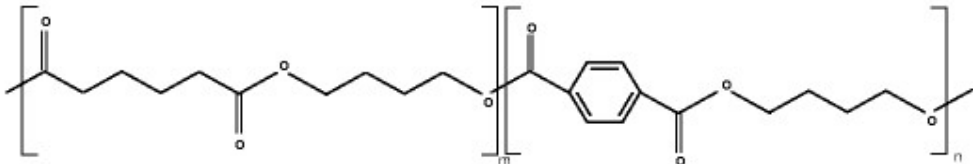
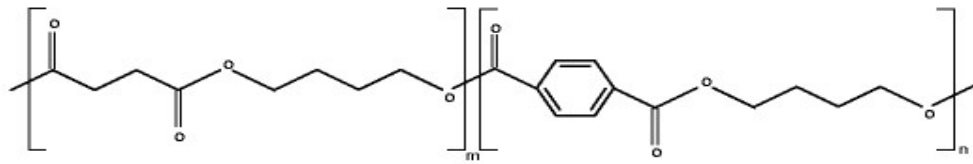
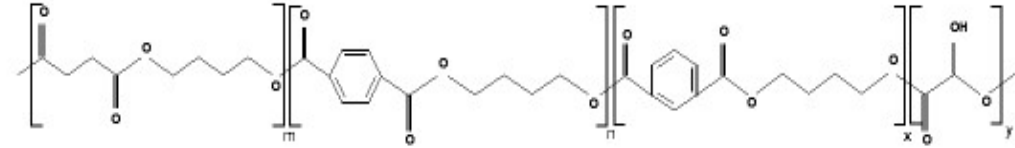
Plastics	Abr.	Chemical structure
Poly(butylene succinate)	PBS	
Poly(butylene succinate-co-adipate)	PBSA	
Poly(ε-caprolactone)	PCL	
Poly(ethylene succinate)	PES	
Poly(L-lactic acid)	PLA	

Table 1-1 Chemical structures of aliphatic, aromatic, and aliphatic-aromatic co-polyester biodegradable plastics (Adapted from Nakajima-Kambe *et al.*, 2009a, 2009b; Shah *et al.*, 2013a, 2013b) - cont'd

Plastics	Abr.	Chemical structure
Poly(3-hydroxybutyrate)	PHB	
Poly(ethylene terephthalate)	PET	
Poly(butylene adipate-co-terephthalate) (Ecoflex™)	PBAT	
Poly(butylene succinate-co-terephthalate)	PBST	
Poly(butylene succinate/terephthalate/isophthalate-co-lactate)	PBSTIL	

occurs mainly as a result of the activity of microorganisms; either by mechanical, chemical and/or enzymatic means (Gu, 2003); that grow on the surface or/and inside a target plastics (Hueck, 2001; Walsh, 2001). Biofragmentation of the polymers into lower molecular mass products by either abiotic reactions (oxidation, photodegradation or hydrolysis), or biotic reactions (degradations by microorganisms) takes place prior to bioassimilation of the polymer fragments by microorganisms (Vroman and Tighzert, 2009) and their mineralization into carbon dioxide and water (Iwata, 2015). The biodegradation routes of biodegradable plastics are illustrated in Figure 1-2.

Biodegradation of a polymer can be estimated using several methods; the evaluation of macroscopic modifications in the materials (surface erosion, formation of holes and cracks, changes in colour, development of microorganisms over the surface) (Lugauskas *et al.*, 2003; Rosa *et al.*, 2004), the measure of the weight loss (Krzan *et al.*, 2006), the monitoring of product formation (Lindström *et al.*, 2004), and the monitoring of formation of a clear halo around the microbial colony (Lucas *et al.*, 2008), among others.

1.5 Polyester-based biodegradable plastics degrading enzyme

The α/β hydrolase superfamily is superfamily of hydrolytic enzymes of widely differing phylogenetic origin and catalytic function that share a common fold (Ollis *et al.*, 1992; Holmquist, 2000). The core of this class of enzymes is an α/β -sheet containing 8 beta strands connected by 6 alpha helices (Ollis *et al.*, 1992; Carr and Ollis, 2009). The α/β hydrolase fold includes proteases, lipases, peroxidases, esterases, epoxide hydrolases and dehalogenases (Nardini and Dijkstra, 1999).

Lipases (EC 3.1.1.3, triacylglycerol hydrolases) and esterases (EC 3.1.1.1, carboxyl ester hydrolases) constitute the major enzymes responsible for the degradation of polyester-based biodegradable plastics. Both esterases and lipases belong to the same family of α/β hydrolases (Hu *et al.*, 2010), distinguishable by their substrate spectra. Esterases preferentially break ester bonds of water-soluble shorter chain fatty acids (Fojan *et al.*, 2000) and are inactive against water-insoluble long-chain triacylglycerols, which are then specifically hydrolyzed by lipases (Chahinian and Sarda, 2009). Cutinases (EC 3.1.1. 74, triacylglycerol acyl hydrolyze), another common α/β hydrolase, are serine esterases that share a common α/β fold with lipases and esterases (Ollis *et al.*, 1992), but lack the hydrophobic lid possessed by other lipases. They are able to hydrolyze a variety of polymers, including low-molecular-weight soluble esters, as well as short- and long-chain triacylglycerols (Martinez *et al.*, 1992).

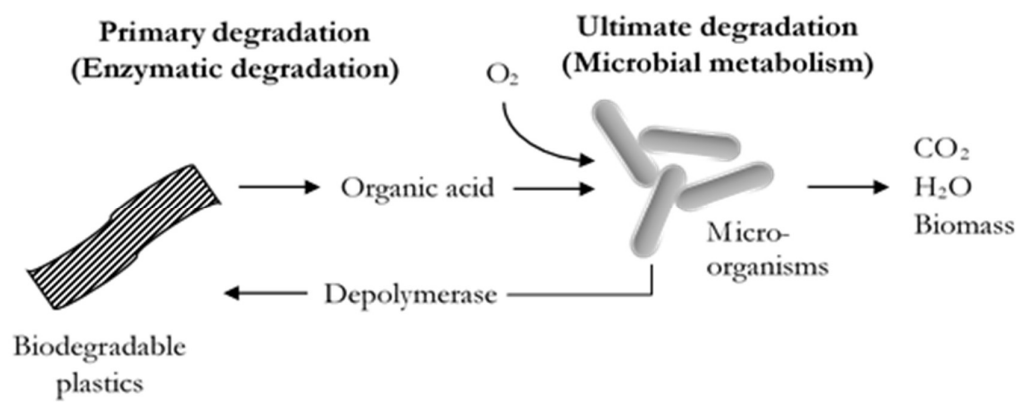


Figure 1-2 Biodegradation routes of biodegradable plastics (Adapted from Iwata, 2015).

1.6 Biochemical monomer recycling

Monomer recycling or chemical recycling is a recycling method in which monomers of depolymerized biodegradable polymers are used to synthesize new polymers. Figure 1-3 summarizes polymer production from waste materials through chemical recycling. Conventional mechanical and thermal chemical recycling of waste polymeric materials into their corresponding monomers generally requires high temperatures thus limiting industrial application. Polymer syntheses using isolated enzymes as a catalyst have received much attention as environmentally friendly processes of polymer production under mild reaction conditions (Kobayashi *et al.*, 2000).

There are two routes for the sustainable chemical recycling of polymers; the enzymatic conversion of polymers into repolymerizable oligomers and the selective depolymerization of polymers into specific monomers. The former is suitable for the reproduction of polymers similar to the original polymers while the monomers generated from the latter route can be used as a comonomer for the production of various kinds of plastics and also as a synthetic intermediate for the production of various compounds (Matsumura, 2002).

One of the advantages of using a hydrolase enzyme as a catalyst for polymer production is the mutually reversible nature of polymerization and degradation. Figure 1-4 illustrates the mechanism of a hydrolase enzyme catalyzing both the polymerization and degradation. Hydrolase enzyme could cleave polymer chains containing enzymatically hydrolyzable moieties, producing potentially repolymerizable low-molecular weight fragments as the primary degradation products. These low-molecular weight fragments are incorporated into microbial cells for further assimilation liberating carbon dioxide and water as the final products during the biodegradation process, whereas during polymer synthesis, these low-molecular-weight fragments having specific terminal structures at both ends can be combined by the enzyme to produce a regenerated polymer chain (Matsumura, 2002). These repetitive production and chemical recycling of polymeric materials between the polymer and monomer using an enzyme is a promising approach for a sustainable chemical recycling of polymers (Okajima *et al.*, 2003).

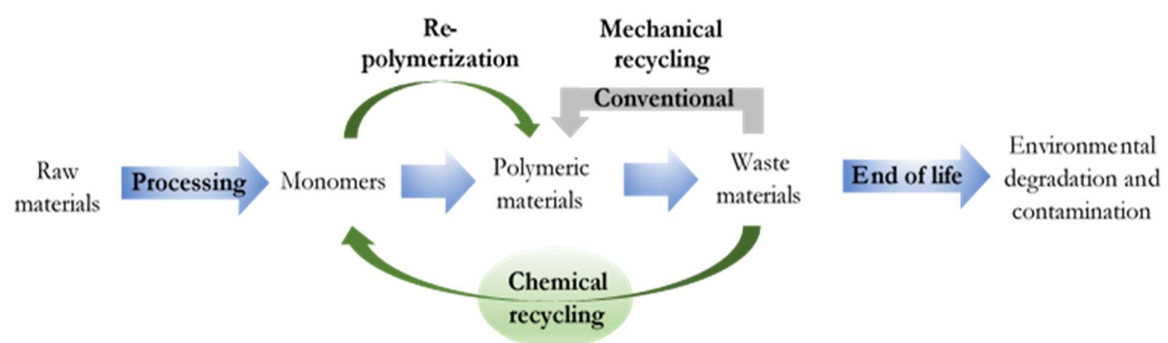


Figure 1-3 Polymer production from waste materials through chemical recycling (Adapted from García, 2016).

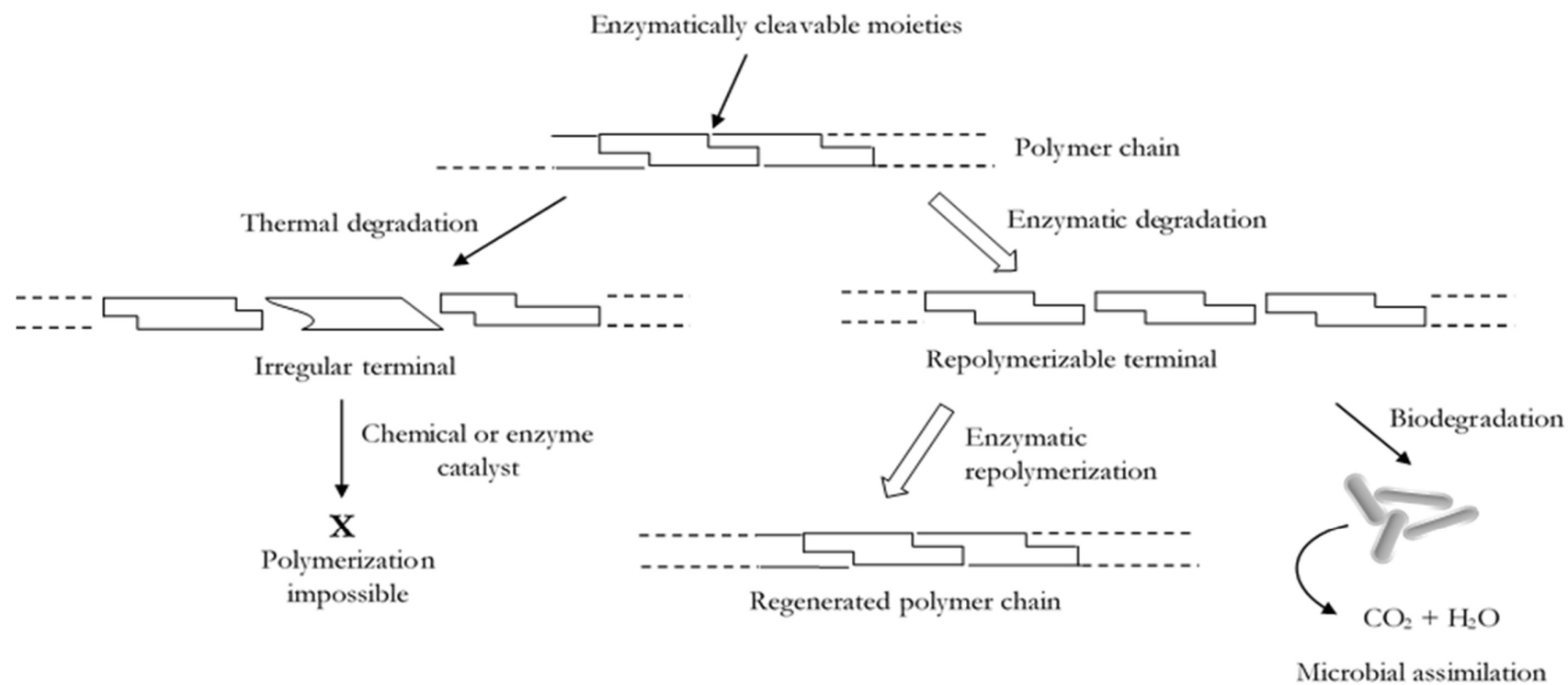


Figure 1-4 Enzymatic degradation products become the raw materials for repolymerization as a chemical recycling technique (Adapted from Matsumura, 2002).

1.7 Review of literature

1.7.1 Microbial degradation of PBS/PBSA

The degradation of biodegradable plastics is heavily depending on their environment. The biodegradability differs under different environmental conditions, such as soil, compost, marine and other aquatic environments (Anstey *et al.*, 2014). Soil and compost environments were found to contain higher microbial biodiversity than that of finding in other environments (Emadian *et al.*, 2017). However, compared to the other aliphatic polyesters such as PCL, the distribution of PBS-degrading microorganisms in a soil environment was quite restricted (Pranamuda *et al.*, 1995; Suyama *et al.*, 1998), which explained the many reports on the isolation of only a single strain from soil environment (Abe *et al.*, 2010). The isolation of PBSA-degrading bacteria and fungi from soil and compost have been reported by many researchers. Lee and Kim (2010) isolated two bacteria; *Burkholderia cepacia* PBSA-1 and *Pseudomonas aeruginosa* PBSA-2, from activated sludge soil and cultivating soil, that could mineralize PBSA into carbon dioxide. The strains were able to mineralize 78% of PBSA with an initial concentration of 0.01% into carbon dioxide during 40 days of the modified Sturm test. Another bacterium, *Bacillus pumilus* strain 1-A that could completely degrade PBSA films, and approximately 90% of PBS films within 14 days, was isolated from soil by Hayase *et al.* (2004). Degradation of PBSA was found to be faster than PBS, probably because of the rapid degradation of adipate units compared to 1,4-butanediol and succinate units, as indicated by the NMR spectra of degradation products.

A fungal strain, *Aspergillus fumigatus* strain NKCM1706, exhibited fast degradation rate for the PBS film ($10.5 \mu\text{gcm}^{-2}\text{h}^{-1}$), was isolated from soil by Ishii *et al.* (2008). In addition to PBS, this strain could also degrade PBSA, PES, P(3HB), and PCL. The isolation of fungi *Aspergillus versicolor* from compost was also reported (Zhao *et al.*, 2005). This strain was able to assimilate 90% of PBSA film within 25 days. Analysis by scanning electron microscopy (SEM) showed a number of cracks and round holes on the eroded film surface. Abe *et al.* (2010) isolated a soil fungal strain, *Fusarium solani* strain WF-6, that can degrade 2.8% of the PBS films in a 14-day experimental run in a sterile soil environment, as determined by measuring CO₂ evolution. Co-culturing of strain WF-6 with the newly isolated bacterial strain *Stenotrophomonas maltophilia* YB-6, that does not show PBS-degrading activity by itself, enhanced the degradability of strain WF-6.

In this laboratory, many PBSA-degrading bacteria have been successfully isolated and characterized (Uchida *et al.*, 2000; Akutsu-Shigeno *et al.*, 2003; Teeraphatpornchai *et al.*, 2003; Nakajima-Kambe *et al.*, 2009b; Shah *et al.*, 2013b).

1.7.2 Characterization of the gene encoding for biodegradable plastic-degrading enzymes

Despite many reports have been published on the isolation and characterization of biodegradable plastics degrading enzymes, very few reports on the genetic structures and/or map of the degrading enzymes-encoding genes are available, particularly those of that esterases. The most similar work to the enzymes in this study was perhaps that of published by Thumarat *et al.* (2015). The genetic map of the gene encoding for cutinase-type polyesterase from *Thermobifida alba* AHK119 revealed the presence of tandem genes, designated as *est1* and *est119*, encoding for enzymes Est1 and Est119. Both enzymes (without signal peptides) shared 95% sequence identity and 98% similarity and possessed similar 3D structures, however, the activity of Est1 towards *p*-nitrophenyl butyrate was higher by approximately 1.6–1.7-fold than that of Est119. Serine hydrolase sequence (G-H-S-M-G) in which Ser169, His247, and Asp215 making up the catalytic triad, were identified in the open reading frame (ORF) of Est1. Amino acid sequences comparison between Est1 and Est119 showed that, instead of α -helices and β -sheets, most of the differences in amino acid sequences were observed in loop regions especially of the Asp215-loop and the His247-loop. The difference in activity and thermostability may be attributed to the differences in the loop domains surrounding the catalytic triad since these domains are considered as a substrate-binding domain.

In another study by Biundo *et al.* (2016), crystallization and determination of the 3D structure of a lipase (PfL1) able to hydrolyze poly(1,4-butylene adipate-*co*-terephthalate) (PBAT), from the anaerobic groundwater organism *Pelosinus fermentans* DSM 17108, displayed the presence of a lid structure and a zinc ion surrounded by an extra domain. These properties classify the enzyme into the I.5 lipase family, further confirmed by examining the thermoalkalophilic properties of the enzyme as well as analysis of sequence and alignment with other bacterial lipases. Structural analysis of PfL1 and GsL1; another lipase belonging to the same I.5 lipase family, showed substitution of the pentapeptide Gly-X-Ser-X-Gly towards the Ala-X-Ser-X-Gly motif. Kleeberg *et al.* (2005) isolated a novel thermophilic hydrolase from *Thermobifida fusca* (TfH) that could hydrolyze aliphatic-aromatic copolyesters. The amino sequence determination showed that the enzyme consists of 261 amino acids, yielding a 28 kDa enzyme, and was classified as a serine hydrolase showing high sequence similarity to a triacylglycerol lipase from *Streptomyces albus* G and triacylglycerol-aclyhydrolase from *Streptomyces* sp. M11. The comparison with other lipases and esterases revealed the TfH exhibits a catalytic behavior between lipase and an esterase, therefore, was regarded as a cutinase.

1.7.3 Recombinant production of biodegradable plastic-degrading enzymes

Heterologous expression in a suitable host cell is a widely used method to produce recombinant proteins and enzymes. This method allows for the expression and purification of the desired protein in a large quantity for various purposes such as for biochemical characterization, for use in industrial processes and for the development of commercial goods (Rosano and Ceccarelli, 2014). Various expression systems are currently being employed in academic and industrial settings, however, some of the systems are too technically challenging, time-consuming and expensive for the application in the average laboratory. *Escherichia coli*, *Pichia pastoris*, baculovirus/insect cell, and mammalian expression systems are some of the most commonly used systems because of the straightforward protocols, are readily accessible and relatively inexpensive for small-scale production (Brondyk, 2009). The choice for an appropriate expression system is determined by the intended application of the recombinant protein and is essential to produce sufficient quantities of the protein (Brondyk, 2009) for downstream studies. For example, bacterial expression system is unable to perform post-translational modifications which are required for proper protein activity; yeasts and filamentous fungi expression systems i.e. eukaryotic expression system, are therefore the most suitable for such purposes (Gasser *et al.*, 2008).

Among all expression system mentioned earlier, *E. coli* is the most commonly used expression system for the production of recombinant protein due to its many advantages such as fast growth kinetics, fast doubling time, easy-to-achieve high-density culture, and fast and easy transformation with exogenous DNA (Sezonov *et al.*, 2007). Dimarogona *et al.* (2015) successfully expressed a functional cutinase from *Fusarium oxysporum* in the periplasm of *E. coli*, to be used for the surface modification of PET synthetic polymers. Two novel esterases from the anaerobe *Clostridium botulinum* ATCC 3502 (Cbotu_EstA and Cbotu_EstB) were expressed in *E. coli* BL21-Gold (DE3) in a study by Perz *et al.* (2016). The enzymes were found to hydrolyze the polyester PBAT, and their crystal structures were successfully determined. Similarly, Biundo *et al.* (2016) accomplished the cloning and expression of a lipase capable to hydrolyze PBAT, from the anaerobic groundwater organism *Pelosinus fermentans* DSM 17108 (Pfl1) in *E. coli* BL21-Gold (DE3). Crystallization and determination of the 3-D structure of the enzymes were also performed following successful expression.

1.7.4 Targeted gene disruption for the elucidation of gene function

The function of a gene can be investigated by observing the effects on a biological system or organism when that gene is missing. Targeted gene disruption is a genetic technique that utilizes homologous recombination to modify an endogenous gene. This technique is employed to investigate the developmental or functional significance of a gene by deleting it (Alberts *et al.*, 2002). Garrido *et al.* (2012) investigated the roles of a FarA transcriptional factor in the regulation of genes; *cutL1* and *hsbA*, that are responsible for the production of cutinase for the degradation of PBSA in *Aspergillus oryzae* by disrupting the FarA-encoding gene, *farA*. When the wild-type and the *farA* gene disruption strains were grown in PBSA-emulsified minimal agar medium, the wild-type formed clear zone around the colonies while the disruptants did not, indicating the significance of the FarA transcriptional factor in the expression of genes essential for the degradation of PBSA. In another study by Gácsér *et al.* (2007), the deletion of lipase locus consisting of adjacent genes *CpLIP1* and *CpLIP2* in the *Candida parapsilosis* genome caused the loss of lipolytic ability in the null mutants. Reconstruction of the *CpLIP2* gene restored lipase activity, similar to those showed by the wild type and heterozygous mutants. In addition, lipase-negative mutants demonstrated inhibited biofilm formation and significant reduced growth in lipid-rich media. Similarly, Nie *et al.* (2011) reported on the disruption of the esterase-encoding gene; *chbH*, that can hydrolyze cyhalofop-butyl (CyB); a widely used aryloxyphenoxy propanoate (AOPP) herbicide for control of grasses in rice fields, to cyhalofop acid (CyA) in *Pseudomonas azotoformans* strain QDZ-1. The disruption produced *dchbH* mutant unable to degrade and utilize CyB, suggesting that *chbH* was the only esterase gene responsible for CyB degradation in strain QDZ-1.

1.8 Background of research

Previously in this laboratory, various biodegradable plastic-degrading bacteria have been isolated and the properties of their degrading enzymes were successfully characterized (Uchida *et al.*, 2000, 2002; Teeraphatpornchai *et al.*, 2003; Shah *et al.*, 2013a, 2013b, 2014). The isolation of freshwater bacterium *Roseateles depolymerans* strain TB-87 (Shah *et al.*, 2013b) and another type of aliphatic-aromatic co-polyester biodegradable plastics degrading bacterium, *Leptothrix* sp. strain TB-71 (Nakajima-Kambe *et al.*, 2009b), were also reported. Strain TB-87 could degrade PBS, PBSA, PES, and PCL while strain TB-71 could effectively degrade PBSA but not PBS. Comparison done on PBSTIL degradation by TB-71 and TB-87 shown that the TB-87 strain demonstrated slightly higher degradation ability than TB-71 (Shah *et al.*, 2013a, 2014).

Unlike strain TB-71 which secretes only one enzyme during degradation, two types of PBSTIL-degrading enzymes were secreted by strain TB-87. The purified enzymes were classified as esterases based on substrate preferences towards *p*-nitrophenyl caproate (C₆) among various *p*-NP acyl esters, therefore, designated as Est-H (high, molecular weight; 31 kDa) and Est-L (low, molecular weight; 27 kDa). Both enzymes having similar substrate specificity and degradation activity formed clear zones on PBSTIL emulsion agar medium. Despite having almost identical molecular masses estimated from SDS-PAGE, both proteins showed different cleavage patterns when cleaved with V8-protease (Cleveland *et al.*, 1977), indicating that both proteins have different amino acids (Shah *et al.*, 2013b). In addition, Est-H showed higher degradation ability against PBS compared to Est-L which further confirm that both proteins are of different proteins.

1.9 Objectives of the study

In many other similar studies, one type of enzyme is usually responsible for the biodegradable plastics' degradation by the isolated strain. However, strain TB-87 in this study secreted two types of enzymes that possess similar characteristic, substrate specificity, and activity. Many previous attempts in this laboratory to elucidate amino acid sequences of the purified enzymes for further biochemical studies have been unsuccessful due to the blocked N-terminus.

The acquisition of high purity enzyme for structural studies is of utmost importance to understand the functions of the genes in the biodegradation of co-polyesters. It was expected that the manipulation of the genes to achieve the final aim which is a monomer recycling, can be performed once the gene elucidation had been understood. Therefore, the principal objectives of this study are

- 1) to analyze the gene-encoding region of an esterase from *Roseateles depolymerans* strain TB-87
- 2) to clone and express esterase from strain TB-87 into suitable host cells for functional expression of the enzymes
- 3) to disrupt esterase-encoding genes for the elucidation of gene function
- 4) to disrupt chaperone-encoding gene for functional analysis studies

CHAPTER 2

Analysis of Gene-encoding Region of Esterase from *Roseateles depolymerans* strain TB-87

2.1 Introduction

Roseateles depolymerans strain TB-87 is a freshwater bacterium that could degrade PBS, PBSA, PES, and PCL previously isolated by Shah *et al.* (2013b). Unlike other strains previously isolated in this laboratory (Uchida *et al.*, 2000, 2002; Teeraphatpornchai *et al.*, 2003; Nakajima-Kambe *et al.*, 2009; Shah *et al.*, 2014) which secreted only one enzyme during degradation, two types of PBSTIL-degrading enzymes were secreted by strain TB-87. The purified enzymes were classified as esterases based on substrate preferences towards *p*-nitrophenyl caproate (C₆) among various *p*-NP acyl esters, therefore, designated as Est-H (high, molecular weight; 31 kDa) and Est-L (low, molecular weight; 27 kDa) (Shah *et al.*, 2013b). Despite having almost identical molecular masses estimated from SDS-PAGE, both proteins showed different cleavage patterns when cleaved with V8-protease (Cleveland *et al.*, 1977), indicating that both proteins have different amino acids (Shah *et al.*, 2013b). In addition, Est-H showed higher degradation ability against PBS compared to Est-L which further confirm that both proteins are of different proteins. The structure of esterase-encoding region from strain TB-87 has not been understood fully. Unfortunately, attempts to elucidate amino acid sequences of the purified enzymes for further studies have been unsuccessful due to the blocked N-terminus. Therefore, esterase-encoding gene region of TB-87 strain was analyzed by combining results from previous internal amino acid sequencing with analysis by using various available software and online databases and the results are presented in this chapter.

2.2 Materials and method

2.2.1 Total genome analysis of TB-87 strain

Extraction of DNA was previously carried out in this laboratory according to ISOPLANT's (Nippon Gene, Tokyo, Japan) standard protocol, and its draft genome analysis was requested to Hokkaido System Science (Hokkaido, Japan).

2.2.2 Determination of ORF of *est-H* and *est-L*

Est-H and Est-L internal amino acid sequences previously obtained in another study were converted into nucleotide sequences using GENETYX ver.11 (Genetics Corporation, Tokyo, Japan). Local BLAST search (<http://blast.ncbi.nlm.nih.gov/Blast.cgi>) against the total translated genome of strain TB-87 using Est-H and Est-L's internal amino acid sequences was performed to find for homology region in Node followed by estimation of ORF by using ORF Finder (<http://www.ncbi.nlm.nih.gov/gorf/>) for Node showing the highest homology. The estimated ORF was then annotated from the base sequence and the amino acid sequence.

2.2.3 Signal peptide analysis

After determining the ORF of Est-H and Est-L, the region presumed to be a signal peptide was examined using SignalP 4.1 Server (<http://www.cbs.dtu.dk/services/SignalP-4.1/>) and Signal-BLAST (<http://sigpep.services.came.sbg.ac.at/signalblast.html>).

2.2.4 Homology search based on the deduced amino acid sequence

Based on the information on the amino acid sequence obtained from the identified homologous region, BLAST program provided by National Center for Biotechnology Information (NCBI) (<https://blast.ncbi.nlm.nih.gov/Blast.cgi>) was used to search for highly homologous proteins.

2.2.5 Multiple sequence alignment

Alignment of amino acid sequences of highly homologous proteins was carried out by using a web server program ClustalW Version 2.1 (<http://clustalw.ddbj.nig.ac.jp/>).

2.2.6 Phylogenetic tree construction

The phylogenetic tree of Est-H, Est-L, and Est-Ch, and similar enzymes reported in other studies were constructed using the MEGA-X software program.

2.3 Results and discussion

2.3.1 Annotation of *est-H*, *est-L*, and chaperone-like gene region

The presence of homologous region in 137 Nodes constituting the whole genome of TB-87 strain was investigated. At Node 98, both internal amino acid sequences (designated as Est-H_a and Est-H_b, respectively) previously obtained in this laboratory, yields 100% query cover


and identities. From the region presumed to be *est-H* and *est-L* genes determined using the NCBI ORF Finder, the open reading frames (ORF) 1083 bp and 870 bp expected to be *est-H* and *est-L*, respectively, were estimated.

The determined nucleotide and amino acid sequences are shown in Figure 2-1. The predicted *est-H* ORF consists of 1083 bp with ATG as the initiation codon and TGA as the stop codon. The probable SD (ribosome binding site) sequence (GGTGAC) is present 7 bp upstream of the translation initiation point (Met). Sequences corresponding to the -10 (TCTACA) and -35 (TGTAAC) regions were identified 33 bp and 53 bp upstream of the translation initiation codon (Met). However, no terminator sequences were found downstream of the termination codons. The presence of a signal peptide could not be confirmed, as no prediction was identified by SignalP 4.1 Server.

The region predicted to be *est-L* consists of an ORF of 870 bp with ATG as the start codon and TGA as the stop codon. The predicted SD sequence (AGGGAG) is located 5 bp upstream of the translation initiation codon (Met). Sequences corresponding to the -10 (TCCAAC) and -35 (TTTCCC) regions of the predicted promoter region were found 21 bp and 53 bp upstream of the translation initiation codon (Met). A GC-rich palindrome sequence (GGGGCTGCTGGGAGA-TCATCTATGCCGCCCCAACGT CC) predicted to serve as a transcription terminator was identified. Analysis by SignalP 4.1 predicted that the 48-amino acid region (144 bp) at the N-terminus formed a signal peptide. A lipase box (-Gly-X1-Ser-X2-Gly-, X1; His, X2; Met) unique to hydrolases were found at amino acid residues 457-471 and 154-159 for Est-H and Est-L, respectively.

Another ORF region consisting of 735 bp was identified within the intergenic region of the predicted *est-H* and *est-L* ORFs. This ORF consisted of an ATG initiation codon located 12 bp downstream of the *est-H* gene and a TGA termination codon located 154 bp upstream of the *est-L* gene. A homology search demonstrated that this region shares homology with bacterial lipase chaperones, thus, this ORF was designated as *est-Ch*. The SD sequence of *est-Ch* was inferred as a sequence (AGGCGT) located 7 bp upstream of the translation initiation codon (Leu). However, a predicted transcription initiation promoter sequence could not be identified. A GC-rich palindrome sequence (CCTCCCGTGCCGGC-GCAGGCACGGGGGG), predicted to be a terminator, was identified 12 bp downstream of the stop codon.

The annotation results of the esterase-encoding region of strain TB-87 presented earlier was summarized into a genetic map as shown in Figure 2-2.

CCACTGCTGGCGTCCACCCATTTCATTGGCGATCAGCAGCTGGGTGTCGGGGTAACTTGCA 60
 CTCATGGTCCGTCCAGCGGATGGCCACGAGCAGGCCACCCGGTTT**TGTAAC**GAAGATGACG 120
 -35
 M T L L A
 CCACT**TCTACAG**CGCCGCCGCACGGCGCATC**GGTGAC**ACGCCGGATGACGCTGTTGGCCGG 180
 -10 SD Sequence  *est-H*
 G W V S P H V N L G G S G H P N T R H S
GTGGGTTTCCCCGCATGTGAATCTAGGGGGGTCAGGTCATCCCAATACAAGGCATTCCGG 240
 G E R F L D S S G R R A R P A P L A P W
CGAACGGTTCCTAGACTCATCCGGCCGCCGTGCGCGTCCGGCTCCGCTTGACCGTGGGA 300
 D R L P L A R P L C R R D A V A A N V T
CCGGCTTCCCCTTGCAAGACCCTTGTGCAGACGGGACGCGGTGGCAGCCAATGTCACGAA 360
 K O G D N M T F T T L W R R H A R A C A
ACAGGGAGACAACATGACCTTCACGACCCTTTGGCGTCGCCATGCGCGCGCCTGCGCGCT 420
 L A A S A A L A L S A G S S F A Q Q T G
CGCGGCCTCTGCCGCGCTGGCACTGTGCGCGGGCAGCAGCTTTGCCAGCAGACCGGCC 480
 P D P T S A S L N A T A G P F A V S T S
CGACCCACCTCCGCCAGCCTGAATGCCACTGCCGGCCCGTTTGCGGTCAGCACGTCGAC 540
 T V T S P V G F G G G T I Y Y P T T A G
GGTGACCTCGCCGGTGGCTTTGGCGGGCGCACCATCTACTACCCACCCACCGCCGGTCA 600
 Q Y G V V A L S P G F T A T Q S S V A W
GTACGGCGTCGTGGCCCTGAGCCCTGGGTTACCGCCACCCAGAGCAGCGTCGCCTGGCT 660
 L G R R I A T H G F V V V T I N T N S T
GGGGCGCCGGATCGCCACCCACGGGTTTCGTGGTGGTCAACATCAACACCAACAGCACGT 720
 Est-H_b

 L D Q P A S R A T Q L I A A L N Y V A N
GGACCAACCAGCCAGCCGGGCGACGCAACTGATCGCCGCGCTGAACTACGTGGCCAACAG 780
 Lipase box
 S A S S T V R S R V D P A R R A V G **G H**
CGCCAGCAGCACGGTGCAGCGCGCTCGACCCCGCGCGTCGCGCCGTGGGCGGGCACTC 840
S M G G G G S L I A A Q N N P S L K A I
GATGGGCGGGCGGGATCCCTGATCGCCGCGCAGAACAACCCAGCCTCAAGGCCATTCT 900
 L P L T P W N L N T N F S G V Q V P T L
TCCGCTGACCCCGTGGAACCTGAACACCAACTTCAGCGGCGTGCAAGTGCCACGCTGAT 960
 Est-H_a

 I V G S D G D V V A P V A S H A R P F Y
CGTGGGCTCGGACGGTGATGTGGTGGCGCCGGTGGCCTCGCATGCCCGGCCCTTCTACGC 1020

 A S L P S T V R K A Y G E L N M A T H S
GAGCCTGCCAGCACCGTGCGCAAGGCCTATGGGGAAGTGAACATGGCCACCCACTCCAC 1080
 T P T S G V N T P I G R Y G V T W M K R
ACCGACCAGCGGGGTGAACACCCCATCGGACGCTACGGCGTCACCTGGATGAAGCGCTT 1140
 F V D G D T R Y S T F L C G A E H Q A Y
CGTCGACGGCGACACCCGCTACTCCACCTTCCTGTGCGGCGCGGAACATCAGGCCTATGC 1200

A T A T V F D R Y S Q N C P Y *
CACGGCCACCGTGTTCGACCGCTACAGCCAGAACTGCCCTACTGACGGAGGTCGCCCAT
SD Sequence → est-Ch 1260

P N P H K R G P G W R I F G L A L I A G
GCCGAATCCGCACAAGCGGGGACCCGGCTGGCGCATCTTTGGCCTGGCCCTGATTGCAGG 1320

G L G A A G L Y A W M A D A T S P E H V
GCTGGGCGCCGCCGGGCTGTATGCCTGGATGGCGGATGCGACCTCCCCGGAGCACGTCGT 1380

V A N Q Q F P W S Q T P G T P G G T A G
CGCCAATCAACAATTCCCTTGGTCCCAGACGCCGGGCACGCCTGGCGGCACCGCGGGGCGC 1440

A P G T A G L S A T E L A A M A A T G A
CCCGGGCACGGCGGGGCTTTCCGCGACCGAGCTGGCGGCGATGGCCGCCACCGGCGCTGG 1500

G D P D A L G S A G G P R Q R P F R V N
AGATCCCGATGCCTTGGGGAGTGCCGGTGGCCCCACGCCAGCGTCCCTTCCGGGTCAATGC 1560

A R G Q L V T D Q A L R L E L E S L L A
GCGGGGTCAGCTCGTGACCGATCAGGCCTTGAGACTGGAGCTGGAATCGCTGCTGGCGCT 1620

L H Q G A A Q T A A L E A Q L S E L P A
GCACCAAGGGGCGCGCAGACCGCCGCCCTGGAGGCGCAACTGTCCGAGCTGCCCCGCCG 1680

A A A A Q A R Q L L S Q F A S Y Q E A Q
AGCGGCTGCGCAGGCGCGGCAACTCCTGAGCCAGTTCCGCCAGTTACCAGGAGGCGCAGCG 1740

R Q A F P P D Q A P L V P E E G L A Q L
TCAAGCCTTCCCGCCGGATCAGGCGCCGCTGGTGCCTGAGGAAGGCTTGGCCCAGCTCAA 1800

N A L Q S L R A T Y L G A E N A R Q M F
CGCCCTGCAGTCCCTGCGCGCCACCTACCTCGGCGCGGAGAACGCACGGCAGATGTTTGC 1860

A Q D D A V S R R L L E L M R E D P S P
GCAGGACGATGCCGTGTCCCGGCGTCTTCTGGAGCTGATGCGGGAGGACCCCTCCCCCAA 1920

N L S M S D K A V R A Q A R Y D L E R N
CCTGTCCATGTCGGACAAGGCCGTGCGGGCGCAGGCCCGTTACGACCTCGAGCGCAACGG 1980

G A Q P *
CGCCCAGCCCTGACGGCGACAGAGGCCTCCCGTGCCGGGCTCCCGCAGGCACGGGGGGTTT 2040

Terminator region

GTCCCGATCGGAGCTAGGGGGCACGGGGGTCTCCCAATACAAGGCATCCCGGGACGGGAT 2100

TCCTAGACTGGCCGGGCCGCGAGCGCAACGGGGTCAGGCGTTTCCCGCCTGCACCGATGCC 2160

-35

M T L T S S L
ACGCGGCATCGTCCAACGTGACATCACAGGGAGACATCATGACCCTCACCTCGAGCTTGC 2220

-10 SD Sequence → est-L

R R Q T R V A A L A A A A A L T G L A L
GTCGTGACACGCGCGTGCCTGCCCGCTGGCGGCTGCTGCGGCCCTACCGGCTTGGCCCTTC 2280

Putative signal peptide

P A S A Q Q T G P D P T S A G L N A T A
CCGCCAGCGCCCGAGCAGACCGGGCGCGGACCCACCTCCGCCGGCCTCAATGCCACCGCGG 2340

G P F A V G S T S V L A P V G F G G G T
GCCCTTTGCCGTGGGCGAGCACGTGGTGGTGGCGCCGGTGGGCTTCGGCGGCGGCACCA 2400

I Y Y P T T A G Q Y G V V A M S P G F T
TCTACTACCCACGACAGCGCGGCAATACGGTGTGGTGGCGATGAGCCCAGGCTTCACCG 2460

A T E S S I A W L G R R L A T H G F V V
CCACCGAGTCCAGCATTGCCTGGCTGGGCCGACGGCTGGCCACGCATGGATTGTCGTGG 2520

Est-L_b

V T I N T L T T L D Q P A S R A T Q L M
TCACCATCAACACGCTCACCACGCTGGACCAGCCCGCCAGCCGCGCCACTCAGCTGATGG 2580

.....
 A A L N H V V N S A S S T V R S R V D P
CGGCGCTCAATCATGTGGTGAACAGTGCGAGCAGCACGGTGCGAAGCCGGGTCGATCCGA 2640

Lipase box

N R R A V A **G H S M G G G G A L I A A E**
ACCGGCGCGCGGTGGCCGGGCATTCGATGGGCGGCGGCGGCCTTGATCGCGGCGGAGA 2700

N N P S L K A A L P L T P W N L T T N F
ACAACCCAGCCTCAAGGCGGCCCTGCCGCTGACGCCCTGGAACCTCACCACCAACTCA 2760

S D V Q V P T L I V G A D G D T I A P V
GCGATGTGCAGGTGCCCCACCCTGATCGTTGGCGCCGACGGTGACACCATCGCGCCAGTGG 2820

Est-L_a

A V H A R P F Y A S L S S S V R K A Y A
CGGTGCATGCAAGGCCCTTCTATGCAAGCCTGTCCAGCTCGGTCCGAAAGGCTTATGCCG 2880

.....
 E L N F S T H F T P N S T N T P I G R Y
AACTGAACTTCTCGACCCACTTCACGCCCACTCCACCAACACGCCGATCGGACGCTATG 2940

G V T W M K R F V D G D T R Y S S F L C
GGGTGACCTGGATGAAGCGCTTTGTGGACGGAGACACCCGGTATTCAAGCTTCCTCTGCG 3000

G A E H N A Y A T S L V F E R Y S Q N C
GCGCTGAGCACAACGCGTACGCCACATCCCTGGTGTTCGAGCGTTACAGCCAGAACTGCC 3060

P Y *
CCTACTGAGCCAGACCGGCCCGGCCGCGGTGGCATCTTGATGACACCGCGGGCAACAGG 3120
GTTCCGTCTTGACGGGCCCGGCGGTGTGCCGGAGCATGCCGTCACGATGCACAAGACATT 3180
GGCGACGCCCCGCTGGGGCTGCTGGGAGACAGCTTCATCTATGCCGGCCCCAACGTCCA 3240

Terminator region

Figure 2-1 *est-H*, *est-Ch*, and *est-L* gene annotation. Annotated ORF for each gene are underlined; translation initiation sequences are indicated with arrows; -10, -35 promoter sequences and SD sequences are bolded; terminator regions are bolded and underlined; putative signal peptide is double-underlined; internal amino acid sequences previously detected are marked with dotted line above the sequences; lipase box are highlighted in italics and bolded.

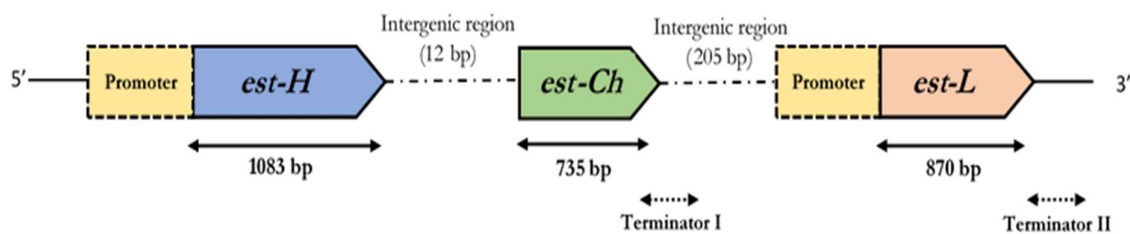


Figure 2-2 Predicted genetic map of esterase-encoding genes based on the combined results of previously obtained internal amino acid sequencing of expressed native esterase and draft genome analysis and gene annotation in the current study. The predicted genetic map of esterase gene region in *R. depolymerans* strain TB-87. *est-H*, *est-Ch*, and *est-L* genes and their respective sizes are as shown. Promoter regions are in yellow. Terminator regions are indicated by a dotted arrow. *est-H* located in the upstream of *est-Ch* with a distance of 12 bp while *est-L* is located in the downstream of *est-Ch* with a distance of 205 bp.

2.3.2 Homology analysis of esterase with other highly-homologous enzymes

Proteins highly homologous to the amino acid sequences of Est-H, Est-L, and Est-Ch were searched from BLAST (<https://blast.ncbi.nlm.nih.gov/Blast.cgi>) and the results are summarized in Table 2-1. Est-H and Est-L's conserved domains showed homology with other α/β -hydrolases. Est-H had about 53-95% homology while Est-L showed about 54-84% homology with cutinase and esterase of other bacteria.

BLAST search performed on Est-Ch revealed homology of conserved domain with lipase chaperones. Est-Ch was shown to have highest homology (90% identities) with a hypothetical protein from *Roseateles terrae* and as low as 31-35% homology with lipase chaperone and another hypothetical protein from *Marinobacter subterrani* and *Aquabacterium* sp. NJ1, respectively.

2.3.3 Multiple sequence alignment of esterase and other homologous enzymes

Amino acid sequence alignment of Est-H and Est-L with various homologous biodegradable plastic degrading enzymes consisting of esterase (Est1, Est119), other similar α/β -hydrolase from *R. terrae* and a cutinase from *T. fusca*, was performed and the results are as shown in Figure 2-3. Consensus sequence making up a lipase box (-Gly-X1-Ser-X2-Gly-, X1; His, X2; Met), specific for hydrolases, are present in all sequences. The amino acid sequence of Est-L analyzed by the SignalP 4.1 Server identified a 31-amino acid sequence at its N-terminus as a signal peptide (MTLTSSLRRQTRVAALAAAAALTGLALPASA). The cleavage site is located between position 31 and 32 (Ala-Gly), yielding mature protein made up of 263 amino acids. Analysis of the amino acid sequence of Est-H, however, predicted no signal peptide's presence. Therefore, the putative signal peptide of Est-H was predicted by using another prediction software, Signal-BLAST (<http://sigpep.services.came.sbg.ac.at/signalblast.html>) and by calculating the differences in molecular weight of Est-H with and without its putative signal sequence. The signal sequence of a secretory protein is usually cleaved-off once they were delivered to the correct subcellular compartment, releasing the mature protein (Tjalsma *et al.*, 2000). The molecular weight of native Est-H and Est-L were 31 kDa and 27 kDa, respectively (Shah *et al.*, 2013b) while the molecular weight of recombinant Est-H and Est-L were predicted, based on the annotated ORF, to be about 37 kDa and 31 kDa, respectively. The differences of 6 kDa and 4 kDa between native and recombinant Est-H and Est-L were presumed to be those of signal sequences, and thus, the signal sequence for Est-H was determined to be a 60-amino acid sequence at its N-terminus (Frank and Sippl, 2008). The cleavage site is located between position 60 and 61 (Val-Ala), yielding a mature protein of 300

Table 2-1 Homology analysis results for esterase in this study and other highly homologous enzymes.

Esterase (this study)	Homologous enzyme	Strain	Identity (%)	GenBank accession number
Est-H	Est-L	<i>Roseateles depolymerans</i> TB-87	80	-
	α/β -hydrolase	<i>Roseateles terrae</i>	95	OWQ89612
	Est1	<i>Thermobifida alba AHK119</i>	55	BAI99230
	Est119	<i>Thermobifida alba AHK119</i>	53	BAK48590
	Cutinase	<i>Thermobifida fusca KW3</i>	59	CBY05530
Est-L	Est-H	<i>Roseateles depolymerans</i> TB-87	80	-
	α/β -hydrolase	<i>Roseateles terrae</i>	84	OWQ89612
	Est1	<i>Thermobifida alba AHK119</i>	56	BAI99230
	Est119	<i>Thermobifida alba AHK119</i>	54	BAK48590
	Cutinase	<i>Thermobifida fusca KW3</i>	60	CBY05530
Est-Ch	Hypothetical protein CDN98_03550	<i>Roseateles terrae</i>	90	OWQ89611
	Hypothetical protein	<i>Mitsuaria</i> sp. PDC51	50	WP_091724599
	Hypothetical protein DBR42_11810	<i>Pelomonas</i> sp. HMWF004	51	PTT87353
	Hypothetical protein JY96_13890	<i>Aquabacterium</i> sp. NJ1	35	KGM40769
	Lipase chaperone	<i>Marinobacter subterrani</i>	31	WP_048496563

amino acids. The cleavage sites for putative signal sequences are demarcated by arrows in Figure 2-3.

2.3.4 Dendrogram of Est-H, Est-L, and Est-Ch

Distance matrices between the esterases examined in this study and other homologous enzymes were measured using the MEGA-X software program and dendrograms were constructed (Figure 2-4) using homologous lipases, esterases, and cutinases. The tree (Figure 2-4A) branched into two; the first branch consisted of Est-H, Est-L, and all other enzymes except for the α/β -hydrolases from *Pelomonas* sp. and *Mitsuaria noduli*, which belong to the second branch. Est-H has a bootstrap value of 100 with an α/β -hydrolase from *R. terrae*, while Est-L has a bootstrap value of 88 with both Est-H and the *R. terrae* α/β -hydrolase, suggesting that these three enzymes are closely related to each other. Est1 and Est119 have a bootstrap value of 100 with each other and a low bootstrap value with Est-H, Est-L, the *R. terrae* α/β -hydrolase, and other α/β -hydrolases from *Pelomonas* sp. and *M. noduli*. Both Est1 and Est119 have approximately 53–56% homology with Est-H and Est-L; however, it is clear that they belong to systematically different groups of enzymes.

The Est-Ch dendrogram was generated using other homologous lipase chaperones and the result showed high bootstrap values of 100 and 65 with hypothetical proteins from *R. terrae* and *Marinobacter subterrani*, respectively, indicating a close relationship with these enzymes. In addition, based on the low bootstrap values, it appears that Est-Ch is distantly related to hypothetical proteins from *Mitsuaria* sp., *Pelomonas* sp., and *Aquabacterium* sp., as well as other lipase chaperones from *Cupriavidus necator* and *Pseudomonas aeruginosa*.

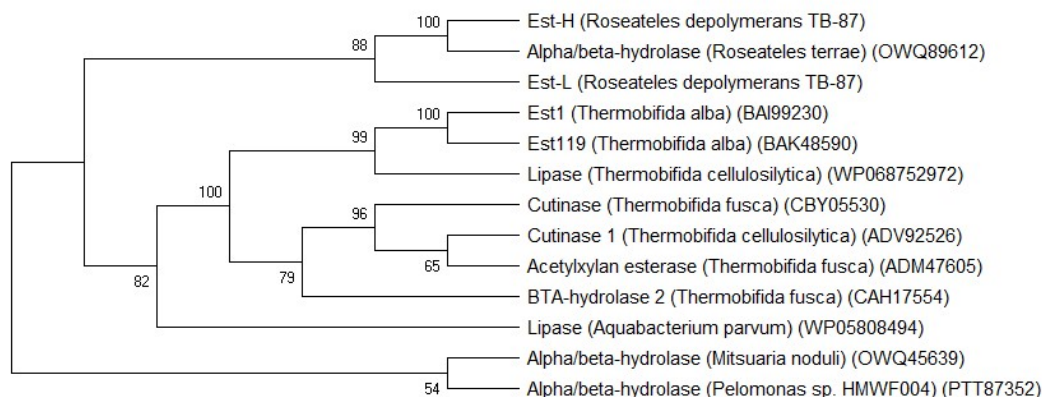
2.3.5 Prediction of the tertiary protein structure of Est-H and Est-L

The tertiary protein structure was predicted using the biodegradable plastic degrading enzyme Est119 secreted by *T. alba* strain AHK119 as the template. The crystal structure of Est119 (PDB ID; 3vis.2) has been well characterized by X-ray crystallography (Kitadokoro *et al.*, 2012). The three-dimensional structures of Est-H and Est-L were constructed using sequences devoid of their respective putative signal sequences. The amino acid sequences encompassing residues 60 to 360 and 32 to 289 were used to create the 3-D structure of Est-H and Est-L, respectively (Figure 2-5B, C). The predicted models of Est-H and Est-L using the Est119 template exhibit similar α -helix and β -pleated sheet structures. The homology of Est-H and Est-L with the Est 119 template was 52.90% and 55.29%, respectively. However, higher identity was observed between a template cutinase from *T. fusca* (PDB ID; 4cg3.1.A, GenBank

Est-H	MTLLAGWVSPHVNLGGSGHPNTRHSGERFLDSSGRRARPAPLAPWDRLPLARPLCRRDAV	60
Est-L	-----	0
Est1	-----	0
Est119	-----	0
Alpha/beta-hydrolase	-----	0
Cutinase	-----	0
	⋮	
Est-H	AANVTKQGDNMTFTTLWRRHARAC-----ALAASAALALSAGSSFAQQTGPDPPTSASLNA	115
Est-L	----- MTLTSSLRRQTRVA ----- ALAAAAALTGLALPASA QQTGPDPPTSAGLNA	45
Est1	-MSVTTPR---REASLLSRAVAVAAA-----AAATVALAAPAQAAANPYERGNPTESMLEA	52
Est119	-MSVTTPR---RETSLLSRALRATAAAATAVVATVALAAPAQAAANPYERGNPTESMLEA	56
Alpha/beta-hydrolase	-----MHFTTLWRRHARAC-----ALAASAVLSLSASSGWAQQTGPDPPTSASLNA	45
Cutinase	-----ANPYERGNPTDALLEA	17
Consensus	gp pt l a	
Est-H	TAGPFAVSTST--VTSVPVFGGGGTIIYYPTTAGQYGVVALSPGFTATQSSVAWLGRRIATH	173
Est-L	TAGPFAVGSTS--VLAPVFGGGGTIIYYPTTAGQYGVVAMSPGFTATESSIAWLGRRLATH	103
Est1	RSGPFSVSEERASRLGADGFGGGGTIIYYPRENNTYGAIAISPGYTGTQSSIAWLGERIASH	112
Est119	RSGPFSVSEERASRFADGFGGGGTIIYYPRENNTYGAIAISPGYTGTQSSIAWLGERIASH	116
Alpha/beta-hydrolase	TAGPFAVSTST--VTSVPVFGGGGTIIYYPTTAGQYGVVALSPGFTATQTSVAWLGRRLATH	103
Cutinase	RSGPFSVSEENVSRLSASGFGGGGTIIYYPRENNTYGAVAISPGYTGTQSSIAWLGERIASH	77
Consensus	gpf v sgfgggtiyy ty a spg t t iawl r a h	
Est-H	GFVVVTINTNSTLDQPASRATQLIAALNYVANSASSTVRSRVDPAARRAVG GHSMGGGGSL	233
Est-L	GFVVVTINTLTLDQPASRATQLMAALNHVNSASSTVRSRVDPNRRAVAG GHSMGGGGAL	163
Est1	GFVVIAIDTNTTLDQPDSSRARQLNAALDYMLTDASSSVNRNIDASRLAVM GHSMGGGGTL	172
Est119	GFVVIAIDTNTTLDQPDSSRARQLNAALDYMLTDASSAVNRNIDASRLAVM GHSMGGGGTL	176
Alpha/beta-hydrolase	GFVVVTINTNSTLDQPASRATQLIAALNYVANSANSTVRSRVDPNRRAVG GHSMGGGGSL	163
Cutinase	GFVVITIDTITLDQPDSSRAEQLNAALNHMINRASSTVRSRIDSSRLAVM GHSMGGGGSL	137
Consensus	gfvv i t tldqp sra ql aal a s vr r d r av ghsmgggg l	
Est-H	IAAQNNPSLKAILPLTPWNLTNFSGVQVPTLIVGSDGDVAPVASHARPFYASLPSTVR	293
Est-L	IAAENNPSSLKAAIPLTPWNLTTNFSQVQVPTLIVGADGTIAPVAVHARPFYASLSSSVR	223
Est1	RLASQRPDLKAAIPLTPWHLNKSQRDITVPTLIIGADLDTIAPVSSHSEPFYNSIPSTSD	232
Est119	RLASQRPDLKAAIPLTPWHLNKSQRDITVPTLIIGAEYDTIASVTLHSPFYNSIPSTPD	236
Alpha/beta-hydrolase	IAAQNNPSLKAILPLTPWNLTNFSGVQVPTLIVGADGDVAPVSSHARPFYASLPSTVR	223
Cutinase	RLASQRPDLKAAIPLTPWHLNKNSSVTPTLIIGADLDTIAPVATHAKPFYNSLPSSIS	197
Consensus	a p lka pltpw l vptli g d a v h pfy s s	
Est-H	KAYGELNMATHSTPTSGVNTPIGRYGVTWMKRFVDGDTRYSTFLCGAEHQAYATATVFDR	353
Est-L	KAYAEINFSHTFTPNS-TNTPIGRYGVTWMKRFVDGDTRYSSFLCGAEHNAYATSLVFER	282
Est1	KAYLELNNATHFAPNI-TNKTIGMYSVAWLKRFVDEDTRYTQFLCPGPRTGLL--SDVDE	289
Est119	KAYLELDGASHFAPNI-TNKTIGMYSVAWLKRFVDEDTRYTQFLCPGPRTGLL--SDVEE	293
Alpha/beta-hydrolase	KAYGELNMATHSTPTSGVNTPIGRYGVTWMKRFVDGDTRYSTFLCGAEHQAYATAAVFDR	283
Cutinase	KAYLELDGATHFAPNI-PNKIIIGKYSVAWLKRFVDNDTRYTQFLCPGPRDGLF--GEVEE	254
Consensus	kay el h p n ig y v w krfvd dtry flc	
Est-H	YSQNCPY 360	
Est-L	YSQNCPY 289	
Est1	YRSTCPF 296	
Est119	YRSTCPF 300	
Alpha/beta-hydrolase	YSQNCPY 290	
Cutinase	YRSTCPF 261	
Consensus	y cp	

Figure 2-3 Multiple sequence alignment of highly homologous biodegradable plastic-degrading enzymes. Sequence making up putative signal peptide are bolded. The possible cleavage site of the signal peptide is indicated by an arrow. Lipase box (-G-X-S-X-G-) specific for the hydrolase have been boxed. Amino acids making up the catalytic triad are indicated by filled circles above each residue. Est-H and Est-L from *R. depolymerans* strain TB-87 from this study; Est1 (BAI99230) and Est119 (BAK48590) from *T. alba* strain AHK119; α/β -hydrolase from *R. terrae* (OWQ89612); cutinase from *T. fusca* (CBY05530).

A



B

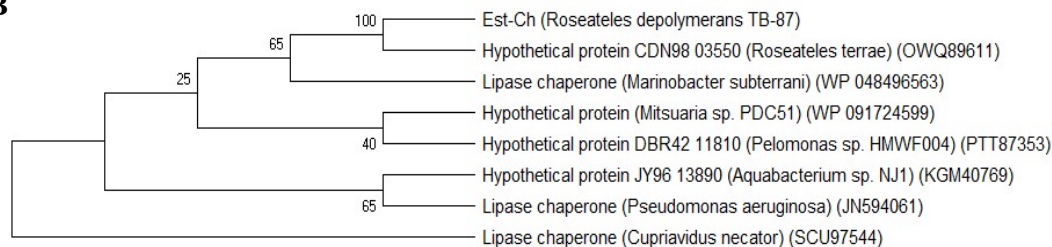


Figure 2-4 Dendrogram showing the level of homology between the esterases examined in this study and similar enzymes reported in other studies. The tree was constructed using the neighbor-joining method. Bootstrap values based on 100 replications are indicated at the nodes. GenBank accession numbers are provided in parentheses. A. Homology of Est-H and Est-L with other α/β -hydrolases; B. Homology of Est-Ch with other lipase chaperones.

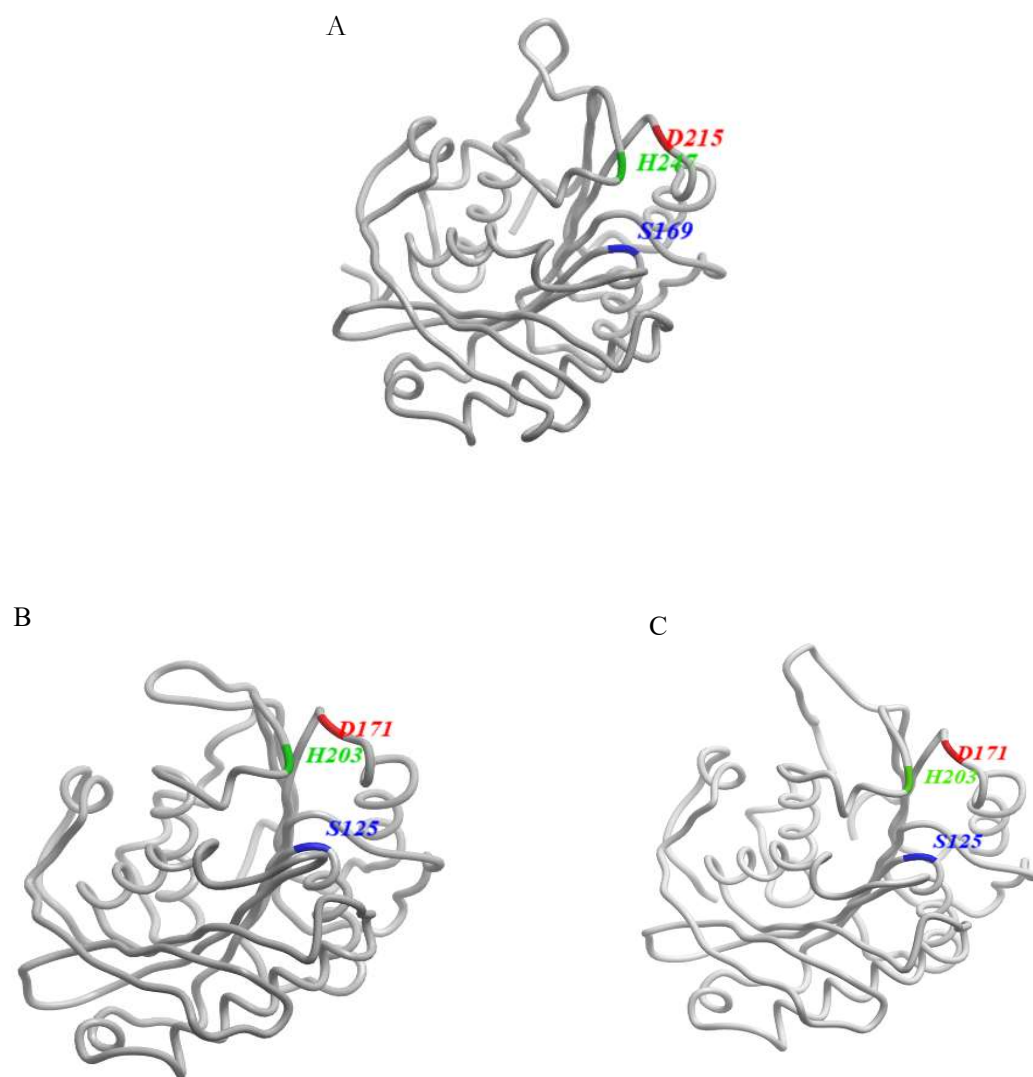


Figure 2-5 3-D structure prediction of the esterases examined in this study using Est119 as the template. A. Est119 from *Thermobifida alba* AHK119 (PBD ID: 3vis.2.A); B. Est-H (without the 60-residue putative signal sequence); C. Est-L (without the 31-residue putative signal sequence). The amino acid residues comprising the catalytic triad and their positions are highlighted in blue (Ser), red (Asp), and green (His).

accession no.; CBY05530) and Est-H (60.24%) and between a template Cutinase 1 from *T. cellulositica* (PDB ID; 5lui.1.A, GenBank accession no.; ADV92526) and Est-L (61.96%). Interestingly, the low bootstrap values for both proteins and Est-H and Est-L suggest both proteins belong to systematically different groups than Est-H and Est-L. The sequences of Est119 and Est-H and Est-L are considerably different; therefore, the quaternary structure of Est-L was not clarified. In both the Est-H and Est-L models the positions of the catalytic triads (Ser, Asp, His) serving as the active centers were predicted to be identical to that of Est119.

between a template Cutinase 1 from *T. cellulositica* (PDB ID; 5lui.1.A, GenBank accession no.; ADV92526) and Est-L (61.96%). Interestingly, the low bootstrap values for both proteins and Est-H and Est-L suggest both proteins belong to systematically different groups than Est-H and Est-L. The sequences of Est119 and Est-H and Est-L are considerably different; therefore, the quaternary structure of Est-L was not clarified. In both the Est-H and Est-L models the positions of the catalytic triads (Ser, Asp, His) serving as the active centers were predicted to be identical to that of Est119.

2.4 Conclusion

As a result of gene annotation in the current study, the presence of chaperone gene (*est-Ch*) located in the intergenic region of esterase-encoding genes (*est-H* and *est-L*) was predicted. The presence of -10, -35 promoter region upstream *est-H* and a terminator region downstream *est-Ch*, strongly suggested that *est-Ch* and *est-H* are expressed polycistronically. *Est-Ch* is possibly expressed to aid in the folding and transport of *Est-H* as a functional protein. Frenken *et al.* (1993) and (Kok *et al.*, 1995) in their respective studies suggested that a lipase chaperone, *LipB*, possibly mediates the formation of a secondary structure on the *LipA* polypeptide and protects the immature *LipA* against proteolytic degradation. Therefore, *LipB* is required for not only lipase production but is also crucial to the producing cell since it prevents membrane damages by the functional lipase (Frenken *et al.*, 1993; Kok *et al.*, 1995; Kim *et al.*, 1996).

Esterases from this study showed high homologies with proteins from *R. terrae*. Gomila *et al.* (2008) proposed two novel species, *Roseateles aquatilis* and *Roseateles terrae* that showed close relation with *Roseateles depolymerans* based on their 16S rRNA gene sequence analysis. Genome analysis of *R. terrae* revealed similarity in structure and position of genes to esterases in this study. A gene encoding for a hypothetical protein (GenBank accession no. OWQ89611) was found in the intergenic region of two genes (GenBank accession no. OWQ89610 and OWQ89612) that showed high homology to *Est-H* and *Est-L* from this study

(95%). Hypothetical protein from *R. terrae* also showed high homology with chaperone protein from this study (Table 2-1). However, the comparison of functional expression of the genes with esterases from this study could not be performed due to the lack of information on expression studies of these genes. In contrast, *Thermobifida alba* AHK119 possess two tandem cutinase gene, *est1* and *est119*, encoding for cutinase-like polyesterses (Thumarat *et al.*, 2015). Sequencing of *est1* and the intergenic region between *est1* and *est119* revealed that *est1* was located upstream of the gene encoding for Est119 (*est119*), with no ORF could be found at the intergenic region of the genes. Despite Est119 showing high homology, high homology in secondary structure prediction, and similar decomposition activity with esterases from this study, it was clear that the enzymes are of different groups, which was confirmed by constructed dendrogram (Figure 2-4) and low identities (Table 2-1) with esterases in this study.

However, very recently, Kitadokoro *et al.* (2019) demonstrated the similarity in structures of cutinase Est119-substrate complex as those of PET hydrolases. It was reported that all known PET hydrolases, including recently isolated PETase (Yoshida *et al.*, 2016), belong to the cutinase group (Tokiwa and Calabia, 2007; Zimmermann and Billig, 2011; Baker *et al.*, 2012). This is because unlike lipase and esterase, cutinase lacks the hydrophobic lid covering the active site; causing exposure of the site to the solvent, resulting in higher PET surface modification's efficiency compared to lipase and esterase (Kawai *et al.*, 2019). Although surface modification of PET is possible with lipases and esterases, the higher activity on short-chain acyl esters of para-nitrophenol (*p*-NP) exhibited by esterases, suggesting that they may not recognize hydrophobic PET (Bornscheuer, 2002), which make the application of esterase for the degradation of PET difficult. As shown in Figure 2-5, 3-D structures of esterases in this study exhibited similar α -helix and β -pleated sheet structures to that of Est-119, thus, it is thought that the esterases from this study may possess the ability to degrade/assimilate PET as well. To confirm this hypothesis, however, further research is necessary.

Cloning and overexpression of annotated *est-H* and *est-L* will be attempted next and will be discussed in the next chapter.

CHAPTER 3

Recombinant Expression of Esterase Genes in *E. coli*

3.1 Introduction

Characterization of wild type esterase from strain *Roseateles depolymerans* strain TB-87 has been performed previously in this laboratory (Shah *et al.*, 2013b). However, information on the function of the esterase is still lacking. For further biochemical characterization studies, the acquisition of the purified protein in large scale is essential. Protein recombination is a method that allows a protein to be expressed in large scale by a suitable bacterial host for many purposes such as for biochemical characterization and for use in industrial processes, among others (Rosano and Ceccarelli, 2014). As mentioned in Chapter 1, *E. coli* is the most widely used organism for the production of recombinant proteins due to its many advantages such as unparallel fast growth kinetics, fast doubling time, easy-to-achieve high-density culture, and fast and easy transformation with exogenous DNA (Sezonov *et al.*, 2007). In this chapter, cloning of esterase genes as annotated in Chapter 2, into a pET vector and their transformation into *E. coli* host cells followed by overexpression of the genes in the same host will be discussed.

3.2 Materials and method

3.2.1 Bacterial strains, plasmids, and chemical reagents

E. coli BL21 (DE3) (*fhuA2 [lon] ompT gal (λ DE3) [dcm] ΔhsdS* λ DE3 = λ *sBamHI* Δ*EcoRI-B int::(lacI::PlacUV5::T7 gene1) i21 Δnin5*) and *E. coli* Lemo21 (DE3) (*fhuA2 [lon] ompT gal (λ DE3) [dcm] ΔhsdS/ pLemo(CamR)*; λ DE3 = λ *sBamHI* Δ*EcoRI-B int::(lacI::PlacUV5::T7 gene1) i21 Δnin5*; pLemo = pACYC184-*PrhaBAD-lysY*) were used as expression hosts. pET21b(+) (Merck KGaA, Darmstadt, Germany) plasmid was used for the construction of expression plasmid. Ampicillin was purchased from Meiji Seika Pharma Co., Ltd. (Tokyo, Japan). Isopropyl-β-D-thiogalactoside (IPTG) and chloramphenicol were purchased from Wako Pure Chemical Industries, Ltd. (Chuo, Osaka, Japan). Molecular mass marker and agarose were purchased from Nippon Gene Co., Ltd. (Toiya-machi, Toyama, Japan). Endonuclease restriction enzymes and ligation high kit were purchased from New England Biolabs (Massachusetts, USA) and Takara Bio Inc., (Shiga, Japan). Protein marker (Amersham Rainbow Molecular Weight Markers) was purchased from GE Healthcare Life

Sciences (Illinois, USA). *p*-nitrophenyl acetate was purchased from Sigma-Aldrich (St. Louis, Missouri, USA).

Unless mentioned otherwise, all reagents and chemicals were purchased from Wako Pure Chemical Industries, Ltd. and of analytical or molecular biology grade.

3.2.2 Construction of expression plasmid

Primers for the construction of expression plasmid in this study are shown in Table 3-1. Genomic DNA of strain TB-87 (100-250 ng per 50 μ L PCR reaction) was used as template DNA for amplification. PCR amplification reactions were performed in a GeneAtlas thermal cycler (Astec, Fukuoka, Japan), with the following conditions: pre-denaturation at 94°C for 5 min, 25 cycles of: denaturation at 94°C for 15 s, annealing at 60°C for 30 s, extension at 68°C for 1 min. After 25 cycles, the temperature was held at 68°C for 10 min. To generate N-terminal deleted pET21b, touchdown (TD) PCR method (Korbie and Mattick, 2008) was employed for the amplification of esterase genes.

The PCR products were electrophoretically resolved on a 1% agarose gel and visualized under Maestrogen UV transilluminator (Maestrogen Inc., Hsinchu, Taiwan). The PCR products were purified using a PCR purification kit (QIAGEN, Venlo, The Netherlands), digested with restriction endonucleases, and ligated into pET21b vector (Merck KgaA) according to the standard method (Green and Sambrook, 2012).

3.2.3 Transformation of pET21b plasmid bearing esterase genes into host cells

pET21b plasmid bearing cloned esterase gene was transformed into *E. coli* competent cells; BL21 (DE3) and Lemo21 (DE3) (New England Biolabs) according to the manufacturer's protocol, spread onto Luria-Bertani (LB) (BD-Difco, Sparks, Maryland, USA) agar plate supplemented with 100 μ g/mL ampicillin (BL21 (DE3)), and 100 μ g/mL ampicillin and 30 μ g/mL chloramphenicol (Lemo21 (DE3)), and incubated overnight at 37°C and 30°C. A clone containing the correct insert was identified by colony PCR using *Taq* DNA Polymerase (Takara Bio Inc.).

3.2.4 Overexpression of recombinant esterase in *E. coli*

3.2.4.1 Overexpression in *E. coli* BL21 (DE3)

A clone containing the correct insert as confirmed by colony PCR was picked up with sterile pipette tips and inoculated into a sterile test tube containing 5 mL of LB supplemented with ampicillin (100 μ g/mL) and were grown overnight at 37°C with shaking at 200 rpm. 1%

Table 3-1 Primers used for the construction of plasmids in this study.

Plasmid	Primer pair	Sequence (5' → 3')
pET- <i>estHF</i>	estHF-fNdeI	ATCAcatatgACGCTGTTGGCCG
	estHL-rSacI	TGATgagctcTCAGTAGGGGCAG
pET- <i>estLF</i>	estLF-fNdeI	ATCAcatatgACCCTCACCTCGAG
	estHL-rSacI	TGATgagctcTCAGTAGGGGCAG
pET- <i>estHM</i>	est-HM-EcoF	TTATgaattcGCAGCAGACCGGCCCCG
	est-HLM-XhoR	ATTctcgagGTAGGGGCAGTTCTGGC
pET- <i>estLM</i>	est-LM-EcoF	TTATgaattcGCAGCAGACCGGGGCCCCG
	est-HLM-XhoR	ATTctcgagGTAGGGGCAGTTCTGGC

Restriction sites recognized by the restriction enzymes NdeI, SacI, XhoI, and EcoRI are in lowercase.

of overnight culture were transferred into 500 mL flask containing 100 mL fresh LB medium and were grown at 37°C with shaking at 200 rpm until OD₆₀₀ reached 0.4-0.5. Protein expression was induced by adding 0.1 mM IPTG and further incubated at 37°C for 3 h. After induction, the cells were harvested by centrifugation at 8000 rpm at 4°C for 5 mins, washed with 20 mM potassium phosphate buffer (pH 7.0) and disrupted by sonication, to release the esterase.

3.2.4.2 Overexpression in *E. coli* Lemo21 (DE3)

A clone containing the correct insert as confirmed by colony PCR was picked up with sterile pipette tips and inoculated into a sterile test tube containing 5 mL of LB supplemented with ampicillin (100 µg/mL) and chloramphenicol (30 µg/mL) followed by overnight incubation at 37°C with shaking at 200 rpm. 1% of the overnight culture was inoculated into a test tube containing 10 mL of LB supplemented with ampicillin (100 µg/mL) and chloramphenicol (30 µg/mL) and incubated overnight with shaking at 37°C, 200 rpm until OD₆₀₀ reached 0.4-0.6. Protein expression was induced by adding 0.4 mM IPTG and further incubated at 37°C for 5 h. To examine different expression levels, L-rhamnose was added at varying concentrations (0-2000 µM). IPTG-induced empty pET21b was used as control. Following induction, the cells were harvested by centrifugation at 8000 rpm at 4°C for 5 mins, washed twice with 20 mM potassium phosphate buffer (pH 7.0), and disrupted using BugBuster protein extraction reagent (Merck KgaA, Darmstadt, Germany) according to the manufacturer's protocol, to release the esterase.

3.2.5 Molecular weight estimation of esterase

Proteins were separated by sodium dodecyl-polyacrylamide gel (SDS-PAGE) (12.5% resolving gel, 4.5% stacking gel) according to the method of Laemmli (1970) using Mini-Slab Size Electrophoresis System AE-6530 (ATTO, Tokyo, Japan). Samples from insoluble and soluble fractions were mixed with 2X Laemmli sample buffer in a 1:1 ratio, boiled for 2 minutes and cooled down. Samples (10 µL) were separated at a constant current of 20 mA. Following electrophoresis, gel staining was performed using Bio-Safe Coomassie G-250 Premixed Staining Solution (BioRad, California, USA) according to the manufacturer's protocol. The stained gel was dried at 65°C for 1 hour with AttoRapidry-Mini (ATTO, Tokyo, Japan). By comparing obtained protein bands with molecular weight marker (Amersham Rainbow Molecular Weight Markers; GE Healthcare Life Sciences, Illinois, USA), the molecular weight of proteins and degree of purification were confirmed.

3.2.6 On-column protein refolding

3.2.6.1 Solubilization and sample preparation

Est-HF and Est-LF (with putative signal peptide; full sequence) that were expressed as inclusion bodies were refolded *in vitro* by affinity chromatography using HisTALON Gravity Columns (Takara Bio Inc.). The pellets containing insoluble proteins were resuspended in solubilization buffer (50 mM Tris-HCl, 6 M guanidine hydrochloride, pH 8.0) and incubated overnight at 4°C. The cell debris and non-solubilized material were removed by centrifugation at 8000 rpm for 1 h. The supernatant was passed through a 0.45 µm filter prior to sample application onto HisTALON column.

3.2.6.2 Purification and refolding

The solubilized protein samples were loaded on the HisTALON column followed by washing with 10 mL 20 mM Tris-HCl, 0.5 M sodium chloride (NaCl), 5 mM imidazole, 6 M guanidine hydrochloride, 1 mM 2-mercaptoethanol, pH 8.0. The column was washed with 10 mL 20 mM Tris-HCl, 0.5 M NaCl, 20 mM imidazole, 1 mM 2-mercaptoethanol, 6 M urea, pH 8.0. Refolding of the bound protein was performed using a linear 6–0 M urea gradient, starting with the wash buffer above and finishing at one without urea, followed by washing with 5 mL of the buffer without urea. The refolded recombinant proteins were eluted with increasing imidazole concentration, starting from 50 mM and ended with 200 mM.

The refolding buffer was removed using PD-10 Desalting Column (GE Healthcare Bio-Sciences, Pittsburgh, Pennsylvania, USA) prior to analysis of folding yields.

3.2.7 Spectrophotometric enzyme assay

The presence of active esterase in the sample supernatant was determined according to the modified method of Kay *et al.* (1993), using *p*-nitrophenyl acetate as a substrate. 0.268 mL *p*-nitrophenyl acetate was mixed with 1.6 mL potassium phosphate buffer (0.1 M, pH 7.0). 0.132 mL enzyme sample was then added into the mix and the absorbance was measured at 405 nm. One unit was defined as the amount of enzyme required to liberate 1 µM of *p*-nitrophenol per min.

3.3 Results and discussion

3.3.1 Recombinant expression of esterase by deleting the N-terminal tag of pET21b

To date, Est-H and Est-L have failed to be expressed in soluble forms despite many attempts i.e. changing parameters such as induction temperature and time, changing host strains

and vectors, and expressing the protein *in vitro*, among others. In a study by Zhu *et al.* (2013), uridine phosphorylase was successfully expressed in soluble form in *E. coli* when it was expressed in its native form (i.e. expression without His-tag attached). When His-tag was fused at either N-terminal or C-terminal of a pET vector, uridine phosphorylase was expressed as inclusion bodies. Therefore, it was hypothesized that the presence of His-tag hinders proper protein folding resulting in the protein being expressed as inclusion bodies despite claims (Carson *et al.*, 2007; Kimple *et al.*, 2013) that fusion tags generally do not affect protein expression due to its small size.

pET21b plasmid, which has been well established for use in this laboratory, possesses two tags; T7-tag at the N-terminal and His-tag at the C-terminal of the plasmid. T7-tag is a short epitope tag (11 peptides) used for the detection of fusion proteins *in vitro* and in cell culture, while His-tag, or polyhistidine-tag, is an affinity tag widely used in protein purification (Kimple *et al.*, 2013). Since the presence of His-tag is essential to facilitate purification of the recombinant esterase, N-terminal T7-tag was deleted instead. This was also based on the assumption that since protein translation initiation occurs at the N-terminal, shall the presence of any tag hinder correct protein folding which in turn impair protein solubility, it will most likely occur at this region. The map of pET21b plasmid and the position of the tags are shown in Figure 3-1.

3.3.1.1 Verification of recombinant *E. coli* BL21 (DE3) bearing the pET-*estHF* and pET-*estLF* constructs

PCR primers for the amplification of *est-H* and *est-L* were designed to include sequences recognized by the restriction enzymes *NdeI* and *SacI* for the insertion into the same site on pET21b plasmid, generating construct devoid of any N-terminal tags. Based on the gene annotation results in Chapter 2, *est-H* and *est-L* consists of 1083 bp and 870 bp nucleotides, respectively. As shown in Figure 3-2A, PCR products at approximately 1100 and 900 bp were observed, which matched the predicted sizes of both genes. The purified PCR products were then digested with *NdeI* and *SacI*, ligated into pET21b followed by transformation into *E. coli* BL21 (DE3). Successfully transformed *E. coli* cells could grow on LB agar plate supplemented with 100 µg/mL ampicillin after overnight incubation at 37°C. Interestingly, this ability to grow on an antibiotic agar plate at 37°C, which was constantly observed in all cloning experiments prior to this experiment, diminished after the deletion of N-terminal tag of pET21b, thus sparked the hypothesis that *est-H* and *est-L* are toxic in their native forms. Although esterases

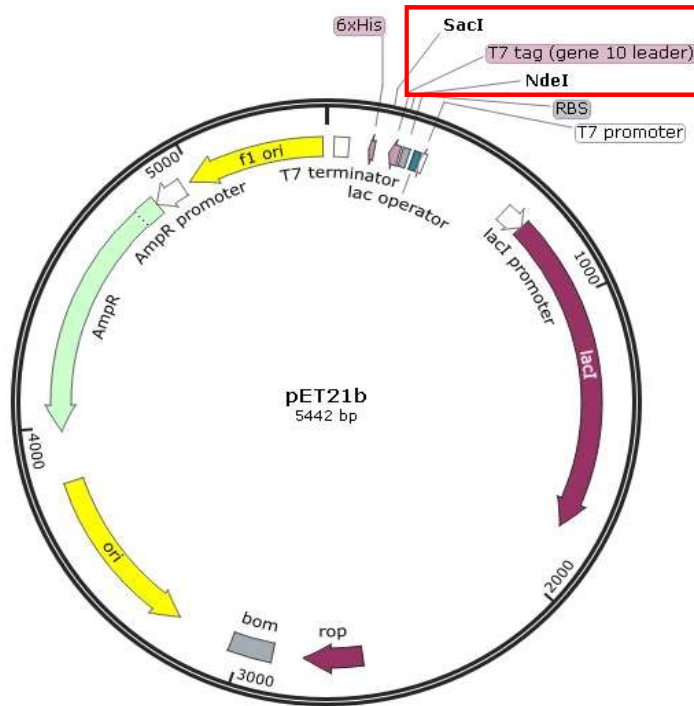
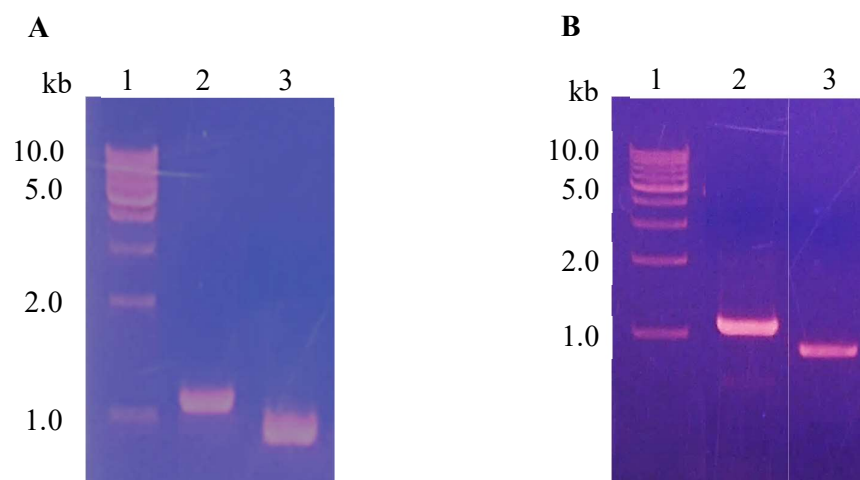


Figure 3-1 The genetic map of pET21b plasmid. The N-terminal T7 tag is located between *NdeI* and *SacI* restriction sites (red box). Linearization of pET21b at these sites would have caused the removal (i.e. deletion) of the tag, leaving only His-tag at the C-terminal.



Lane 1: Molecular mass marker

Lane 2: *est-H*

Lane 3: *est-L*

Figure 3-2 Amplification, digestion, and cloning of *est-H* and *est-L* into pET21b to generate plasmid pET-*estHF* and pET-*estLF*. DNA bands with molecular masses of approximately 1100 and 870 bp were observed for *est-H* and *est-L*, respectively. A. PCR amplified products; B. PCR amplified products using *est-H* and *est-L* ligated into pET21b as a template.

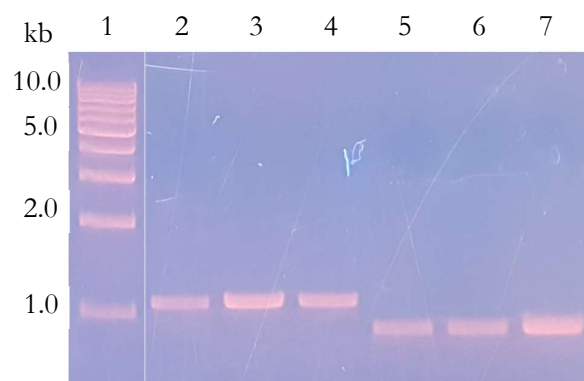
in this study were “not native” since the protein needs to be free of any tag at either terminal for them to be expressed in their native form as demonstrated by Zhu *et al.* (2013), this result seems to partially corroborate their results.

To confirm whether the lost ability to grow on an antibiotic agar plate at 37°C was because of the tag deletion instead of failed ligation, the successful insertion of esterase genes into pET21b were reconfirmed by PCR using ligated pET21b as a template. As shown in Figure 3-2B, PCR products of the same size as *est-H* and *est-L* were observed. Further, the transformed cultures were replated on the same antibiotic agar plate. For a toxic gene of interest, they can benefit from incubation at a lower temperature (25-30°C) (Hoseini and Sauer, 2015), thus the plates were incubated at 30°C for 24 h. Following 24 h of incubation, substantial colonies formation (>100 colonies) were observed on the agar plates. Six randomly picked colonies, three from each pET-*estHF*/*E. coli* BL21 and pET-*estLF*/*E. coli* BL21 plates, respectively, were subjected to colony PCR using primers listed in Table 3-1 and the results are shown in Figure 3-3. All tested clones produced PCR products with sizes matched those of *est-H* and *est-L*, thus confirming the earlier hypothesis that the inability of *est-H* and *est-L* to grow at 37°C was attributed to the toxicity of the genes.

Positive clones bearing the recombinant pET-*estHF* and pET-*estLF* plasmids were cultivated in LB liquid culture medium to be used for subsequent overexpression experiments.

3.3.1.2 Analysis of overexpressed recombinant Est-H and Est-L

The SDS-PAGE analysis of overexpressed Est-H and Est-L (Figure 3-4) revealed the presence of protein bands at approximately 29 kDa for both proteins in the insoluble fraction of the cells while no bands are visible in the soluble fractions, indicating insoluble expression of both proteins. However, the obtained molecular weight of both proteins was different than estimated; Est-H is estimated at 37 kDa while Est-L is at 31 kDa. The different-than-estimated molecular weight of proteins may be attributed to the gel shifting, which refers to the migration of proteins on SDS-PAGE that does not correlate with formula molecular weights. Rath *et al.* (2009) suggested that gel shifting appears to be common for some proteins such as membrane proteins, due to the aggregation of SDS molecules at hydrophobic protein residues, which transmembrane sequences of membrane proteins contain an abundance of (Imamura, 2006), resulting in an increase of the negative charge. As a result, the mobility of the protein in SDS-PAGE gel is increased, thus appearing to be smaller than expected. To confirm this hypothesis,

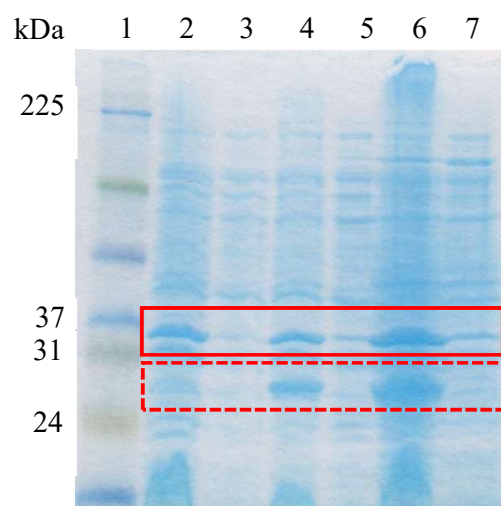


Lane 1: Molecular mass marker

Lane 2-4: Colony PCR of transformants bearing pET-*estHF*

Lane 5-7: Colony PCR of transformants bearing pET-*estLF*

Figure 3-3 PCR amplified products of six randomly picked colonies successfully grown on LB agar plates supplemented with 100 $\mu\text{g/mL}$ ampicillin after overnight incubation at 30°C. The colonies possibly bearing recombinant pET-*estHF* and pET-*estLF* were confirmed by colony PCR using corresponding primers listed in Table 3-1.



- Lane 1: Molecular weight marker
- Lane 2: Insoluble fraction of pET21b (control)
- Lane 3: Soluble fraction of pET21b (control)
- Lane 4: Insoluble fraction of Est-H
- Lane 5: Soluble fraction of Est-H
- Lane 6: Insoluble fraction of Est-L
- Lane 7: Soluble fraction of Est-L

Figure 3-4 SDS-PAGE profile of insoluble and soluble fraction of expressed Est-H and Est-L. SDS-PAGE was performed using 12.5% gel at a constant current 20 mA, and the proteins were CBB-stained.

similar *pET-estHF* and *pET-estLF* plasmids constructed previously in another study using primers listed in Table 3-1, were isolated for the transformation in *E. coli* Lemo21 (DE3).

Despite the non-soluble expression, the deletion of the N-terminal tag of pET21b has led both proteins to be successfully expressed in *E. coli*. Until now, all attempts to express esterase in its full form (with putative signal sequence) in *E. coli* have failed as no expression could be obtained.

3.3.2 Recombinant expression of esterase in *E. coli* Lemo21 (DE3)

Recombinant expression of esterase genes thus far has yet to produce soluble expression despite changing many conditions. The problems commonly associated with toxic proteins expressions such as the formation of inclusion bodies and plasmid instability (Dumon-Seignovert *et al.*, 2004) and decreased expression yields (Saïda, 2007), have been observed which lead to the assumption that the recombinant esterase is possibly toxic. When the proteins were expressed without any N-terminal tag, the recombinant colonies could no longer grow at 37°C, suggesting that *est-H* and *est-L* are toxics in their native form. Therefore, expression in *E. coli* Lemo21 (DE3) was attempted as this strain has been proven to successfully express many difficult and toxic proteins, membrane proteins as well as proteins prone to insoluble expression. Lemo21 (DE3) possesses a titratable rhamnose promoter, rhaBAD promoter (PrhaBAD), to allow for gradual gene expression. This restrained expression avoids saturation of the capacity of the machinery involved in the production of the protein which could cause misfolding and aggregation of proteins in the cytoplasm (Wagner *et al.*, 2007, 2008; Klepsch *et al.*, 2011; Schlegel *et al.*, 2012).

3.3.2.1 Verification of recombinant *E. coli* Lemo21 (DE3) bearing the pET-*estHF*, pET-*estLF*, pET-*estHM* and pET-*estLM*

As mentioned in Section 3.3.1.2, the smaller-than-estimated molecular mass of the protein may be due to SDS binding behavior with the protein, thus affecting its migration behavior on the SDS-PAGE gel. To confirm whether this behavior was indeed because of the hydrophobic amino acid residues as per discussed earlier, similarly constructed plasmids from other unpublished study were isolated from their respective host cells and transformed into Lemo21 (DE3). On the other hand, overexpression in BL21 (DE3) produced insoluble proteins, probably due to the presence of a native signal sequence of Est-H and Est-L. Yazdani and Mukherjee (1998) suggested that a non-*E. coli* signal peptide may lead to the low expression

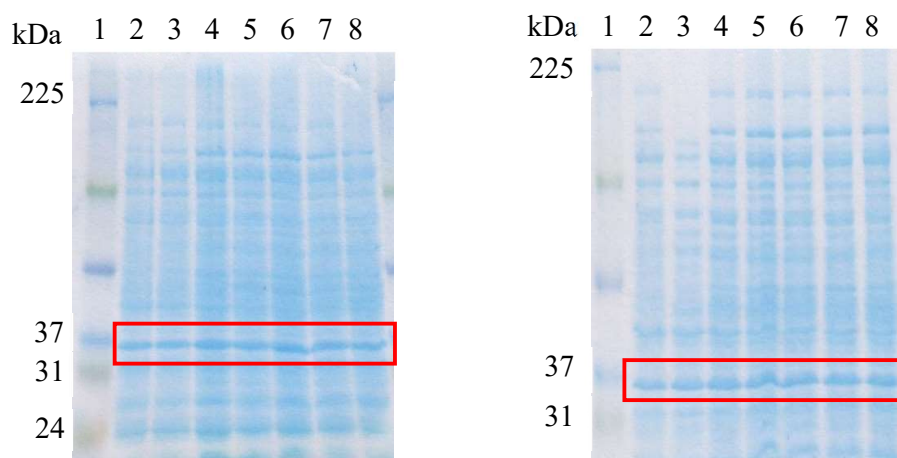
levels of the recombinant protein; therefore new constructs devoid of their signal sequences; Est-HM and Est-LM, were developed.

As discussed in Chapter 2, signal sequences for Est-H and Est-L were determined to be a 60-amino acid and 31-amino acid sequences, respectively, at its N-terminus. The plasmids with the genes devoid of these signal sequences (*pET-estHM*, *pET-estLM*) that were previously constructed in another study using primers listed in Table 3-1, were transformed into Lemo21 (DE3). Positive clones confirmed by colony PCR were isolated for subsequent overexpression experiments.

3.3.2.2 Analysis of overexpressed recombinant Est-HF, Est-LF, Est-HM, and Est-LM in Lemo21 (DE3)

To elucidate the functions of genes encoding for Est-H and Est-L, *est-H* and *est-L* were cloned into the pET21b vector and transformed into *E. coli* Lemo21 (DE3) cells. To investigate the influence of signal sequence on protein solubility, Est-H and Est-L were expressed with and without their putative signal sequence, designated as Est-HF and Est-LF (with putative signal peptide; full sequence/premature), and Est-HM and Est-LM (without putative signal peptide; mature), respectively. The signal sequence of a newly expressed secretory protein, recognized by the cell machinery, directs the protein to the bacterial periplasm, where the sequence is removed by a signal peptidase (Singh *et al.*, 2013). A constant oxidizing environment of the periplasm allows correct folding of the protein prior to signal sequence cleavage followed by secretion into the extracellular environment (Karkhane *et al.*, 2012). Although the presence of native signal sequence is preferable since it allows for periplasm localization thus aids in the correct folding of a protein, few studies suggested that the presence of native signal peptide of a protein is substantially less stable and more aggregation-prone than the corresponding mature protein (Krishnan *et al.*, 2009; Kulothungan *et al.*, 2009). As the expression of Est-H and Est-L with their putative signal sequence attached were unsuccessful, the expression without the signal sequences was then attempted.

SDS-PAGE analysis of both insoluble and soluble fraction of Est-HF, Est-LF, Est-HM, and Est-LM, revealed the presence of proteins with molecular weight (MW) of approximately 37 kDa in all samples (solid box), including control sample (empty pET21b; Figure 3-5), regardless of L-rhamnose concentrations added. This protein is possibly a pET-derived protein. All protein bands at their approximate sizes were observed in insoluble fractions, suggesting non-soluble expressions of Est-H and Est-L. The constant reducing environment in the cell cytoplasm prevents the correct folding of the newly expressed protein, therefore most proteins



Lane 1: Molecular weight marker

Lane 2: 0 μ M L-rhamnose

Lane 3: 100 μ M L-rhamnose

Lane 4: 250 μ M L-rhamnose

Lane 5: 500 μ M L-rhamnose

Lane 6: 750 μ M L-rhamnose

Lane 7: 1000 μ M L-rhamnose

Lane 8: 2000 μ M L-rhamnose

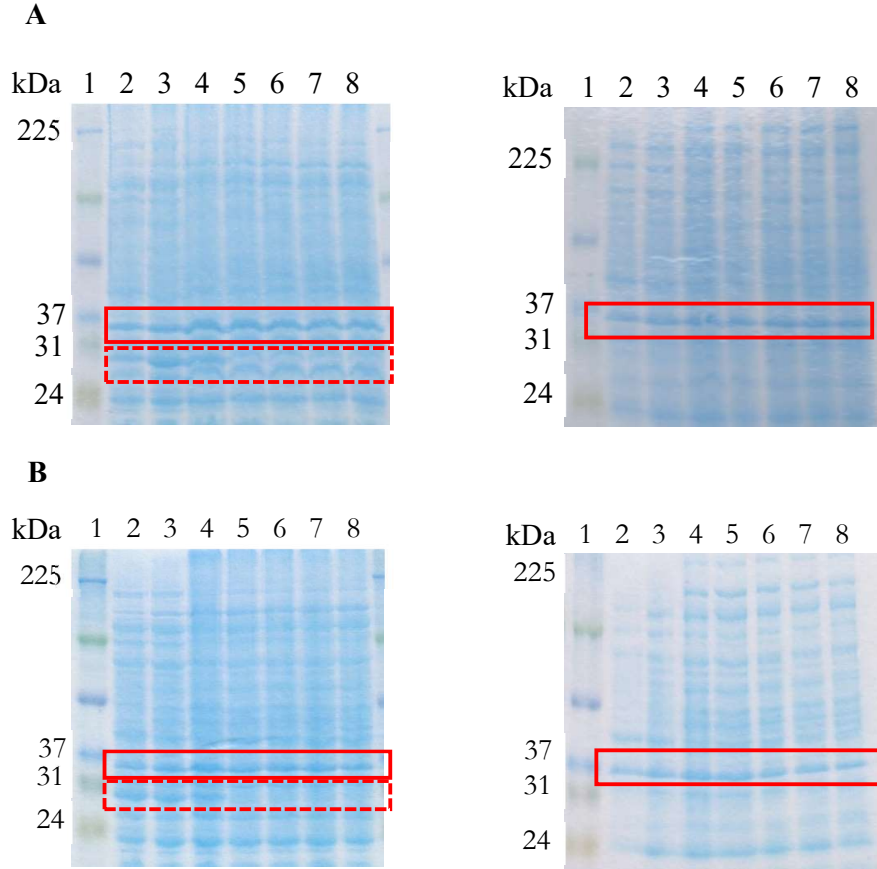
Figure 3-5 SDS-PAGE profile of (left) insoluble fraction and (right) soluble fraction of empty pET21b (without cloned esterase gene) as a control after induction with 0.4 mM IPTG. pET21b was subjected to the same expression experiment as Est-H and Est-L. SDS-PAGE was performed using 12.5% gel at a constant current 20 mA, and the proteins were CBB-stained.

destined for the secretory pathway are usually transported to the periplasm for signal sequence cleavage and proper folding prior to the secretion. However, the results obtained suggest that the localization of Est-H and Est-L may not be the determining factor for the incorrect folding of both proteins. Unfortunately, no data is available to support this hypothesis.

Protein bands with a molecular weight of approximately 30 kDa were observed in the SDS-PAGE gels of both Est-HF and Est-HM (Figure 3-6). A 30 kDa protein band was observed in the insoluble fraction of Est-HF (dotted box) (Figure 3-6A) which matched the size of Est-HM's protein band (Figure 3-6B). While Est-HM's band obtained was as per estimated (30 kDa), the size for Est-HF was incorrect (estimated at 37 kDa). The same migration behavior was exhibited by both Est-HF's construct, which in agreement with the hypothesis discussed earlier in Section 3.3.1.2.

Expression of Est-LF and Est-LM yielded proteins with a molecular weight of approximately 30 kDa and 27 kDa, respectively. Both bands matched their predicted sizes. Two Est-LF protein bands were observed at 30 kDa and 27 kDa with the addition of 250 μ M L-rhamnose (Figure 3-7A, Lane 4), which match the sizes of both Est-LF and Est-LM. It is possible that at this concentration, Est-L exists in both premature and mature forms, signifying the signal peptide cleavage by the Lemo21 (DE3) translational machinery to yield a mature protein. The expression band intensities for all proteins decreased with increasing L-rhamnose concentration; darker bands observed for 0-250 μ M L-rhamnose, which decreased as the L-rhamnose concentration was increased to 500-2000 μ M, suggesting that expression of all proteins was enhanced at low L-rhamnose concentration. The level of lysozyme (lysY), the natural inhibitor of T7 RNA polymerase modulated by L-rhamnose. For difficult soluble proteins, tuning the expression level by varying the level of lysozyme, may also result in more soluble and properly folded protein (Schlegel *et al.*, 2012). Spectrophotometric enzyme activity assay (A_{405}) using supernatant samples and *p*-nitrophenyl acetate as the substrate, detected no esterase activity (data not shown). Moreover, the addition of L-rhamnose did not seem to affect expression as the proteins were still expressed insolubly.

As discussed in Chapter 2, Est-H and Est-Ch are possibly expressed polycistronically. Although the cause of the lack of soluble expression of Est-L could not be identified, the absence of *est-Ch* during the expression of Est-H is probably the cause for insoluble expression of Est-H. Many studies have reported on the inability of the lipase-encoding genes to be expressed in their active and soluble forms when expressed without their "lipase activator" (Hobson *et al.*, 1993; Sullivan *et al.*, 1999; Su *et al.*, 2004).



Lane 1: Molecular weight marker

Lane 2: 0 μM L-rhamnose

Lane 3: 100 μM L-rhamnose

Lane 4: 250 μM L-rhamnose

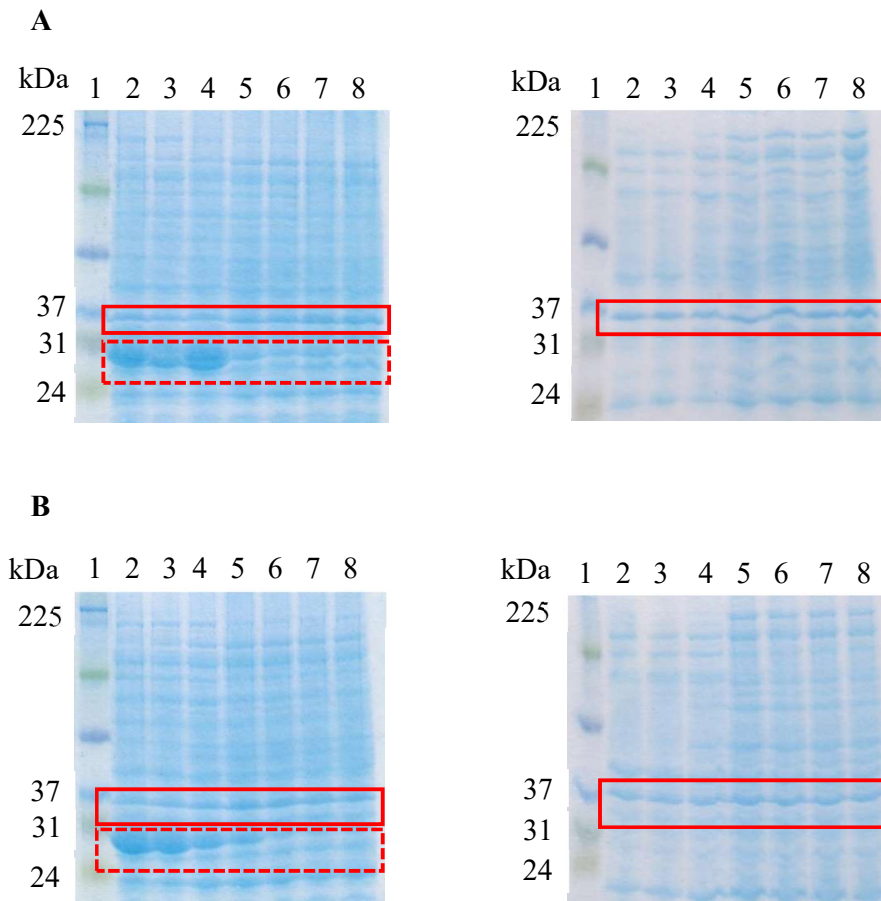
Lane 5: 500 μM L-rhamnose

Lane 6: 750 μM L-rhamnose

Lane 7: 1000 μM L-rhamnose

Lane 8: 2000 μM L-rhamnose

Figure 3-6 SDS-PAGE profile of (left) insoluble fraction and (right) soluble fraction of expressed crude Est-H with and without its putative signal peptide after induction with 0.4 mM IPTG. Level of expression was investigated by adding a varied concentration of L-rhamnose (0-2000 μM). SDS-PAGE was performed using 12.5% gel at a constant current 20 mA, and the proteins were CBB-stained. A. Est-HF (with putative signal peptide; full sequence); B. Est-HM (without putative signal peptide; mature).



Lane 1: Molecular weight marker

Lane 2: 0 μ M L-rhamnose

Lane 3: 100 μ M L-rhamnose

Lane 4: 250 μ M L-rhamnose

Lane 5: 500 μ M L-rhamnose

Lane 6: 750 μ M L-rhamnose

Lane 7: 1000 μ M L-rhamnose

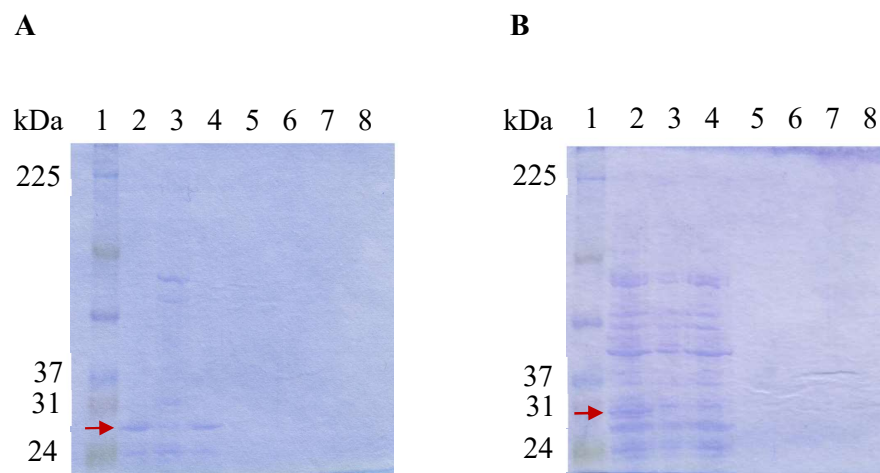
Lane 8: 2000 μ M L-rhamnose

Figure 3-7 SDS-PAGE profile of (left) insoluble fraction and (right) soluble fraction of expressed crude Est-L with and without its putative signal peptide. Level of expression was investigated by adding a varied concentration of L-rhamnose (0-2000 μ M). SDS-PAGE was performed using 12.5% gel at a constant current 20 mA, and the proteins were CBB-stained. A. Est-LF (with putative signal peptide; full sequence); B. Est-LM (without putative signal peptide; mature).

3.3.3 On-column refolding of insoluble esterase

As insoluble proteins were still expressed after many attempts of varying growth conditions and parameters, *in vitro* refolding of expressed proteins aggregated into inclusion bodies were performed. The refolding was performed simultaneously with purification; specifically, affinity column purification, termed on-column refolding. Refolding of insoluble recombinant proteins could employ conventional methods such as slow dialysis or dilution into a buffer of near-neutral pH. Purification and refolding in a single chromatographic step are possible due to the presence of affinity tag i.e. His-tag. The binding of the histidine to immobilized divalent metal ions can take place in the presence of a high concentration of chaotropic agent (such as urea or guanidine hydrochloride), therefore, His-tagged inclusion body protein can be solubilized by chaotropic extraction followed by direct bound to an affinity matrix (Hoess *et al.*, 1988; Werner *et al.*, 1994).

SDS-PAGE profile of all collected fractions during on-column refolding under denaturing condition (Figure 3-8) showed opposing behavior exhibited by Est-H and Est-L during refolding. The presence of Est-H protein bands in the sample and wash flow-through fraction (Figure 3-8A) suggesting protein's inability to binding to the column resin, while the absence of Est-L protein band in all fractions (Figure 3-8B) indicating strong binding of the protein to the column resin. The cause for this may be attributed to the protein aggregation. In the case of Est-H, the protein aggregate prior to sample loading onto the column, causing the protein passing through the column unable to bind the column resin, while the protein aggregate in the column in the case of Est-L, unable to be eluted out with imidazole. This could happen when the pH of the solubilized protein is very near to the theoretical isoelectric point (pI) value of the protein. Est-L has a theoretical pI value of approximately 9.7. Although protein aggregation should not be a concern during Est-L's refolding as the pH of all buffers used for solubilization and refolding was set at pH 8.0, which was more than 1.5 lower than Est-L's theoretical pI value, it is not unlikely that the protein aggregated in the column for various other unknown factors. It was suggested that the addition of salt (NaCl), although could help to keep proteins soluble, is not favorable for the refolding of some proteins i.e. membrane proteins and proteins having abundance of hydrophobic residues; due to the hydrophobic chains being clustered upon being exposed to salt ions, resulting in aggregation (Song, 2009). However, when the buffers were replaced with those without NaCl, a similar result was observed (data not shown). Protein elution by pH changing was also attempted to no avail. The exact reason for the failed refolding remains unclear.



Lane 1: Molecular weight marker
 Lane 2: Solubilized protein (before refolding)
 Lane 3: Sample flow through
 Lane 4: Wash flow through
 Lane 5: Eluate (20 mM imidazole)
 Lane 6: Eluate (50 mM imidazole)
 Lane 7: Eluate (100 mM imidazole)
 Lane 8: Eluate (200 mM imidazole)

Figure 3-8 SDS-PAGE profile of collected fractions during on-column refolding of Est-H and Est-L using HisTALON Gravity Column. The purified and refolded proteins were eluted with increasing imidazole concentration (50-200 mM). Red arrows indicate estimated molecular weight for each protein. SDS-PAGE was performed using 12.5% gel at a constant current 20 mA, and the proteins were CBB-stained. A. Est-H; B. Est-L.

3.3.4 Measurement of active esterase activity

Eluted samples were measured spectrophotometrically for the presence of active esterase following on-column refolding using *p*-nitrophenyl acetate as the substrate. The presence of active esterase is measured by measuring the intensity of the yellow color of *p*-nitrophenol, released as a result of ester bond hydrolysis of *p*-nitrophenyl acetate; the intensity of the yellow color is directly related to the amount of active esterase in the sample. As many attempts to elute the proteins out the column have failed, no esterase activity can be detected in the samples (data not shown).

3.4 Conclusion

Many attempts to obtain soluble expression of Est-H and Est-L have failed previously. Although some insoluble expression of the enzymes was observed in the past, the results could not be replicated despite using the same constructed plasmid, which indicated possible gene toxicity. To test the hypothesis, the enzymes were expressed in their native forms. This was achieved by employing the plasmid devoid of any tags at the N-terminal. As predicted, the ability of the clones to grow on antibiotic agar plates at 37°C diminished following the tag deletion, which confirmed the earlier hypothesis, therefore, *E. coli* Lemo21 (DE3) was chosen as the host cells for subsequent overexpression experiments.

Overexpression of Est-H and Est-L in Lemo21 (DE3) with and without their putative signal peptides, designated as Est-HF and Est-LF, and Est-HM and Est-LM, respectively, were attempted to obtain soluble expression. Protein bands with a molecular weight of approximately 30 kDa, were observed in the SDS-PAGE gels of both Est-HF and Est-HM. Expression of Est-LF, and Est-LM, however, yielded proteins with a molecular weight of approximately 30 kDa and 27 kDa, respectively, which matched their predicted sizes. Interestingly, with the addition of 250 μ M L-rhamnose, two Est-L protein bands were observed at 30 kDa and 27 kDa, which matched the sizes of both Est-LF and Est-LM, suggesting the occurrence of signal peptide cleavage by the Lemo21 (DE3) translational machinery to yield a mature protein. The addition of L-rhamnose, although showed no effect to the soluble expression of both proteins, enhanced the expression when added at the low concentration (0-250 μ M). The spectrophotometric enzyme activity assay of the sample supernatant using *p*-nitrophenyl acetate as the substrate, detected no esterase activity.

Successful expression of Est-HM, Est-LF, and Est-LM in Lemo21 (DE3) seems to confirm the earlier hypothesis that the native esterase is possibly toxic, which may explain all

problems associated with toxic protein encountered thus far. Despite the incorrect size of Est-HF and insoluble expression of Est-HM, Est-LF and Est-LM obtained, expression in Lemo21 (DE3) seems promising for the future expression experiments.

Further, insoluble Est-H and Est-L were refolded *in vitro* using immobilized metal affinity column chromatography (IMAC). Simultaneous refolding and purification of the proteins are achieved as the proteins pass through the column, however, both Est-H and Est-L could not be retrieved after purification and refolding, suggesting possible aggregation before and during refolding step. Many attempts to elute the proteins out the column have failed; thus, no esterase activity was detected during spectrophotometric enzyme assay.

Overall, although the expression and refolding of Est-H and Est-L reported in this chapter were unsatisfactory, the characteristic and behavior of the proteins have been made clear, which will be useful to design future strategies when dealing with these proteins.

Gene annotation data presented in Chapter 2 revealed the presence of *est-Ch* in the intergenic region of *est-H* and *est-L*, and that *est-H* and *est-Ch* are possibly co-expressed *in vivo*, thus, the next attempt to investigate the roles of *est-Ch* in the soluble expression of either *est-H* and/or *est-L* shall take into consideration the deletion as well as the co-expression of the genes. This will be explored and discussed further in the next chapter.

CHAPTER 4

Disruption of Esterase-encoding Genes of *R. depolymerans* Strain TB-87

4.1 Introduction

Gene annotation of the esterase-encoding region of *R. depolymerans* strain TB-87 comprised of a cluster of gene consisting of *est-H*, *est-Ch*, and *est-L*. The different strategies adopted to obtain (soluble) expression of the genes as discussed in the previous chapter have failed to produce the soluble enzyme. This has made further downstream studies impossible as no active enzyme could be obtained. The difficulty of getting the enzymes express, particularly that of *est-H*, is probably because the N-terminal region of *est-H* was not sequenced. As attempts to sequence this region previously had failed due to the blocked N-terminus, the exact location of the translation initiation codon or ORF of *est-H* is unknown. Since all primers in this study were designed according to the gene annotation data, it is not unlikely that the failed expression was because internal methionine codons were mistaken for start codons (Guigó *et al.*, 1992) and that there was a different ORF of *est-H* than that proposed in Chapter 2. In addition, few studies suggested on the possibility of alternative start codons in prokaryotes (Panicker *et al.*, 2015; Tripp *et al.*, 2015; Belinky *et al.*, 2017; Omasits *et al.*, 2017). Although there is no data available from this study to support this theory, the occurrence of alternative start codon is not unlikely. Nevertheless, to elucidate the functions of the esterase gene cluster annotated in Chapter 2, the entire esterase gene cluster was disrupted by homologous recombination using antibiotic cassette and the results are presented in this chapter.

4.2 Materials and method

4.2.1 Bacterial strains, plasmids, and chemical reagents

E. coli HST08 (F^- , *endA1*, *supE44*, *thi-1*, *recA1*, *relA1*, *gyrA96*, *phoA*, $\text{Fai80d } lacZ$ Derutaemu15, $\Delta(lacZYA-argF)$ U169, $\Delta(mrr-hsdRMS-mcrBC)$, $\Delta mcrA$, λ (Takara Bio Inc.), *E. coli* JM109 (*recA1*, *endA1*, *gyrA96*, *thi-1*, *hsdR17* ($r_{\kappa^- m \kappa^+}$), *e14^-* (*mcrA^-*), *supE44*, *relA1*, $\Delta(lac-proAB)/F'[traD36, proAB^+, lacI^q, lacZ \Delta M15]$) (Takara Bio Inc.) and *E. coli* S17-1 (F^- , *thi*, *pro*, *hsdR*, [RP4-2 Tc::Mu Km::Tn7

(*Tp Sm*)] (ATCC) were used as transformation hosts. pUC19 (Takara Bio Inc.) and pGMS1 (laboratory stock collection) plasmids was used for the construction of cloning plasmid.

PBSA (Bionolle® #3020; MW = 1.4×10^5) were supplied by Showa Denko K.K. (Minato, Tokyo, Japan). Ampicillin was purchased from Meiji Seika Pharma Co., Ltd. (Chuo, Tokyo, Japan). Molecular mass marker and agarose were purchased from Nippon Gene Co., Ltd. (Toiya-machi, Toyama, Japan). Kanamycin and gentamicin were purchased from Wako Pure Chemical Industries, Ltd. (Chuo, Osaka, Japan).

Unless mentioned otherwise, all reagents and chemicals were purchased from Wako Pure Chemical Industries, Ltd. and of analytical or molecular biology grade.

4.2.2 Growth medium and culture conditions

R. depolymerans strain TB-87 and derived mutant strains were cultivated at 30°C and 200 rpm in liquid nutrient agar containing 0.2% (w/v) PBSA emulsion (Showa Denko K.K.). *E. coli* strains were grown in Luria Bertani (LB) broth at 37°C supplemented with appropriate antibiotics. For growth on solid medium, 1.5% (w/v) agar was added. Sucrose sensitivity of TB-87 mutant strains was tested on nutrient agar supplemented with 10% (w/v) sucrose.

4.2.3 Template DNA preparation, primers, and PCR conditions

Total DNA extracted from *R. depolymerans* strain TB-87 using the Wizard Genomic DNA Purification Kit (Promega, WI, USA) served as the template for esterase gene amplification (10 ng per 20 µL PCR reaction). DNA purification (QIAGEN, Venlo, The Netherlands), transformation, and electrophoresis were performed according to a standard method (Green and Sambrook, 2012). An in-fusion cloning method using the In-Fusion HD Cloning Kit (Clontech, Takara Bio Inc., Shiga, Japan) was used for all ligation steps in this study, thus all primers were designed to include a 15 bp sequence homologous to the cloning plasmid. PrimeSTAR GXL DNA Polymerase (Takara Bio Inc.) was used for PCR according to the manufacturer's protocol. Forward and reverse primers for the amplification of the esterase gene region were designed to amplify the *est-H-est-Ch-est-L* gene cluster flanked by a 500 bp sequence homologous to the genome of strain TB-87 (homology arm) on either side of the cluster, to allow for homologous recombination with wild type TB-87 (wt-TB-87). All primers used for PCR amplification and plasmid linearization are detailed in Table 4-1. PCR amplification reactions were performed using a GeneATLAS thermal cycler (Astec Co., Ltd., Fukuoka, Japan), with the following conditions: 30 cycles of denaturation at 98°C for 10 s,

Table 4-1 Primers used for the construction of plasmids in this study.

Primer	Sequence (5'→ 3')	Description
est region-pUC19_fwd	CGACTCTAGAGGATCCGCCAGGTTGCGGGAATG	Amplification of esterase gene region
est region-pUC19_rev	CGGTACCCGGGGATCATGCAGGCAGACG	
est region-inverse pUC19_fwd	CCATGGCTAATTCCCAGCCAGACCG	Linearization of pUC19 bearing the esterase gene region for insertion of the kanamycin cassette
est region-inverse pUC19_rev	GCAGCTCCAGCCTACACACCGGCGTGTACCGATGCGC	
Km cassette-pUC19_fwd	TGTGTAGGCTGGAGCTGC	Amplification of the kanamycin cassette for in-fusion cloning into linearized pUC19
Km cassette-pUC19_rev	TGGGAATTAGCCATGGTC	
est region-pGMS1_fwd	CTCTAGAGGATCCCCCGCCAGGTTGCGGGATGGCA	Amplification of the kanamycin cassette inserted-esterase gene region for in-fusion cloning into pGMS1
est region-pGMS1_rev	TCGAGCTCGGTACCCATGCAGGCAGACG	

The esterase gene region (est region) refers to the *est-H-est-Ch-est-L* gene cluster flanked by a 500 bp sequence homologous to the genome sequence of wt-TB-87 at either side of the cluster.

annealing at 60°C for 15 s, and extension at 68°C (1 kb/min). After the 30 cycles, the temperature was held at 4°C until the reactions were removed from the thermal cycler.

4.2.4 Gene deletion of the entire esterase gene region

Primers est region-pUC19_fwd and est region-pUC19_rev were used to amplify the esterase gene region. The amplified fragment was purified and ligated into the linearized pUC19 vector at the *Bam*HI site (Clontech, Takara Bio Inc). The plasmid (est region- pUC19) was transformed into *Escherichia coli* HST08 (Takara Bio Inc.) for conventional blue-white selection. Positive clones (white colonies containing the plasmid) were confirmed by colony PCR using the EmeraldAmp PCR Master Mix (Takara Bio Inc.) and the plasmid was extracted using the QIAprep Spin Miniprep Kit (QIAGEN); the plasmid was then used as the template (1 ng per 20 µL PCR reaction) for plasmid linearization by PCR with primers est region-inverse pUC19_fwd and est region-inverse pUC19_rev. The kanamycin cassette was amplified, purified, and ligated into the purified linearized est region-pUC19 plasmid and then transformed into *E. coli* JM109 competent cells (New England BioLabs, MA, USA), plated on Luria-Bertani (LB) agar plates supplemented with 100 µg/mL ampicillin and 50 µg/mL kanamycin, and incubated overnight at 37°C. The resulting plasmid was extracted from a positive clone (confirmed by colony PCR) and used as the template for amplification using primers est region-pGMS1_fwd and est region-pGMS1_rev. The resulting fragment was purified and ligated into pGMS1 (laboratory stock collection) and the plasmid was transformed into *E. coli* JM109, plated on LB agar plates supplemented with 50 µg/mL kanamycin and 10 µg/mL gentamicin, and incubated overnight at 37°C. Positive clones harboring plasmids bearing knocked-out esterase genes were confirmed by colony PCR.

4.2.5 Bacterial conjugation between *E. coli* S17-1 with wild type strain TB-87

Following confirmation by colony PCR, the plasmid was extracted, purified, transformed into *E. coli* S17-1 (laboratory stock collection), and introduced into *R. depolymerans* strain TB-87 by conjugation. Colonies of both wild type TB-87 and *E. coli* S17-1 strains were harvested from the nutrient agar plates supplemented with appropriate antibiotics and grown overnight at 37°C in 20 mL NB medium supplemented with 0.2% PBSA emulsion and 20 mL LB medium supplemented with kanamycin (50 µg/mL) and gentamicin (10 µg/mL), respectively, followed by subculturing into the same medium *sans* the antibiotics, until OD₆₀₀ reached 0.4-0.9. Aliquots of 10 mL of both strains were mixed together and filtered through a 0.45 µm membrane. The membrane filter was picked up with sterile forceps, overlaid on a nutrient agar

plate and incubated overnight at 30°C, followed by suspension in 20 mL saline water (0.85%). 100 µL of the suspension were plated on nutrient agar supplemented with either 50 µg/mL kanamycin, 1% PBSA emulsion, or both kanamycin and PBSA emulsion, and incubated at 30°C for 48 h. Δest -TB-87 mutants, in which the esterase gene-region was knocked-out, were selected based on growth without the formation of a clear zone on PBSA-emulsified nutrient agar plates supplemented with 50 µg/mL kanamycin, 10 µg/mL gentamicin, and 10% sucrose and then further confirmed by colony PCR.

The general workflow of targeted gene disruption experiments is summarized in Figure 4-1.

4.3 Results and discussion

4.3.1 Construction of plasmids for the conjugation with wild type strain TB-87

4.3.1.1 PCR amplification and cloning of the esterase gene region into pUC19

The results for the construction of pUC19 plasmid carrying the esterase gene cluster for the transformation into *E. coli* HST08 is shown in Figure 4-2. Esterase gene region consisting of *est-H-est-Ch-est-L* genes cluster as annotated in Chapter 2, and two 500 bp sequence homologous to the genome sequence (homology arm) of wild type TB-87 (wt-TB-87), were amplified using TB-87 genome as the template (Figure 4-2A). The PCR amplified product obtained matched the size of the entire esterase gene cluster (approximately 2.7 kb) and 1.0 kb of homology arm (Figure 4-2B). The amplified product produced smear on agarose gel probably due to the use of whole-genome of TB-87 as a template. The primers may anneal unspecifically with other places on the genome causing smeared product. Nevertheless, the DNA band was excised off the gel and was purified with gel extraction kit prior to transformation into *E. coli* HST08 for the conventional blue/white screening. Following overnight incubation at 37°C, the colonies growth was observed on the selection plate (Figure 4-2C). Colony PCR performed on three randomly selected white colonies yield products with an approximate size of 3.5 kb as expected. The confirmed positive clone was cultivated in LB medium to isolate the plasmid to serve as a template for plasmid linearization by PCR.

4.3.1.1 Insertion of kanamycin cassette at the *est-H-est-Ch-est-L* genes cluster's site

pUC19 bearing the esterase gene cluster flanked by two 500 bp homology arm was isolated from 5 mL overnight culture and used as the template for plasmid linearization by inverse PCR. The amplified region and starting point for the plasmid linearization is shown in

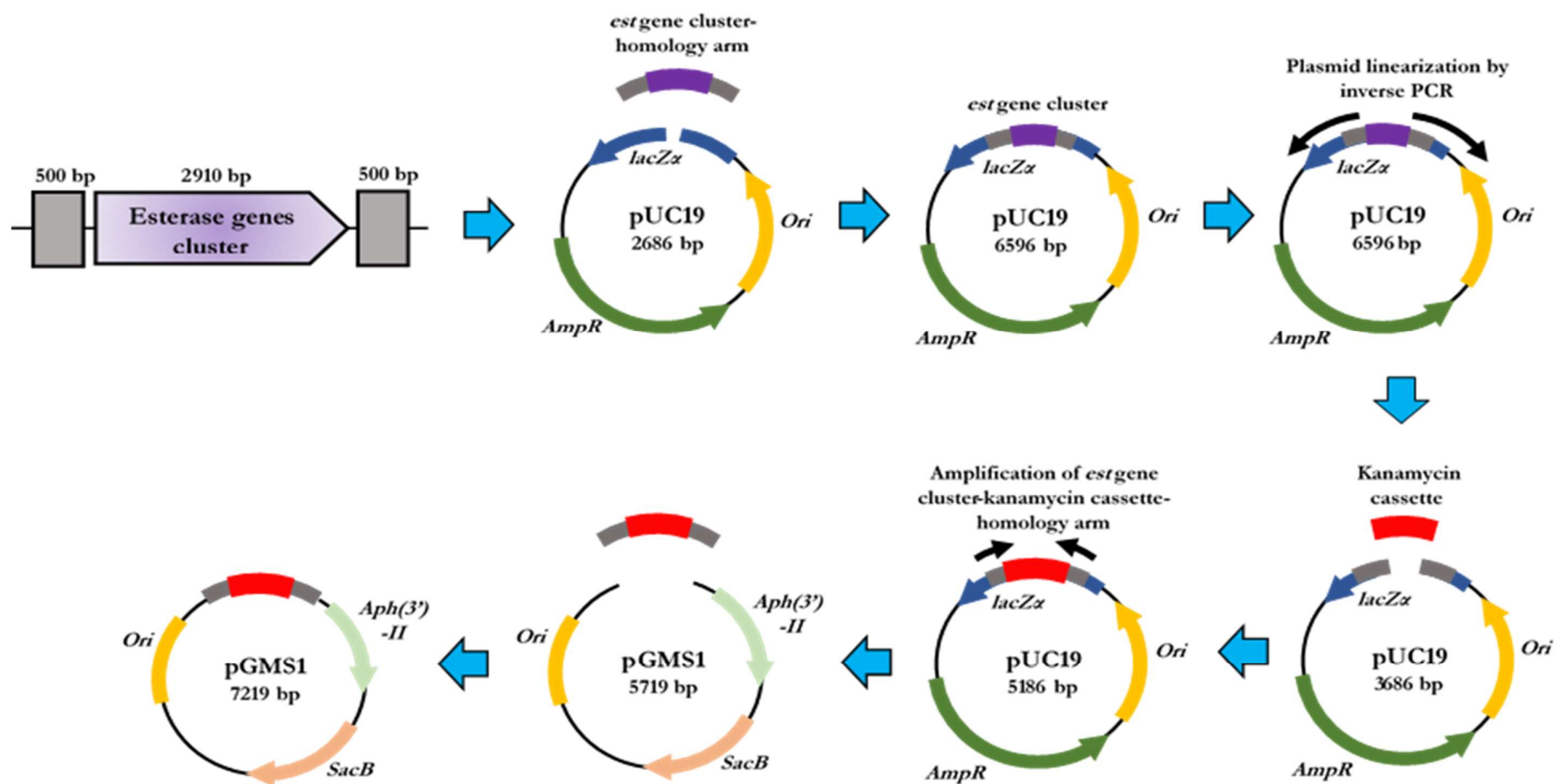
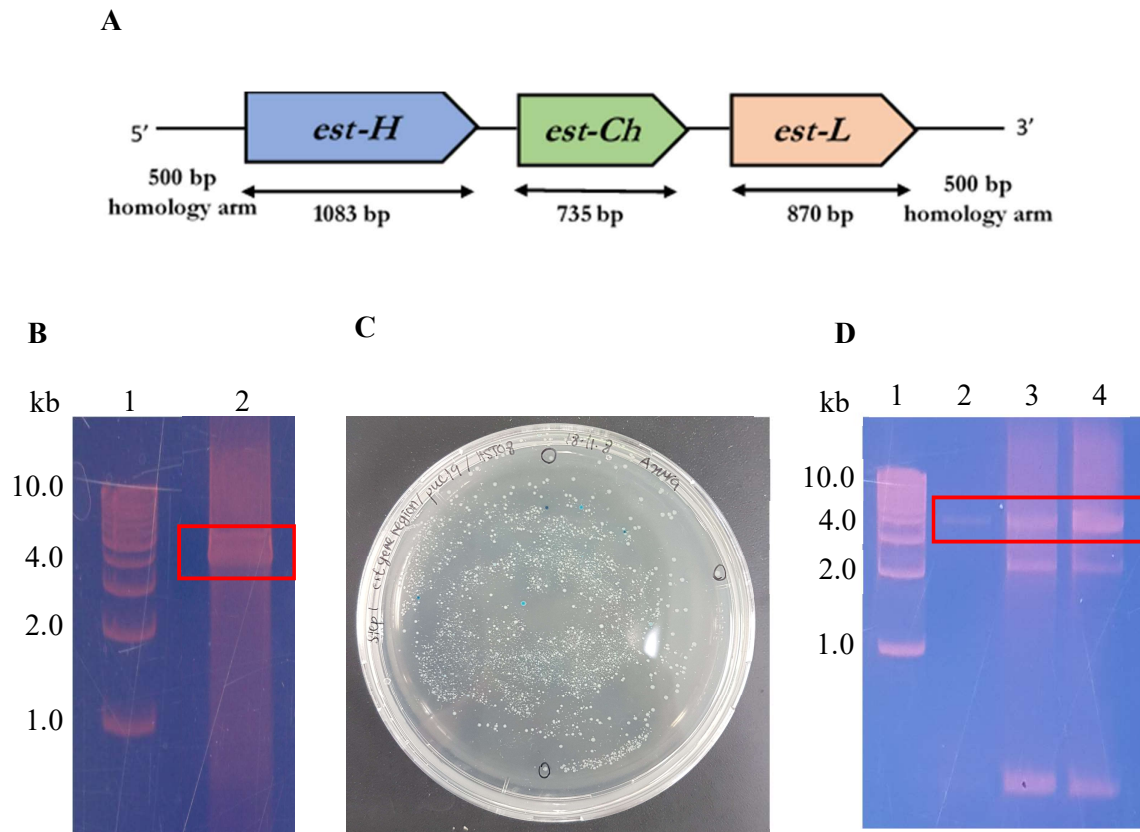


Figure 4-1 General workflow of the targeted disruption of the entire esterase gene region using kanamycin antibiotic cassette. Linearization of plasmids *pUC19* and *pGMS1* were performed at *Bam*HI and *Sma*I, respectively. 3-step PCR for the amplification of the esterase gene clusters used primers as listed in Table 4-1.



Lane 1: Molecular mass marker

Figure B, Lane 2: PCR product amplification of the esterase gene region

Figure D, Lane 2-4: Colony PCR product amplification

Figure 4-2 Amplification of esterase gene region for the cloning into pUC19 and transformation into *E. coli* HST08. A. Esterase gene region consisting of *est-H*-*est-Ch*-*est-L* genes cluster (total size of approximately 2.7 kb) flanked by two 500 bp homology arm; B. PCR product amplification of esterase gene region using wt-TB-87's genome as the template; C. Colonies growth on an LB agar plate supplemented with 100 µg/mL ampicillin; D. Colony PCR of three randomly selected colonies grown on LB agar plate supplemented with 100 µg/mL ampicillin.

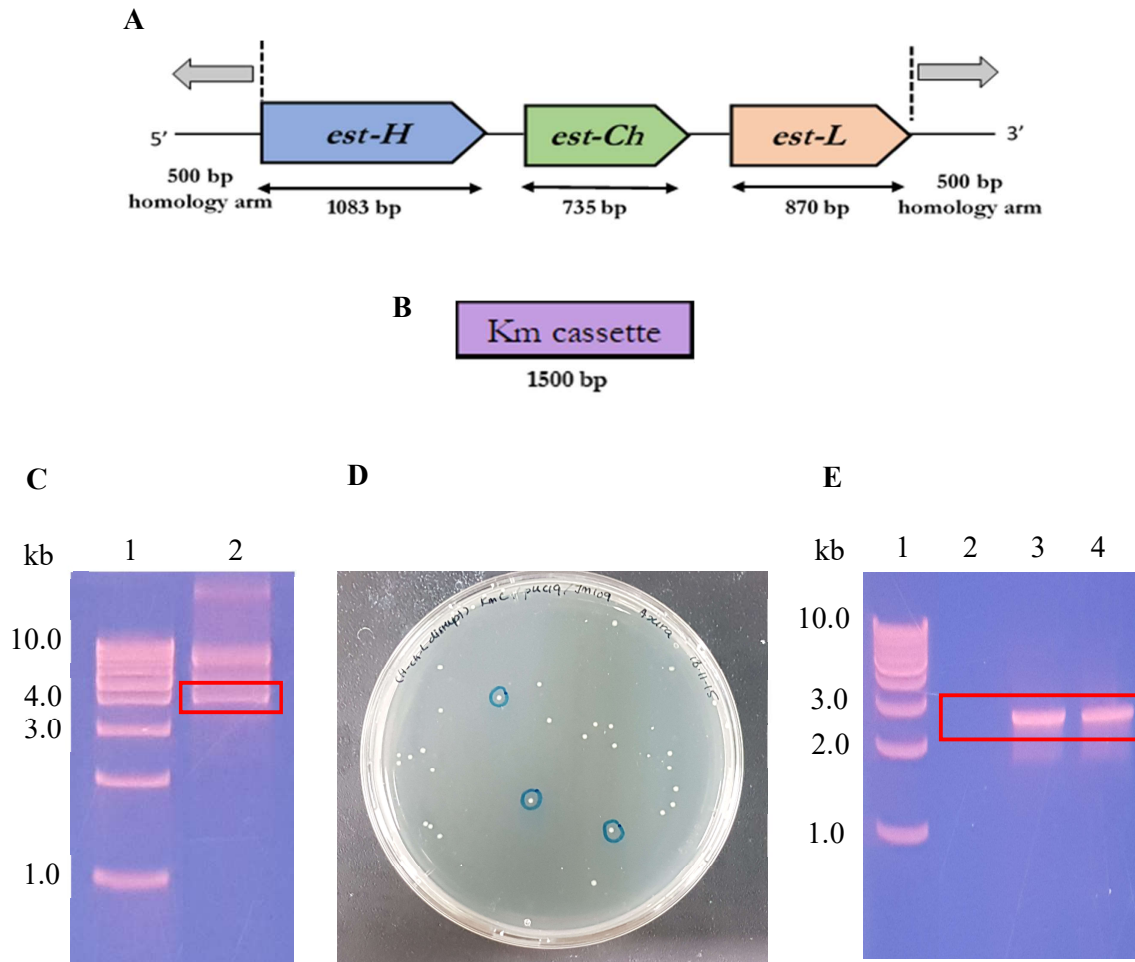
Figure 4-3A. The whole plasmid was linearized without the *est-H-est-Ch-est-L* genes cluster; therefore, the forward primer and reverse primer were designed to anneal precisely with the sequences adjacent to stop codon of *est-L*, and start codon of *est-H*, respectively. Agarose gel electrophoresis showed the PCR product of approximately 3.7 kb, which matched the size of pUC19 (2686 bp) and homology arm (1.0 kb) (Figure 4-3C). The 1.5 kb-kanamycin cassette (Figure 4-3B) was then inserted at these sites by in-fusion cloning, creating a pUC19 plasmid with the knocked-out esterase genes flanked by homology arm, followed by transformation of the cloned plasmid into *E. coli* JM109. Colony PCR (with primers *est* region-pUC19_fwd and *est* region-pUC19_rev) of three randomly picked colonies growth on selection agar plate (Figure 4-3C) produced products for two out of the three tested colonies, with sizes of approximately 2.5 kb (Figure 4-3D) which matched the size of the kanamycin cassette (1.5 kb) and homology arm (1.0 kb). pUC19 plasmid from the confirmed positive clone was isolated and used as the template for amplification of homology arm-flanking kanamycin cassette.

4.3.1.3 Cloning of homology arm flanking-kanamycin cassette into pGMS1

PCR amplification of homology arm flanking-kanamycin cassette using isolated pUC19 bearing the cassette as the template yield 2.5 kb product (Figure 4-4) which matched the total size of the cassette and the homology arm. The purified product was then cloned into pGMS1 followed by transformation into *E. coli* JM109. Transformation of pGMS1 bearing the kanamycin cassette into *E. coli* JM109 produced only one colony (data not shown). The sole colony was grown in LB medium for plasmid miniprep (Figure 4-5A) and used for transformation in *E. coli* S17-1. Figure 4-5B showed colonies grow on the selection plate. A positive clone as confirmed by colony PCR (data not shown) was cultivated to be used for bacterial conjugation with wt-TB-87.

4.3.2 Screening of Δ *est*-TB-87 mutants bearing knocked-out esterase genes

The esterase-encoding genes in the genome of wt-TB-87 were replaced with the knocked-out version by homologous recombination. Two 500 bp homology arm flanking the kanamycin cassette recognizes the same sequence in the genome, allowing the recombination to occur, creating TB-87 mutants lacking the esterase genes (Δ *est*-TB-87). It was hypothesized that shall the annotated esterase genes in Chapter 2 are indeed the genes responsible for the degradation of polyester-based biodegradable plastics by strain TB-87, the strain shall lose the ability to degrade the PBSA in this study.



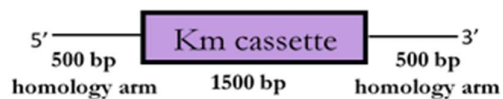
Lane 1: Molecular mass marker

Figure C, Lane 2: Linearized pUC19 by inverse PCR

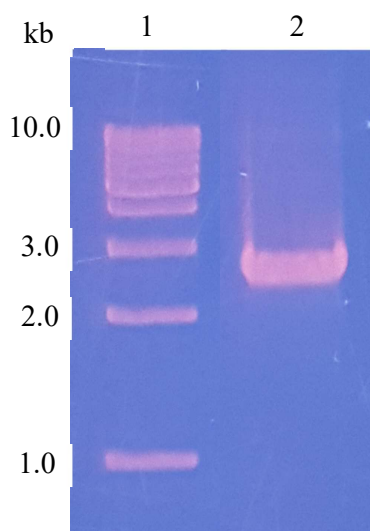
Figure E, Lane 2-4: Colony PCR product amplification

Figure 4-3 Linearization of *est* region-pUC19 by inverse PCR for the insertion of kanamycin cassette (KmC) and transformation into *E. coli* JM109. pUC19 was linearized precisely starting from start codon and stop codon of *est-H* and *est-L*, respectively, followed by the insertion of KmC at the linearized site. A. Linearization site indicated by dotted line and arrows; B. Amplified kanamycin cassette was inserted into linearized pUC19 by in-fusion cloning to produce 2.5 kb product (kanamycin cassette, 1.5 kb; homology arm, 1.0 kb); C. Linearized pUC19 by inverse PCR; D. Colonies growth on a LB agar plate supplemented with 100 µg/mL ampicillin, 50 µg/mL kanamycin, 40 µg/mL X-Gal and 0.1 mM IPTG, for blue/white screening; E. Colony PCR of three randomly selected colonies grown on LB agar plate in (D).

A



B



Lane 1: Molecular mass marker

Lane 2: PCR amplified product using kanamycin cassette
inserted-pUC19 as the template

Figure 4-4 PCR amplification of homology arm flanking-kanamycin cassette using miniprep pUC19 bearing the cassette as the template. A. Amplified region; B. PCR amplified product.

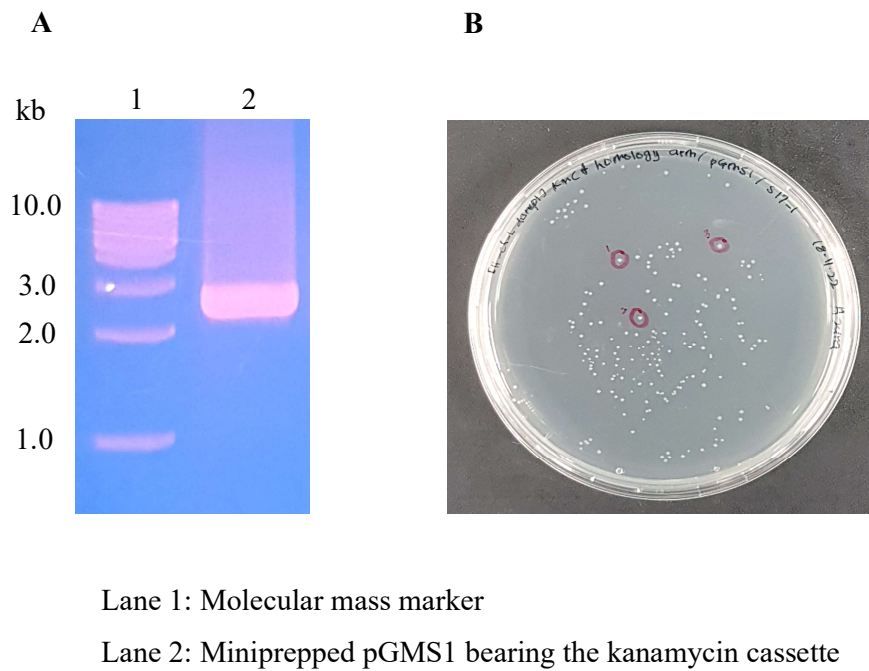


Figure 4-5 Cloning of homology arm flanking-kanamycin cassette into pGMS1 followed by transformation into *E. coli* S17-1 for the conjugation with wt-TB-87. A. Isolated pGMS1 bearing the kanamycin cassette; B. Colony growth on LB agar plate supplemented with 50 µg/mL kanamycin and 10 µg/mL gentamicin.

Figure 4-6 showed the mutant colonies growth on various agar plates. The mutant cultures were grown on nutrient agar and PBSA emulsion-overlaid nutrient agar without the addition of kanamycin, as controls. A lawn of bacteria was observed on the nutrient agar plate only control (Figure 4-6A) while fewer colonies' growth was observed on nutrient agar plates supplemented with kanamycin (Figure 4-6B). In figure 4-6C, with the addition of kanamycin, the growth of colonies able to form clear zone on PBSA emulsion overlaid-nutrient agar plate was observed, indicating incomplete recombination of kanamycin cassette with wt-TB-87's genome. Few colonies (in red circle), lost their ability to form clear zone on PBSA emulsion overlaid-nutrient agar plate despite able to grow in the presence of kanamycin, suggesting that the complete recombination had occurred. To further confirm the complete removal of pGMS1 after recombination, these colonies and three other randomly selected colonies that able to form clear zone on the plate were streaked on the same plate with the added addition of 10% sucrose and the result are shown in Figure 4-6D. To confirm that the complete recombination has occurred, second screening with the addition of sucrose was performed. Three randomly selected colonies from nutrient agar plates supplemented with kanamycin, and kanamycin and 1% PBSA emulsion (from plates in Figure 4-6B and 4-6C) were streak on nutrient agar plate supplemented with kanamycin and sucrose. Among the colonies tested, colonies that grow without forming clear zone on the plate in Figure 4-6C (colonies 1-3) are able to grow well on the plate, while colonies that could form clear zone on the same plate (colonies 4-6) produced few colonies on the sucrose added-nutrient agar plate, indicating complete and partial recombination have occurred for colonies 1-3 and colonies 4-6, respectively. pGMS1 carrying the *sacB* gene, could not grow on media containing sucrose (Hynes *et al.*, 1989), therefore, only strains which no longer contain pGMS1 are able to grow on media containing sucrose. Colony 1 was picked for cultivation in LB medium for plasmid isolation to be used as a template for PCR to further confirm the kanamycin cassette insertion.

4.3.3 Verification of gene deletion of the *Δest*-TB-87 mutants

Insertion of the kanamycin cassette into the esterase gene cluster site was confirmed by PCR (Figure 4-7) using genomic DNA from the wt-TB-87 and *Δest*-TB-87 strains as the template. PCR amplification of the esterase gene region of wt-TB-87 with the *est* region-pUC19 (Table 4-1) primer pair resulted in products with an approximate size of 3.9 kb, which matched the total length of the entire esterase gene cluster (2.9 kb) flanked by two 500 bp homology arms (Figure 4-7, Lane 3). Successful insertion of the kanamycin cassette (1.5 kb) into the *est-H-est-Ch-est-L* gene cluster yields a shorter PCR product (total length 2.5 kb) when

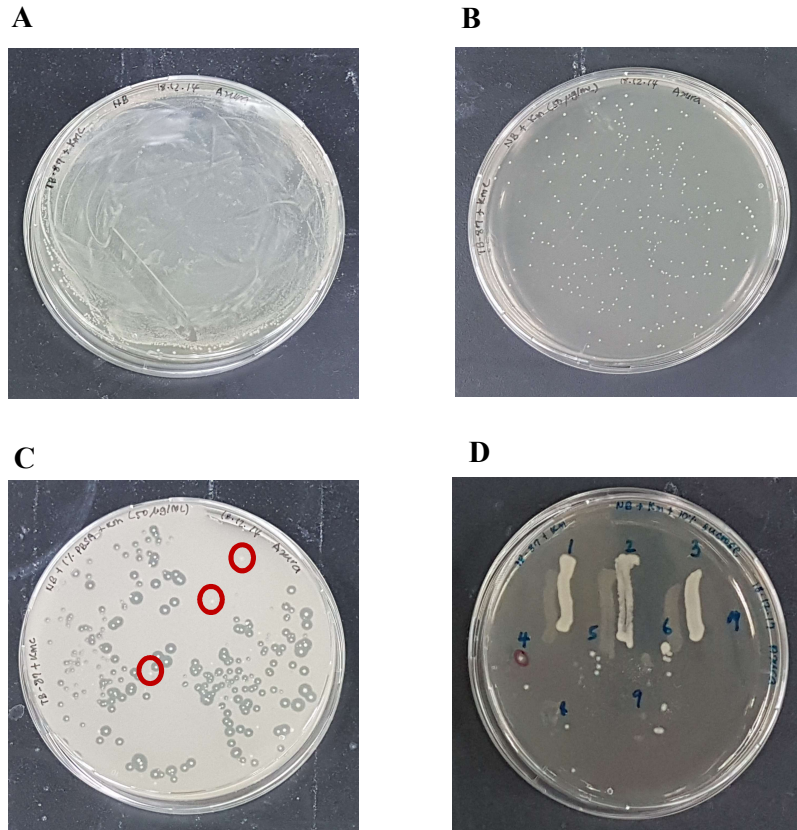
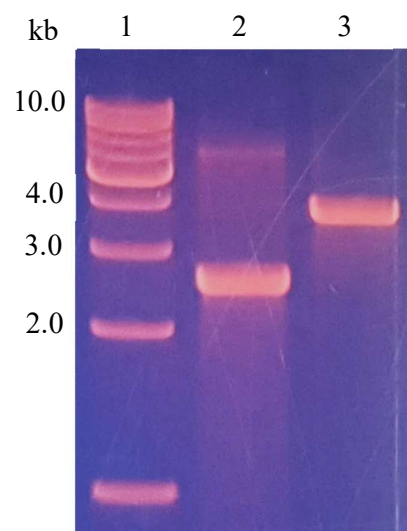


Figure 4-6 Colonies growth on nutrient agar plates and PBSA emulsion-overlaid nutrient agar plates. Colonies in red circles indicate *Δest*-TB-87 mutants with complete recombination. A. Nutrient agar only (control); B. Nutrient agar supplemented with 50 µg/mL kanamycin; C. PBSA emulsion-overlaid nutrient agar supplemented with 50 µg/mL kanamycin; D. Nutrient agar supplemented with 50 µg/mL kanamycin and 10% sucrose. Colony 1-3: Colonies circled in red from the plate in (C); Colony 4-6: Randomly selected colonies from the plate in (C); Colonies 7-9: Randomly selected colonies from the plate in (B).

amplified using the same primer pair and Δest -TB-87 genomic DNA as the template (Figure 4-7, Lane 2). Restriction digestion of the amplified products with *Nde*I and *Bst*API further confirmed the successful insertion of the kanamycin cassette (data not shown).

4.3.4 Assessment of the degradation ability of Δest -TB-87 mutants

To assess the degradation ability of strain TB-87 following gene deletion, a single colony of the Δest -TB-87 mutant and wt-TB-87 were streaked on a PBSA emulsion-overlaid nutrient agar plate and incubated for 48 h at 30°C. The ability of strain TB-87 to form a clear zone on the PBSA emulsion-overlaid agar plate diminished (Figure 4-8) following the deletion of the esterase-encoding genes, thus confirming that the annotated esterase genes in this study are indeed the genes responsible for PBSA degradation by strain TB-87.



Lane 1: Molecular marker

Lane 2: Δest -TB-87 genomic DNA

Lane 3: wt-TB-87 genomic DNA

Figure 4-7 PCR amplification product of the esterase gene region using genomic DNA from wt-TB-87 and Δest -TB-87 as the template.

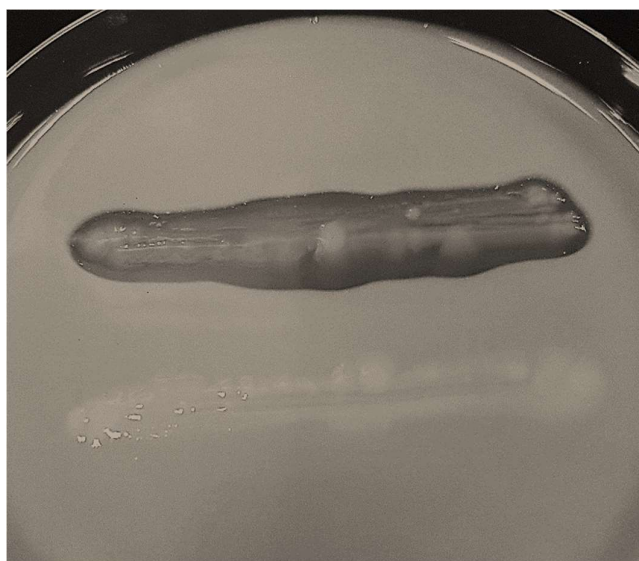


Figure 4-8 Formation of a clear zone of hydrolysis surrounding the wt-TB-87 streak (upper line) and Δest -TB-87 streak (lower line) on a PBSA emulsion-overlaid nutrient agar plate following 48 h of incubation at 30°C.

5.4 Conclusion

To investigate the function of the esterase-encoding genes annotated in this study, the entire cluster of esterase-encoding genes consisting of *est-H*, *est-L*, and *est-Ch*, was deleted using a homologous recombination method with a kanamycin antibiotic cassette. The mutant strain lost the ability to form a clear zone on PBSA emulsion-overlaid nutrient agar plates, suggesting that the annotated esterase-encoding genes in Chapter 2 are indeed the genes responsible for the PBSA degradation ability of *R. depolymerans* strain TB-87. However, the exact mechanism of PBSA-degradation at the molecular level remains unclear. As all attempts to express these genes individually have failed to produce a soluble enzyme, it would be interesting to determine whether these three genes work individually or synergistically to degrade PBSA or whether deletion of any one gene would affect the activity of the other two genes. Disruption of *estB*, a gene encoding for an esterase able to utilize dibutyl phthalate (DBP) as a sole carbon source in *Sphingobium* sp. SM42, resulted in increased degradation ability in the mutant strain compared with the parent strain. The *estB* mutant demonstrates increased expression of *estG*, which encodes for another DBP degrading esterase, EstG, thus compensating for the loss of EstB (Whangsuk *et al.*, 2015). Similarly, disruption of a gene encoding for Factor B, a serine protease essential for the function of the alternative pathway of complement activation, leads to the downregulation of gene expression of two adjacent genes, *C2* and *D17H6S45*, resulting in the complete loss of classical pathway function (Taylor *et al.*, 1998). The complementation study to restore the esterase activity is currently ongoing.

The functions of the entire esterase encoding genes have been confirmed by deleting the genes encoding for the enzymes, however, as the presence of the chaperon-encoding gene in the intergenic region of two genes encoding for two similar enzymes is unusual in many other similar studies, the investigation of the exact function of the gene is of utmost importance. Therefore, the deletion of *est-Ch* will be performed next and the results will be discussed in Chapter 5.

CHAPTER 5

Functional Analysis of Chaperone

5.1 Introduction

Gene annotation data presented in Chapter 2 revealed the presence of a chaperone-encoding gene in the intergenic region of *est-H* and *est-L*. Many previous attempts in this laboratory to express the genes have failed as the proteins could not be expressed in their soluble forms. In most cases, no expression could be observed at all. This has prompted the hypothesis that the proteins may need a helper protein to aid in the proper folding to yield soluble and functional proteins. This hypothesis was backed by many other similar studies (Hobson *et al.*, 1993; Su *et al.*, 2004; Sullivan *et al.*, 1999). They reported on the inability of lipase-encoding genes to be expressed in their active and soluble forms when expressed without their “lipase activator”. Furthermore, as discussed in Chapter 3, many strategies adopted to express the proteins in their soluble forms have failed, suggesting that the presence of a chaperone protein may be essential to aid in correct protein folding, thus preventing protein aggregation and inclusion bodies’ formation. Therefore, the disruption of *est-Ch* was attempted to elucidate the function of the chaperone and the results are presented in this chapter.

5.2 Materials and method

5.2.1 Bacterial strains, plasmids, and chemical reagents

The suppliers for and genotypes of *E. coli* HST08, *E. coli* JM109 and *E. coli* S17-1 used as transformation hosts as well as cloning plasmids (pUC19 and pGMS1), PBSA (Bionolle® #3020; MW = 1.4×10^5), ampicillin, molecular mass marker, agarose kanamycin and gentamicin, and all reagents and chemicals, are as per listed in Section 4.2.1.

5.2.2 Growth medium and culture conditions

R. depolymerans strain TB-87 and derived mutant strains were cultivated and maintained as per described in Section 4.2.2.

5.2.3 Template DNA preparation, primers, and PCR conditions

Template DNA preparation for PCR amplification, primers, and PCR conditions follow the method described in Section 4.2.3.

Table 5-1 Primers used for the construction of plasmids for *est-Ch* deletion.

Primer	Sequence (5'→ 3')	Description
est region-pUC19_fwd	CGACTCTAGAGGATCCGCCAGGTTGCGGGAATG	Amplification of the esterase gene region
est region-pUC19_rev	CGGTACCCGGGGATCATGCAGGCAGACG	
est region-inverse pUC19_fChdel	CCATGGCTAATTCCCACGGCGACAGAGGCCT	Linearization of pUC19 bearing the esterase gene region sans the <i>est-Ch</i> for insertion of the kanamycin cassette
est region-inverse pUC19_rChdel	GCAGCTCCAGCCTACACAGGCGGACCTCCGTCAGTAG	
Km cassette-pUC19_fwd	TGTGTAGGCTGGAGCTGC	Amplification of the kanamycin cassette for in-fusion cloning into linearized pUC19
Km cassette-pUC19_rev	TGGGAATTAGCCATGGTC	
est region-pGMS1_fwd	CTCTAGAGGATCCCCCGCCAGGTTGCGGGATGGCA	Amplification of the kanamycin cassette inserted (at <i>est-Ch</i> 's site)-esterase gene region for in-fusion cloning into pGMS1
est region-pGMS1_rev	TCGAGCTCGGTACCCATGCAGGCAGACG	

The esterase gene region (est region) refers to the *est-H-est-Ch-est-L* gene cluster flanked by a 500 bp sequence homologous to the genome sequence of wt-TB-87 at either side of the cluster.

5.2.4 Construction of plasmid bearing knocked-out *est-Ch*

The deletion of *est-Ch* by using kanamycin antibiotic cassette follows the method described in Section 4.2.4, therefore with the exception of primers *est* region-inverse pUC19_fChdel and *est* region-inverse pUC19_rChdel, all primers used in this study are similar to those used in Chapter 4 (Table 5). Knocking-out of *est-Ch* was achieved by inserting kanamycin cassette at the *est-Ch*'s site generated as a result of pUC19 linearization at the sites immediately upstream and downstream of *est-Ch*.

5.2.5 Bacterial conjugation between *E. coli* S17-1 with wild type strain TB-87

Positive clones harboring plasmid bearing knocked-out *est-Ch* gene prepared according to the method described in Section 4.2.4, was cultivated in LB medium for the introduction into wild type *R. depolymerans* by conjugation following the method described in Section 4.2.5. TB-87 Δ *est-Ch* mutants carrying the knocked-out *est-Ch* were screened by colony PCR.

The general workflow of targeted gene disruption of *est-Ch* is summarized in Figure 5-1.

5.3 Results and discussion

5.3.1 Deletion of the putative Est-Ch-encoding gene by homologous recombination

Preliminary co-expression of Est-Ch with Est-H and Est-L results done in this laboratory presented caused the loss of expression, even in insoluble forms (data not shown), previously observed during individual expression of Est-H and Est-L as demonstrated in Chapter 3. This prompted the hypothesis that the *est-Ch* can only function when it is in full cluster i.e. *est-H-est-Ch-est-L*. As mentioned earlier, many other studies reported on soluble expression of a lipase gene when expressed with their chaperone protein (Hobson *et al.*, 1993; Sullivan *et al.*, 1999; Su *et al.*, 2004), however, co-expression of Est-Ch seems to suppress the expression of Est-H and Est-L in this study (data not shown), therefore, the deletion of *est-Ch* was attempted to elucidate the functions of *est-Ch* in the expression of *est-H* and *est-L*.

5.3.1.1 Insertion of kanamycin cassette at the *est-Ch* genes cluster's site

pUC19 bearing the esterase gene cluster flanked by two 500 bp homology arm obtained previously in Section 4.3.1.1 was used as the template for plasmid linearization by inverse PCR. The amplified region and starting point for the plasmid linearization is shown in Figure 5-2A. The whole plasmid was linearized without the *est-Ch* gene; therefore, the forward and the reverse primers were designed to anneal precisely with the sequence adjacent to stop and start

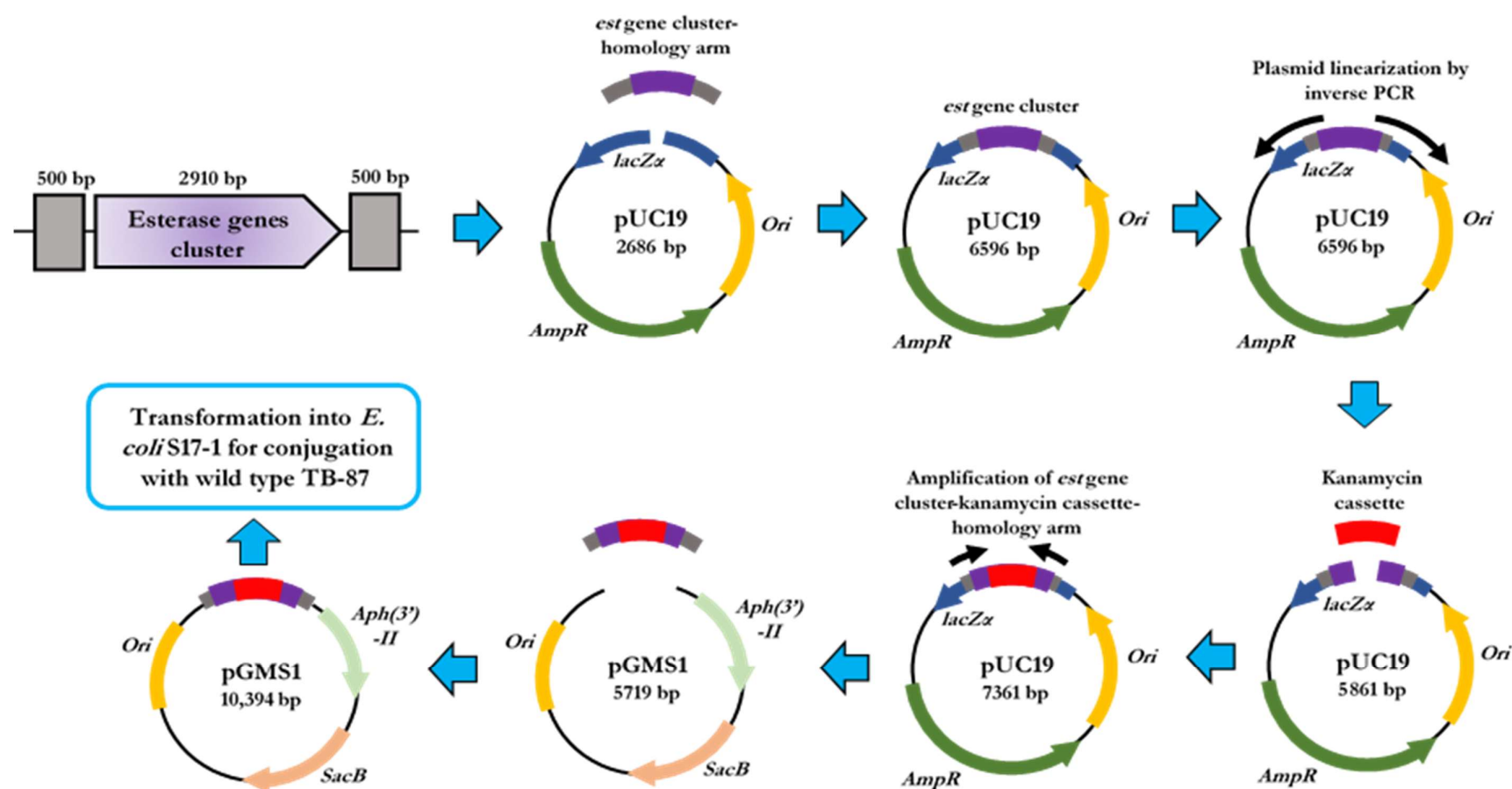


Figure 5-1 General workflow of the targeted disruption of the *est-Ch* gene using kanamycin antibiotic cassette. Linearization of plasmids *pUC19* and *pGMS1* were performed at the *Bam*HI and *Sma*I sites, respectively. 3-step PCR for the amplification of the esterase gene clusters used primers as listed in Table 5-1.

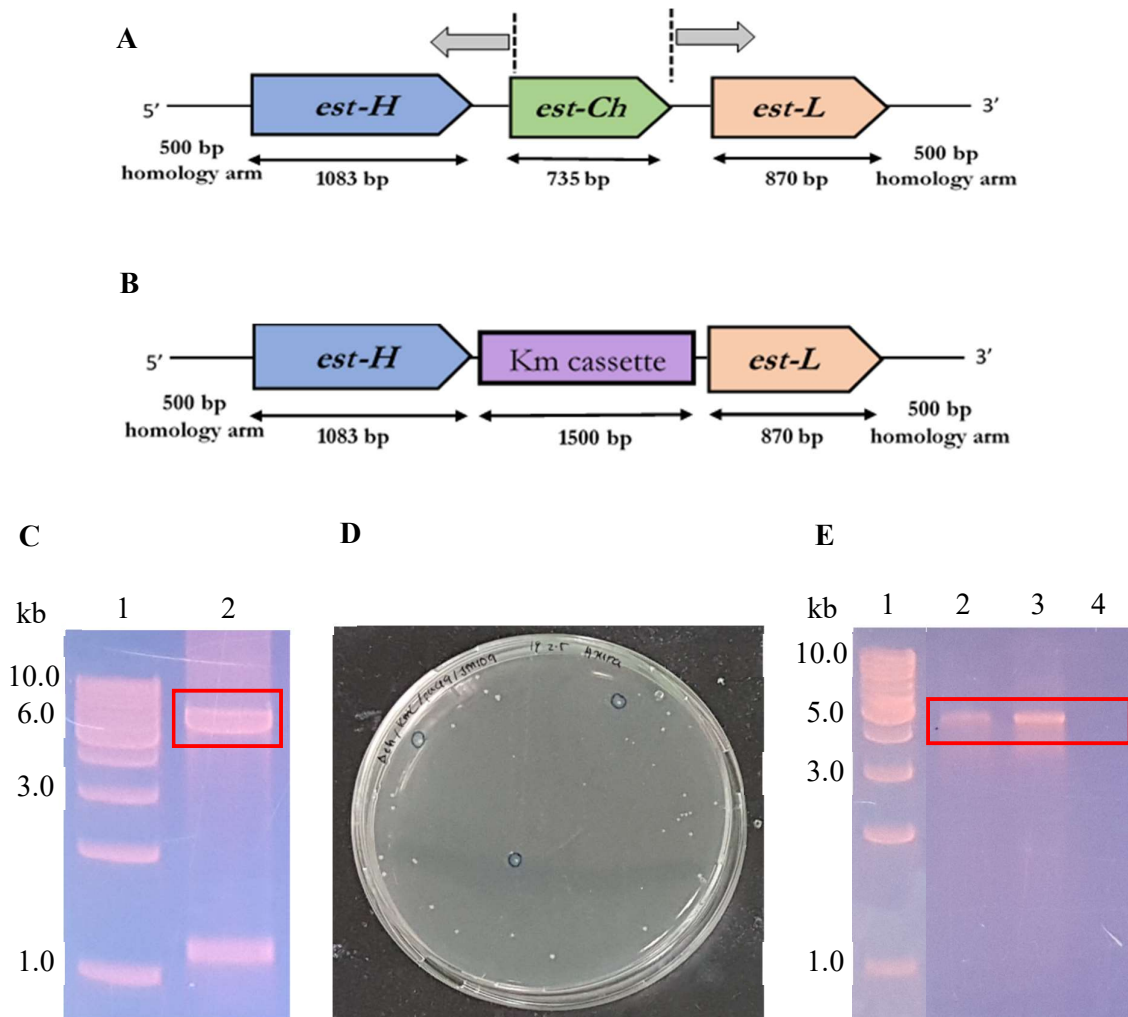
codon of *est-Ch*, in which amplified kanamycin cassette (1.5 kb) was later inserted at these sites (Figure 5-2B). Agarose gel electrophoresis showed the PCR products of approximately 5.9 kb which matched the size of pUC19 (2686 bp), *est-L-est-H* (2175 bp) and homology arm (1.0 kb) (Figure 5-2C). A non-specific DNA band at approximately 1.2 kb was also observed. As multiple bands were still observed even after changing conditions, the DNA band with the correct size was excised off the gel, purified and used for in-fusion cloning with kanamycin cassette, creating a pUC19 plasmid with the knocked-out *est-Ch* flanked by homology arm. The plasmid was then transformed into *E. coli* JM109. Colony PCR (with primers *est* region-pUC19_fwd and *est* region-pUC19_rev) of three randomly picked colonies growth on selection agar plate (Figure 5-2D) produced products for two out of the three tested colonies, with sizes of approximately 4.7 kb (Figure 5-2E) which matched the size of the kanamycin cassette (1.5 kb), *est-H*-intergenic region-*est-L* (2.2 kb), and homology arm (1.0 kb). pUC19 plasmid from the confirmed positive clone was isolated and used as the template for amplification of homology arm-flanking kanamycin cassette.

5.3.1.2 Cloning of homology arm flanking-kanamycin cassette into pGMS1

PCR amplification of homology arm flanking-kanamycin cassette using isolated pUC19 bearing the cassette as the template yield 4.7 kb product (Figure 5-3) which matched the total size of the cassette flanked by the *est-H* and *est-L*, and the homology arm. The purified product was then cloned into pGMS1 followed by transformation into *E. coli* JM109. Transformation of pGMS1 bearing the kanamycin cassette into *E. coli* JM109 produced approximately 100 colonies (Figure 5-3C). Colony PCR of three randomly selected colonies were done to confirm clones containing the correct insert (Figure 5-3D). All tested samples produced multiple products on an agarose gel, suggesting non-specific binding of the primers with the template DNA, similar as observed previously (Figure 5-2C). Clone number three (Figure 5-3D, Lane 4), although yield non-specific product, produced PCR product at the expected size (4.7 kb), therefore the colony was picked and grown in LB medium for plasmid miniprep to be used for transformation in *E. coli* S17-1.

5.3.1.3 Screening of TB-87 *est-Ch* mutants bearing knocked-out *est-Ch* gene

The putative chaperone-encoding gene in the genome of wt-TB-87 was replaced with the knocked-out version by homologous recombination. As mentioned in Chapter 4, two 500 bp homology arm flanking the kanamycin cassette recognizes the same sequence in the genome, allowing the recombination to occur, creating TB-87 mutants lacking the *est-Ch* gene



Lane 1: Molecular mass marker

Figure C, Lane 2: Linearized pUC19 by inverse PCR

Figure E, Lane 2-4: Colony PCR product amplification

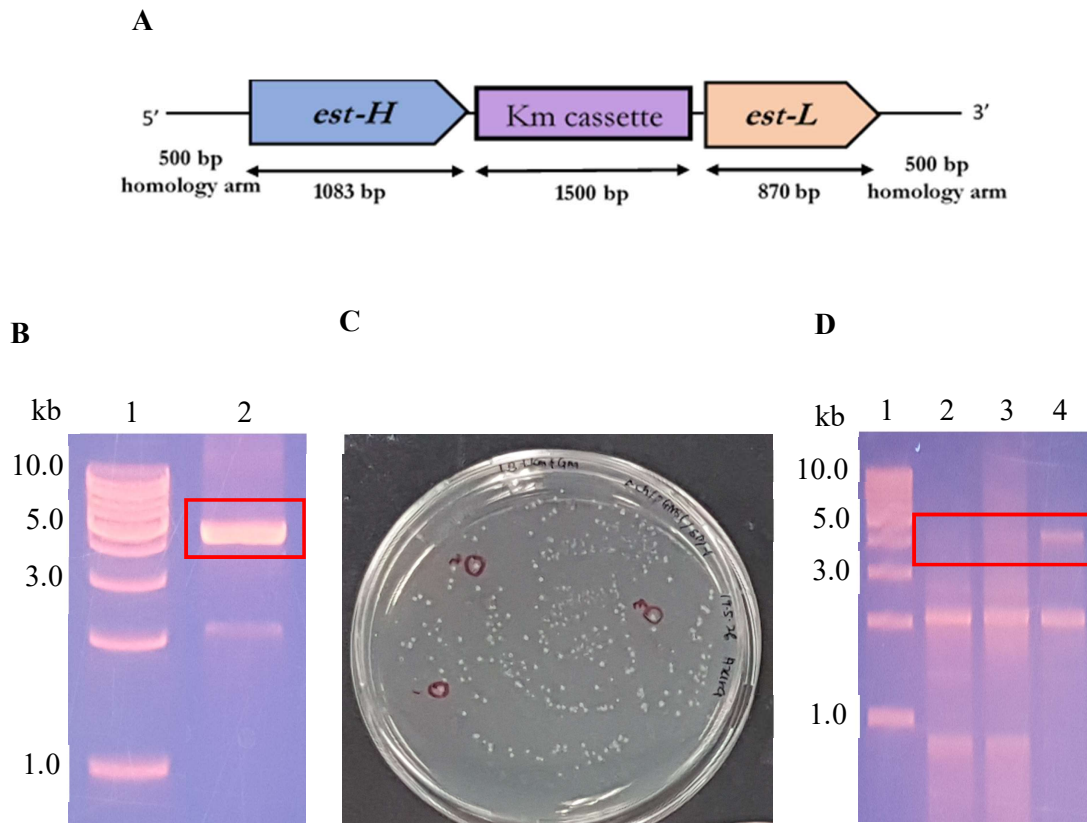
Figure 5-2 Linearization of *est* region-pUC19 by inverse PCR for the insertion of kanamycin cassette (KmC) and transformation into *E. coli* JM109. pUC19 was linearized precisely starting from start codon and stop codon of *est-Ch*, followed by the insertion of KmC at the linearized site. A. Linearization site indicated by dotted line and arrows; B. Amplified kanamycin cassette was inserted into linearized pUC19 by in-fusion cloning to produce 4.7 kb product (kanamycin cassette, 1.5 kb; *est-H-estL*, 2.2 kb; homology arm, 1.0 kb); C. Linearized pUC19 by inverse PCR; D. Colonies growth on a LB agar plate supplemented with 100 µg/mL ampicillin, 50 µg/mL kanamycin, 40 µg/mL X-Gal and 0.1 mM IPTG, for blue/white screening; E. Colony PCR of three randomly selected colonies grown on LB agar plate in (D).

(TB-87 Δ *est-Ch*).

Figure 5-4 showed the mutant colonies growth on various agar plates. The mutant cultures were grown on nutrient agar and PBSA emulsion-overlaid nutrient agar without the addition of 10% sucrose, as controls. A lawn of bacteria was observed on the nutrient agar plate only control (Figure 5-4A) while fewer colonies' growth was observed on nutrient agar plates supplemented with kanamycin and 10% sucrose (Figure 5-5B-D). Unlike gene deletion experiments in Chapter 4, where the addition of 10% sucrose to select for the mutants containing no active pGMS1 was done during the second screening, the addition of sucrose was done from the beginning to eliminate clones with incomplete recombination, thus, the esterase gene region of colonies able to grow on agar plates in the presence of kanamycin and sucrose were assumed to be completely recombined with knocked-out *est-Ch*. Colony PCR performed on three randomly selected mutant colonies from selection agar plate in Figure 5-4D, yields very faint DNA bands at the expected size (4.7 kb). Louwrier and Van Der Valk (2001) suggested that the presence of sucrose during the PCR reaction at low denaturation temperatures (90°C), produced lower yields of PCR product. The increase of temperature to 95°C, however, increased the stabilization of the DNA duplex, causing increased denaturation of the template. This provides higher template copy number, resulting in higher PCR product yields. Although the denaturation temperature used for colony PCR here was 95°C, the relatively high sucrose concentration used (10%) possibly caused a similar effect, hence the faint DNA bands.

Nevertheless, colony PCR of *E. coli* S17-1 transformed with TB-87- Δ *est-Ch* (Figure 5-2E) prior to conjugation with wt-TB-87 yield correct PCR product, indicating successful recombination had occurred (data not shown). Interestingly, the deletion of only *est-Ch* produced mutants that lost the ability to form halo zone on PBSA emulsion-nutrient agar plate; an effect similar to that observed after the deletion of the entire esterase gene as discussed in Chapter 4, which prompted the hypothesis that the esterase genes in this study possibly exist as a subunit or as a protein complex. If a number of proteins function exclusively in a complex, organisms would be expected to encode in their genomes the genes for either all or none of them (Kensche *et al.*, 2008; Pellegrini, 2012), thus, the deletion of the gene for either protein should have the same impact on the organism's competency as the deletion of all genes together (Costanzo *et al.*, 2011). However, to confirm this hypothesis, further studies are essential.

As mentioned previously, pGMS1 carrying the *sacB* gene, could not grow on media containing sucrose (Hynes *et al.*, 1989), therefore, only strains which no longer contain active



Lane 1: Molecular mass marker

Figure B, Lane 2: Amplified esterase gene region bearing the kanamycin cassette at the *est-Ch*'s site

Figure E, Lane 2-4: Colony PCR product amplification

Figure 5-3 Cloning of homology arm flanking-kanamycin cassette into pGMS1 followed by transformation into *E. coli* S17-1 for the conjugation with wt-TB-87. A. Amplified esterase gene region bearing the kanamycin cassette at the *est-Ch*'s site; B. PCR product of amplified region shown in (A); C. Colony growth on LB agar plate supplemented with 50 µg/mL kanamycin and 10 µg/mL gentamicin; D. Colony PCR of three randomly selected colonies grow on antibiotic agar plate in (B).

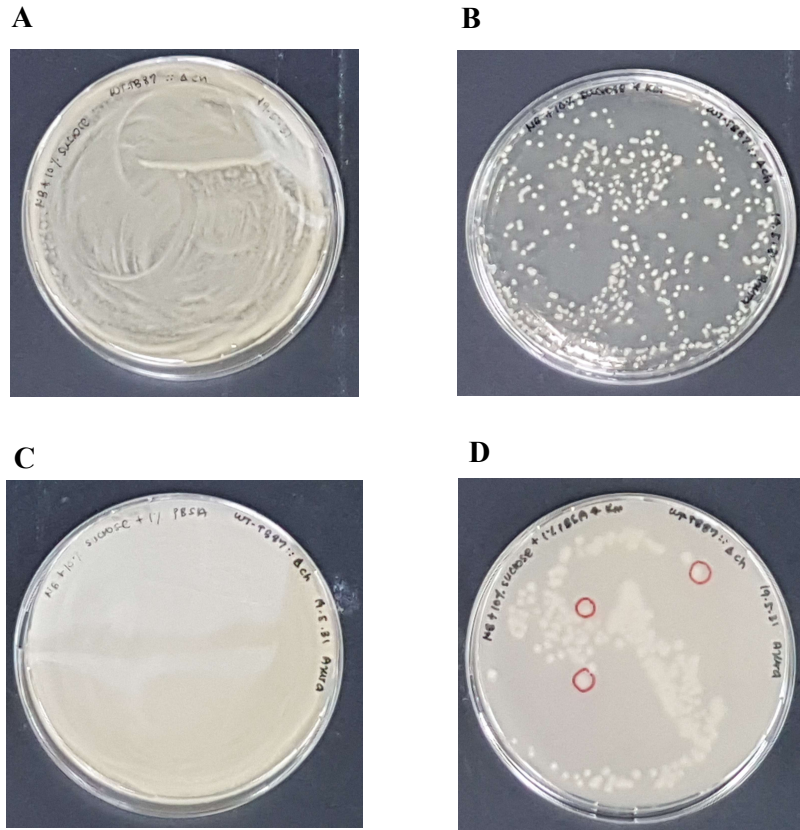


Figure 5-4 Colonies growth on nutrient agar plates and PBSA emulsion-overlaid nutrient agar plates. Colonies in red circles indicate TB-87 Δ *estCh* mutants with complete recombination. A. Nutrient agar only (control); B. Nutrient agar supplemented with 50 μ g/mL kanamycin and 10% sucrose; C. PBSA emulsion-overlaid nutrient agar supplemented with 50 μ g/mL kanamycin; D. PBSA emulsion-overlaid nutrient agar supplemented with 50 μ g/mL kanamycin and 10% sucrose. Three randomly selected colonies circled in red were picked for colony PCR to confirm positive clones.

pGMS1 are able to grow on media containing sucrose. Colony 1 was picked for cultivation in LB medium for plasmid isolation to be used as the template for PCR to further confirm the kanamycin cassette insertion and for gene reconstruction to investigate the restoration of enzyme activity.

5.4 Conclusion

Based on results presented thus far, although the roles of *est-Ch* have yet to be understood, the roles and functions of esterase-encoding genes have been made slightly clear. The presence of chaperone-encoding gene annotated in Chapter 2 and the inability of Est-H and Est-L to be expressed in their soluble forms when expressed individually, prompted the hypothesis that the presence of chaperone gene is essential to aid in correct protein folding. Hence, the current study was attempted to clarify the roles of *est-Ch* in *est-H* and/or *est-L*'s expression. The results of preliminary *est-Ch*'s deletion experiments presented in this chapter, suggesting that the Est-Ch possibly exists as a subunit or as part of a protein complex with Est-H and Est-L. This assumption was based on the fact that the deletion of only one gene i.e. *est-Ch*, showed a similar effect as that exhibited when the entire esterase gene cluster was deleted. The loss of ability to form halo zone on PBSA emulsion-nutrient agar plate was observed, suggesting that the PBSA degradation ability is conferred to the strain TB-87 by the esterase gene cluster in its entirety. Unfortunately, no current data is available to support this hypothesis; thus, further studies are needed.

CHAPTER 6

General Conclusion and Suggestions for Future Work

6.1 Conclusion

Plastic waste pollution is one of the major environmental concerns in recent years caused by the rapid growth of plastic utilizing industries. To overcome many problems associated with plastics waste, the development of biodegradable plastics for use especially in packaging, has been gaining attention since these plastics can be degraded into low molecular weight monomer generating carbon dioxide, methane, and water by suitable microorganisms. However, in recent years, new concerns regarding the fate of biodegradable plastics have arisen; the production of micro- and nanoplastics as a result of the breakdown of the plastics. The development of biodegradable plastics comprise of recyclable monomers is, therefore, the more economical and environmentally benign approach to the problems. The central idea of such a system relies on the recycling of monomers generated as a result of partial degradation of biodegradable plastics by microorganisms, into a new polymer. To achieve this final aim, the biodegradation mechanism by microorganisms first needs to be clarified.

Previously in this laboratory, the isolation and characterization of polyester-degrading enzymes, designated as Est-H and Est-L from a freshwater bacterium, *Roseateles depolymerans* strain TB-87, capable to degrade various polyester-based biodegradable plastics such as PBS, PBSA, and PCL, have been reported. Although both Est-H and Est-L have similar substrate specificity and degradation activity as well as nearly identical molecular masses, studies suggested that both proteins are of different proteins. While many other similar studies reported on the single enzyme responsible for the degradation, strain TB-87 possesses two identical enzymes with similar functions. The functions of the genes encoding of these enzymes are still unknown, therefore, the current study aims to understand the roles of the genes in the degradation of polyester-based biodegradable plastics.

In Chapter 2, the gene-encoding region of esterase previously isolated from *Rosetaeles depolymerans* strain TB-87 was annotated. Two open reading frames (ORFs) consisting of 873 bp and 870 bp nucleotides, corresponding to *est-H* and *est-L*, encoding enzymes of 361 and 290 amino acids, respectively, were predicted. In addition, another ORF consisting of 735 bp encoding a chaperone-like protein (Est-Ch) of 244 amino acids was identified in the intergenic

region of *est-H* and *est-L*. The presence of chaperone gene (*est-Ch*) located in the intergenic region of esterase-encoding genes (*est-H* and *est-L*) was predicted. The presence of -10, -35 promoter region and a terminator region flanking *est-H-est-Ch* genes cluster, suggested that *est-Ch* and *est-H* are expressed polycistronically. Est-Ch is possibly expressed to aid in the folding and transport of Est-H as a functional protein. Est-H and Est-L showed homology with plastic degrading enzymes, such as esterase and cutinase while Est-Ch showed homology with bacterial lipase chaperone. The presence of consensus lipase sequences (-Gly-His-Ser-Met-Gly-) was observed in these enzymes, thus Est-H and Est-L were hypothesized to be hydrolases with serine (Ser) in their active center.

Overexpression of Est-H and Est-L in *E. coli* BL21 (DE3) to obtain purified protein for further biochemical characterization studies was attempted in Chapter 3. Both proteins were cloned into pET21b devoid of N-terminal T7-tag, producing proteins in their “native forms”. The ability of the clones to grow on antibiotic agar plates at 37°C diminished following the tag deletion, which pointed at possible gene toxicity; therefore, *E. coli* Lemo21 (DE3) was chosen as the host cells for subsequent overexpression experiments. Overexpression of Est-H and Est-L in Lemo21 (DE3) with and without their putative signal peptides, designated as Est-HF and Est-LF, and Est-HM and Est-LM, respectively, were performed. Protein bands with a molecular weight of approximately 30 kDa, were observed in the SDS-PAGE gels of both Est-HF and Est-HM. Expression of Est-LF and Est-LM, however, yielded proteins with a molecular weight of approximately 30 kDa and 27 kDa, respectively, which matched their predicted sizes. Interestingly, with the addition of 250 µM L-rhamnose, two Est-L protein bands were observed at 30 kDa and 27 kDa, which matched the sizes of both Est-LF and Est-LM, suggesting the occurrence of signal peptide cleavage by the Lemo21 (DE3) translational machinery to yield a mature protein. The addition of L-rhamnose, although showed no effect on the soluble expression of both proteins, enhanced the expression when added at the low concentration (0-250 µM). The spectrophotometric enzyme activity assay of the sample supernatant using *p*-nitrophenyl acetate as the substrate detected no esterase activity. Since the expression of Est-H and Est-L still produced insoluble proteins, *in vitro* refolding of both proteins was done using immobilized metal affinity column chromatography (IMAC). The proteins could not be retrieved even after changing many buffers and refolding conditions, suggesting aggregation of the proteins in the column during simultaneous refolding and purification. Many attempts to elute the proteins out the column have failed.

In Chapter 4, the deletion of the entire cluster of esterase-encoding genes consisting of *est-H*, *est-L*, and *est-Ch* using a homologous recombination method with a kanamycin

antibiotic cassette was performed to investigate the function of the esterase-encoding genes annotated in this study. The mutant strain lost the ability to form a clear zone on PBSA emulsion-overlaid nutrient agar plates, suggesting that the annotated esterase-encoding genes in Chapter 2 are indeed the genes responsible for the PBSA degradation ability of *R. depolymerans* strain TB-87. However, the exact mechanism of PBSA-degradation at the molecular level remains unclear. As all attempts to express these genes individually have failed to produce a soluble enzyme, it would be interesting to determine whether these three genes work individually or synergistically to degrade PBSA or whether the deletion of any one gene would affect the activity of the other two genes.

Following the successful deletion of the entire esterase gene cluster, the deletion of *est-Ch* to elucidate the functions of the putative chaperon-encoding gene was attempted in Chapter 5. Interestingly, the deletion of only *est-Ch* produced mutants that showed similar loss of degradation ability i.e. unable to form halo zone on PBSA emulsion-nutrient agar plate, with that observed after the deletion of the entire esterase gene cluster. Unpublished preliminary results obtained suggested that the *est-Ch* is possibly existed as a subunit or as a part of a protein complex with Est-H and Est-L. To confirm this hypothesis, however, further studies are needed.

A point of interest in this study focuses on the unique structure of esterase from strain TB-87. As mentioned earlier, strain TB-87 secreted two identical enzymes that have very similar substrate specificity and nearly identical molecular masses, while only one enzyme is usually responsible for biodegradation in many other similar studies. Furthermore, very few reports are available on the structure of the genes encoding for plastic-degrading enzymes. Even very few reports can be found on the gene cluster of three enzymes with almost identical characteristics and functions. The elucidation of the genes' functions is therefore of utmost importance to understand the biodegradation mechanism of esterase in the degradation of polyester-based biodegradable plastics.

Overall, the functional studies of esterase genes from strain TB-87 have been challenging. Although many strategies have been adopted when the results obtained were not in agreement with expected results, successful strategies have yet to be observed. Nevertheless, the characteristics and behavior of the proteins have been made clear, which will be useful to design future strategies when working with these proteins. Understanding of function of the genes encoding for plastic-degrading enzymes could lead to the elucidation of the decomposition activity and substrate specificity exclusive to the biodegradable plastic enzymes. This will allow manipulation and modification of the genes to obtain enzymes having more

specific properties particularly for the development of enzyme-based monomer recycling systems in the future.

6.2 Suggestions and recommendations for future work

Future work could focus on the resequencing of the N-terminus region of esterase, particularly that of Est-H. To achieve this, the acquisition of purified protein on a large scale is necessary. As all attempts and strategies adopted in this study had failed to obtain (soluble) expression, a different approach for protein expression could be employed. Different expression systems; fungal (using yeast *Pichia Pastoris*) and *Brevibacillus* Expression System, have been proven to successfully express recombinant proteins (Udaka and Yamagata, 1993; Yashiro *et al.*, 2001; Tanaka *et al.*, 2003; Miyauchi *et al.*, 2005) otherwise could not be expressed in *E. coli* (Tanio *et al.*, 2009).

Preliminary gene deletion experiments suggested the possibility that the Est-H, Est-L, and Est-Ch are expressed as a cluster i.e. they exist as a subunit or as a protein complex. To confirm this hypothesis, the deletion of the genes can be done in a cluster of two genes i.e. *est-H-est-Ch* and *est-Ch-est-L*. If the proteins have indeed existed as a subunit, the deletion of any one or two genes shall give similar results as the deletion of the entire esterase gene region.

In addition, the functions of esterase-encoding genes are still unknown, therefore, the study of gene transcription and expression by employing the reverse transcriptase PCR (RT-PCR). DNA microarray; able to monitor the expression of multiple genes simultaneously (Lashkari *et al.*, 1997), can be attempted in the future.

Finally, gene modification to improve the enzyme function can be employed. DNA shuffling and error-prone PCR are recommended to achieve this objective. Much research reported on the improvement of the function of their target enzymes through these two methods (Glieder *et al.*, 2002; Fasan *et al.*, 2007; Goda, 2012).

It is expected that by employing these strategies, the functions of esterase genes at the molecular level can be made clear, which will aid in achieving the final aim of the development of biodegradable plastics comprising of recyclable monomers.

REFERENCES

- Alberts, B., Johnson, A., and Lewis, J. (2002) 'Studying Gene Expression and Function', in *Molecular Biology of the Cell* [Online], 4th edn., New York: Garland Science. Available at: <https://www.ncbi.nlm.nih.gov/books/NBK26818/> [Accessed 26 April 2019].
- Abe, M., Kobayashi, K., Honma, N. and Nakasaki, K. (2010) 'Microbial degradation of poly(butylene succinate) by *Fusarium solani* in soil environments', *Polymer Degradation and Stability*, 95 (2), pp. 138-143.
- Akutsu-Shigeno, Y., Teeraphatpornchai, T., Teamtisong, K., Nomura, N., Uchiyama, H., Nakahara, T. and Nakajima-Kambe, T. (2003) 'Cloning and sequencing of a poly(DL-lactic acid) depolymerase gene from *Paenibacillus amylolyticus* strain TB-13 and its functional expression in *Escherichia coli*', *Applied and Environmental Microbiology*, 69(5), pp. 2498-2504.
- Anstey, A., Muniyasamy, S., Reddy, M. M., Misra, M. and Mohanty, A. (2014) 'Processability and biodegradability evaluation of composites from poly(butylene succinate) (PBS) bioplastic and biofuel co-products from Ontario', *Journal of Polymers and the Environment*, 22(2), pp. 209–218
- Babak, G. and Hadi, A. (2013). 'Biodegradable Polymers', in Chamy, R. and Rosenkranz, F. (eds.), *Biodegradation - Life of Science* [Online], London: IntechOpen. Available at: <https://www.intechopen.com/books/biodegradation-life-of-science/biodegradable-polymers> [Accessed 29 March 2019].
- Baker, P. J., Poultney, C., Liu, Z., Gross, R. and Montclare, J. K. (2012) 'Identification and comparison of cutinases for synthetic polyester degradation', *Applied Microbiology and Biotechnology*, 93(1), pp. 229-240.
- Belinky, F., Rogozin, I. B. and Koonin, E. V. (2017) 'Selection on start codons in prokaryotes and potential compensatory nucleotide substitutions', *Scientific Reports*, 7(12422), pp. 1-10.
- Biundo, A., Hromic, A., Pavkov-Keller, T., Gruber, K., Quartinello, F., Haernvall, K., Perz, V., Arrell, M. S., Zinn, M., Ribitsch, D. and Guebitz, G. M. (2016) 'Characterization of a

- poly(butylene adipate-co-terephthalate)-hydrolyzing lipase from *Pelosinus fermentans*', *Applied Microbiology and Biotechnology*, 100(4), pp. 1753–1764.
- Bornscheuer, U. T. (2002) 'Microbial carboxyl esterases: Classification, properties and application in biocatalysis', *FEMS Microbiology Reviews*, 26(1), pp. 73–81.
- Bouwmeester, H., Hollman, P. C. H. and Peters, R. J. B. (2015) 'Potential health impact of environmentally released micro- and nanoplastics in the human food production chain: experiences from nanotoxicology', *Environmental Science and Technology*, 49(15), pp. 8932-8947.
- Brondyk, W. H. (2009) 'Chapter 11: Selecting an appropriate method for expressing a recombinant protein', in *Methods in Enzymology*, 463, pp. 131-147.
- Carr, P. D. and Ollis, D. L. (2009) 'Alpha/beta hydrolase fold: An update', *Protein and Peptide Letters*, 16(10), pp. 1137–1148.
- Carson, M., Johnson, D. H., McDonald, H., Brouillette, C. and DeLucas, L. J. (2007) 'His-tag impact on structure', *Acta Crystallographica Section D: Biological Crystallography*, 63(3), pp. 295-301.
- Chahinian, H. and Sarda, L. (2009) 'Distinction between esterases and lipases: Comparative biochemical properties of sequence-related carboxylesterases', *Protein and Peptide Letters*, 16(10), pp. 1149–1161.
- Chandra, R. and Rustgi, R. (1998) 'Biodegradable Polymers', *Progress in Polymer Science*, 23(7), pp. 1273-1335.
- Cleveland, D. W., Fischer, S. G., Kirschner, M. W. and Laemmli, U. K. (1977) 'Peptide mapping by limited proteolysis in sodium dodecyl sulfate and analysis by gel electrophoresis.', *The Journal of Biological Chemistry*, 252(3), pp. 1102–1106.
- Costanzo, M., Baryshnikova, A., Myers, C. L., Andrews, B. and Boone, C. (2011) 'Charting the genetic interaction map of a cell', *Current Opinion in Biotechnology*, 22(1), pp. 66-74.
- Cozar, A., Echevarria, F., Gonzalez-Gordillo, J. I., Irigoien, X., Ubeda, B., Hernandez-Leon, S., Palma, a. T., Navarro, S., Garcia-de-Lomas, J., Ruiz, A., Fernandez-de-Puelles, M. L. and Duarte, C. M. (2014) 'Plastic debris in the open ocean', *Proceedings of the National Academy of Sciences*, 111(28), pp. 10239-10244.

- Dimarogona, M., Nikolaivits, E., Kanelli, M., Christakopoulos, P., Sandgren, M. and Topakas, E. (2015) 'Structural and functional studies of a *Fusarium oxysporum* cutinase with polyethylene terephthalate modification potential', *Biochimica et Biophysica Acta - General Subjects*, 1850(11), pp. 2308–2317.
- Dumon-Seignovert, L., Cariot, G. and Vuillard, L. (2004) 'The toxicity of recombinant proteins in *Escherichia coli*: A comparison of overexpression in BL21(DE3), C41(DE3), and C43(DE3)', *Protein Expression and Purification*, 37(1), pp. 203–206.
- Emadian, S. M., Onay, T. T. and Demirel, B. (2017) 'Biodegradation of bioplastics in natural environments', *Waste Management*, 59, pp. 526–536.
- Fasan, R., Chen, M. M., Crook, N. C. and Arnold, F. H. (2007) 'Engineered alkane-hydroxylating cytochrome P450BM3 exhibiting natively catalytic properties', *Angewandte Chemie - International Edition*, 46(44), pp. 8414–8418.
- Finch, C. A. (2003) 'Polyesters II. Properties and chemical synthesis', *Polymer International*, 52, pp. 185–187.
- Fojan, P., Jonson, P. H., Petersen, M. T. N. and Petersen, S. B. (2000) 'What distinguishes an esterase from a lipase: A novel structural approach', *Biochimie*, 82(11), pp. 1033–1041.
- Frank, K. and Sippl, M. J. (2008) 'High-performance signal peptide prediction based on sequence alignment techniques', *Bioinformatics Original Paper*, 24(19), pp. 2172–2176.
- Frenken, L. G. J., Bos, J. W., Visser, C., Müller, W., Tommassen, J. and Verrips, C. T. (1993) 'An accessory gene, *lipB*, required for the production of active *Pseudomonas glumae* lipase', *Molecular Microbiology*, 9(3), pp. 579–589.
- Fujimaki, T. (2002) 'Processability and properties of aliphatic polyesters, "BIONOLLE", synthesized by polycondensation reaction', *Polymer Degradation and Stability*, 59(1-3), pp. 209–214.
- Gácsér, A., Trofa, D., Schäfer, W. and Nosanchuk, J. D. (2007) 'Targeted gene deletion in *Candida parapsilosis* demonstrates the role of secreted lipase in virulence', *Journal of Clinical Investigation*, 117(10), pp. 3049–3058.
- García, J. M. (2016) 'Catalyst: Design challenges for the future of plastics recycling', *Chem* 1(6), pp. 813–815.

- Garrido, S. M., Kitamoto, N., Watanabe, A., Shintani, T. and Gomi, K. (2012) 'Functional analysis of FarA transcription factor in the regulation of the genes encoding lipolytic enzymes and hydrophobic surface binding protein for the degradation of biodegradable plastics in *Aspergillus oryzae*', *Journal of Bioscience and Bioengineering*, 113(5), pp. 549-555.
- Gasser, B., Saloheimo, M., Rinas, U., Dragosits, M., Rodríguez-Carmona, E., Baumann, K., Giuliani, M., Parrilli, E., Branduardi, P., Lang, C., Porro, D., Ferrer, P., Tutino, M., Mattanovich, D. and Villaverde, A. (2008) 'Protein folding and conformational stress in microbial cells producing recombinant proteins: A host comparative overview', *Microbial Cell Factories*, 7(11), pp. 1-18.
- Geyer, R., Jambeck, J. R. and Law, K. L. (2017). Production, use, and fate of all plastics ever made. *Science Advances*, 3(7): pp. 1700782.
- Gigault, J., Halle, A. ter, Baudrimont, M., Pascal, P.Y., Gauffre, F., Phi, T. L., El Hadri, H., Grassl, B., Reynaud, S. (2018) 'Current opinion: What is a nanoplastic?', *Environmental Pollution*, 235: pp. 1030–1034.
- Glieder, A., Farinas, E. T. and Arnold, F. H. (2002) 'Laboratory evolution of a soluble, self-sufficient, highly active alkane hydroxylase', *Nature Biotechnology*, 20, pp. 1135–1139.
- Goda, S. K. (2012) 'DNA shuffling and the production of novel enzymes and microorganisms for effective bioremediation and biodegradation process', *Journal of Bioremediation and Biodegradation*, 3(8), pp. e116.
- Gomila, M., Bowien, B., Falsen, E., Moore, E. R. B. and Lalucat, J. (2008) 'Description of *Roseateles aquatilis* sp. nov. and *Roseateles terrae* sp. nov., in the class Betaproteobacteria, and emended description of the genus *Roseateles*', *International Journal Of Systematic And Evolutionary Microbiology*, 58(1), pp. 6–11.
- Green, M. R. and Sambrook, J. (2012) *Molecular Cloning: A Laboratory Manual*, 4th edn, New York: Cold Spring Harbor Laboratory Press.
- Gu, J. D. (2003) 'Microbiological deterioration and degradation of synthetic polymeric materials: Recent research advances', *International Biodeterioration and Biodegradation*, 52(2), pp. 69-91.

- Guigó, R., Knudsen, S., Drake, N. and Smith, T. (1992) 'Prediction of gene structure', *Journal of Molecular Biology*, 226(1), pp. 141-157.
- Hayase, N., Yano, H., Kudoh, E., Tsutsumi, C., Ushio, K., Miyahara, Y., Tanaka, S. and Nakagawa, K. (2004) 'Isolation and characterization of poly(butylene succinate-co-butylene adipate)-degrading microorganism', *Journal of Bioscience and Bioengineering*, 97(2), pp. 131–133.
- Hidalgo-Ruz, V., Gutow, L., Thompson, R. C. and Thiel, M. (2012) 'Microplastics in the marine environment: A review of the methods used for identification and quantification', *Environmental Science and Technology*, 46(6), pp. 3060-3075.
- Holmquist, M. (2000) 'Alpha/Beta-hydrolase fold enzymes: Structures, functions and mechanisms.', *Current Protein & Peptide Science*, 1(2), pp. 209–235.
- Hobson, A. H., Buckley, C. M., Aamand, J. L., Jorgensen, S. T., Diderichsen, B. and McConnell, D. J. (1993) 'Activation of a bacterial lipase by its chaperone.', *Proceedings of the National Academy of Sciences*, 90(12), pp. 5682–5686.
- Hoess, A., Arthur, A. K., Wanner, G. and Fanning, E. (1988) 'Recovery of soluble, biologically active recombinant proteins from total bacterial lysates using ion exchange resin', *Bio/Technology*, 6, pp. 1214–1217.
- Hoseini, S. and Sauer, M. G. (2015) 'Molecular cloning using polymerase chain reaction, an educational guide for cellular engineering', *Journal of Biological Engineering*, 9(1), pp. 1-12.
- Hu, X., Thumarat, U., Zhang, X., Tang, M. and Kawai, F. (2010) 'Diversity of polyester-degrading bacteria in compost and molecular analysis of a thermoactive esterase from *Thermobifida alba* AHK119', *Applied Microbiology and Biotechnology*, 87(2), pp. 771-779.
- Hueck, H. J. (2001) 'The biodeterioration of materials - An appraisal', *International Biodeterioration and Biodegradation*, 48(1-4), pp. 5-11.
- Hynes, M. F., Quandt, J., O'Connell, M. P. and Pühler, A. (1989) 'Direct selection for curing and deletion of *Rhizobium* plasmids using transposons carrying the *Bacillus subtilis* *sacB* gene', *Gene*, 1(15), pp. 111-120.

- Imamura, T. (2006) 'Protein-surfactant interactions', in Somasundaran, P. (ed), *Encyclopedia of Surface and Colloid Science*, New York: Taylor & Francis, pp 5251–5263.
- Ishii, N., Inoue, Y., Tagaya, T., Mitomo, H., Nagai, D. and Kasuya, K. (2008) 'Isolation and characterization of poly(butylene succinate)-degrading fungi', *Polymer Degradation and Stability*, 93(5), pp. 883–888.
- Ishioka R., Kitakuni E. and Ichikawa Y. (2002) 'Aliphatic polyesters: 'Bionolle'', in Doi, Y. and Steinbüchel, A. (eds), *Biopolymers Online: Biology • Chemistry • Biotechnology • Applications*, Weinheim: Wiley, pp. 275–297.
- Iwata, T. (2015) 'Biodegradable and bio-based polymers: future prospects of eco-friendly plastics', *Angewandte Chemie International Edition*, 54(11), pp. 3210–3215.
- Jacquel, N., Freyermouth, F., Fenouillot, F., Rousseau, A., Pascault, J. P., Fuertes, P. and Saint-Loup, R. (2011) 'Synthesis and properties of poly(butylene succinate): Efficiency of different transesterification catalysts', *Journal of Polymer Science Part A: Polymer Chemistry*, 49(24), pp. 5301–5312.
- Karkhane, A. A., Yakhchali, B., Jazii, F. R., Hemmat, J., Shariati, P., Khodabandeh, M. and Zomorodipoor, A. (2012) 'Periplasmic expression of *Bacillus thermocatenuatus* lipase in *Escherichia coli* in presence of different signal sequences', *Iranian Journal of Biotechnology*, 10(4), pp. 255-262.
- Karlsson, S. and Albertsson, A. C. (1998) 'Biodegradable polymers and environmental interaction', *Polymer Engineering and Science*, 38(8), pp. 1251-1253.
- Kay, M. J., McCabe, R. W. and Morton, L. H. G. (1993) 'Chemical and physical changes occurring in polyester polyurethane during biodegradation', *International Biodeterioration and Biodegradation*, 31(3), pp. 209–225.
- Kensche, P. R., Van Noort, V., Dutilh, B. E. and Huynen, M. A. (2008) 'Practical and theoretical advances in predicting the function of a protein by its phylogenetic distribution', *Journal of the Royal Society Interface*, 5, pp. 151–170.
- Kim, H. K., Lee, J. K., Kim, H. and Oh, T. K. (1996) 'Characterization of an alkaline lipase from *Proteus vulgaris* K80 and the DNA sequence of the encoding gene', *FEMS Microbiology Letters*, 135(1), pp. 117–121.

- Kimple, M. E., Brill, A. L. and Pasker, R. L. (2013) 'Overview of affinity tags for protein purification', *Current Protocols in Protein Science*, 73(1), pp 9.9.1-9.9.23.
- Kitadokoro, K., Kakara, M., Matsui, S., Osokoshi, R., Thumarat, U., Kawai, F. and Kamitani, S., (2019) 'Structural insights into the unique polylactate-degrading mechanism of *Thermobifida alba* cutinase', *FEBS Journal*, 286(11), pp. 2087-2098.
- Kleeberg, I., Welzel, K., VandenHeuvel, J., Müller, R. J. and Deckwer, W. D. (2005) 'Characterization of a new extracellular hydrolase from *Thermobifida fusca* degrading aliphatic-aromatic copolyesters', *Biomacromolecules*, 6(1): pp. 262-270.
- Klepsch, M. M., Persson, J. O. and De Gier, J. W. L. (2011) 'Consequences of the overexpression of a eukaryotic membrane protein, the human KDEL receptor, in *Escherichia coli*', *Journal of Molecular Biology.*, 407(4), pp. 532-542.
- Kobayashi, S., Uyama, H. and Takamoto, T. (2000) 'Lipase-catalyzed degradation of polyesters in organic solvents. A new methodology of polymer recycling using enzyme as catalyst', *Biomacromolecules*, 1(1), pp. 3-5.
- Kok, R. G., Thor, J. J., Nugteren-Roodzant, I. M., Brouwer, M. B. W., Egmond, M. R., Nudel, C. B., Vosman, B. and Hellingwerf, K. J. (1995) 'Characterization of the extracellular lipase, LipA, of *Acinetobacter calcoaceticus* BD413 and sequence analysis of the cloned structural gene', *Molecular Microbiology*, 15(5), pp. 803–818.
- Korbie, D. J. and Mattick, J. S. (2008) 'Touchdown PCR for increased specificity and sensitivity in PCR amplification', *Nature Protocols*, 3(9), pp. 13–15.
- Krishnan, B., Kulothungan, S. R., Patra, A. K., Udgaonkar, J. B. and Varadarajan, R. (2009) 'SecB-mediated protein export need not occur via kinetic partitioning', *Journal of Molecular Biology*, 385(4), pp. 1243-56
- Krzan, A., Hemjinda, S., Miertus, S., Corti, A. and Chiellini, E. (2006) 'Standardization and certification in the area of environmentally degradable plastics', *Polymer Degradation and Stability*, 91(12), pp. 2819-2833.
- Kulothungan, S. R., Das, M., Johnson, M., Ganesh, C. and Varadarajan, R. (2009) 'Effect of crowding agents, signal peptide, and chaperone SecB on the folding and aggregation of *E. coli* maltose binding protein', *Langmuir*, 25(12), pp. 6637-6648.

- Laemmli, U. K. (1970) 'Cleavage of Structural Proteins during the Assembly of the Head of Bacteriophage T4', *Nature*, 227(5259), pp. 680–685.
- Lashkari, D. A., DeRisi, J. L., McCusker, J. H., Namath, A. F., Gentile, C., Hwang, S. Y., Brown, P. O. and Davis, R. W. (1997) 'Yeast microarrays for genome wide parallel genetic and gene expression analysis', *Proceedings of the National Academy of Sciences of the United States of America*, 94(24), pp. 13057-13062.
- Lee, S. H. and Kim, M. N. (2010) 'Isolation of bacteria degrading poly(butylene succinate-co-butylene adipate) and their *lipA* gene', *International Biodeterioration & Biodegradation*, 64(3), pp. 184–190.
- Leja, K. and Lewandowicz, G. (2010) 'Polymer biodegradation and biodegradable polymers - A review', *Polish Journal of Environmental Studies*, 19(2), pp. 255-266.
- Li, W. C., Tse, H. F. and Fok, L. (2016) 'Plastic waste in the marine environment: A review of sources, occurrence and effects', *Science of the Total Environment*, 566-567, pp. 333-349.
- Lindström, A., Albertsson, A. C. and Hakkarainen, M. (2004) 'Quantitative determination of degradation products an effective means to study early stages of degradation in linear and branched poly(butylene adipate) and poly(butylene succinate)', *Polymer Degradation and Stability*, 83(3), pp. 487-493.
- Lucas, N., Bienaime, C., Belloy, C., Queneudec, M., Silvestre, F. and Nava-Saucedo, J. E. (2008) 'Polymer biodegradation: Mechanisms and estimation techniques - A review', *Chemosphere*, 73(4), pp. 429–442.
- Lugauskas, A., Levinskaite, L. and Pečiulyte, D. (2003) 'Micromycetes as deterioration agents of polymeric materials', *International Biodeterioration and Biodegradation*, 52(4), pp. 233-242.
- Martinez, C., De Geus, P., Lauwereys, M., Matthyssens, G. and Cambillau, C. (1992) '*Fusarium solani* cutinase is a lipolytic enzyme with a catalytic serine accessible to solvent', *Nature*, 356(6370), pp. 615–618.
- Matsumura, S. (2002) 'Enzyme-catalyzed synthesis and chemical recycling of polyesters', *Macromolecular Bioscience*, 2(3), pp. 105-126.

- Miyauchi, A., Ozawa, M., Mizukami, M., Yashiro, K., Ebisu, S., Tojo, T., Fujii, T. And Takagi, H. (2005) 'Structural conversion from non-native to native form of recombinant human epidermal growth factor by *Brevibacillus choshinensis*', *Bioscience, Biotechnology, and Biochemistry*, 63(11), pp.1965-1969
- Nair, L. S. and Laurencin, C. T. (2007) 'Biodegradable polymers as biomaterials', *Progress in Polymer Science*, 32(8-9), pp. 762-798.
- Nakajima-Kambe, T., Ichihashi, F., Matsuzoe, R., Kato, S. and Shintani, N. (2009a) 'Degradation of aliphatic-aromatic copolyesters by bacteria that can degrade aliphatic polyesters', *Polymer Degradation and Stability*, 94(11), pp. 1901–1905.
- Nakajima-Kambe, T., Toyoshima, K., Saito, C., Takaguchi, H., Akutsu-Shigeno, Y., Sato, M., Miyama, K., Nomura, N. and Uchiyama, H. (2009b) 'Rapid monomerization of poly(butylene succinate)-co-(butylene adipate) by *Leptothrix* sp.', *Journal of Bioscience and Bioengineering*, 108(6), pp. 513–516.
- Narancic, T., Verstichel, S., Chaganti, S. R., Morales-Gamez, L., Kenny, S. T., De Wilde, B., Padamati, R. B. and O'connor, K. E. (2018) 'Biodegradable plastic blends create new possibilities for end-of-life management of plastics but they are not a panacea for plastic pollution', 52(18), pp. 10441-10452.
- Nardini, M. and Dijkstra, B. W. (1999) ' α/β hydrolase fold enzymes: The family keeps growing', *Current Opinion in Structural Biology*, 9(6), pp. 732–737.
- Nie, Z. J., Hang, B. J., Cai, S., Xie, X. T., He, J. and Li, S. P. (2011) 'Degradation of cyhalofop-butyl (CyB) by *Pseudomonas azotoformans* strain QDZ-1 and cloning of a novel gene encoding CyB-hydrolyzing esterase', *Journal of Agricultural and Food Chemistry* 59(11), pp.6040-6046.
- Nikolic, M. S. and Djonlagic, J. (2001) 'Synthesis and characterization of biodegradable poly(butylene succinate-co-butylene adipate)s', *Polymer Degradation and Stability* 74(2), pp. 263-270.
- Okajima, S., Kondo, R., Toshima, K. and Matsumura, S. (2003) 'Lipase-catalyzed transformation of poly(butylene adipate) and poly(butylene succinate) into repolymerizable cyclic oligomers', *Biomacromolecules*, 4(6), pp. 1514-1519.

- Ollis, D. L., Cheah, E., Cygler, M., Dijkstra, B., Frolow, F., Franken, S. M., Harel, M., Remington, S. J., Silman, I., Schrag, J., Sussman, J. L., Verschueren, K. H. G. and Goldman, A. (1992) 'The α / β hydrolase fold', *Protein Engineering, Design and Selection*, 5(3), pp. 197–211.
- Omasits, U., Varadarajan, A. R., Schmid, M., Goetze, S., Melidis, D., Bourqui, M., Nikolayeva, O., Québatte, M., Patrignani, A., Dehio, C., Frey, J. E., Robinson, M. D., Wollscheid, B. and Ahrens, C. H. (2017) 'An integrative strategy to identify the entire protein coding potential of prokaryotic genomes by proteogenomics', *Genome Research*, 27, pp. 2083–2095.
- Palmisano, A. C. and Pettigrew, C. A. (1992) 'Biodegradability of plastics', *BioScience*, 42(9), pp. 680–685.
- Panicker, I. S., Browning, G. F. and Markham, P. F. (2015) 'The effect of an alternate start codon on heterologous expression of a PhoA fusion protein in mycoplasma gallisepticum', *PLoS ONE*, 10(5), pp. e0127911.
- Pellegrini, M. (2012) 'Using phylogenetic profiles to predict functional relationships', *Methods in Molecular Biology*, 804, pp.167-177.
- Perz, V., Baumschlager, A., Bleymaier, K., Zitzenbacher, S., Hromic, A., Steinkellner, G., Pairitsch, A., Łyskowski, A., Gruber, K., Sinkel, C., Küper, U., Ribitsch, D. and Guebitz, G. M. (2016) 'Hydrolysis of synthetic polyesters by *Clostridium botulinum* esterases', *Biotechnology and Bioengineering*, 113(5), pp. 1024-1034.
- Pranamuda, H., Tokiwa, Y. and Tanaka, H. (1995) 'Microbial degradation of an aliphatic polyester with a high melting point, poly(tetramethylene succinate)', *Applied and Environmental Microbiology*, 61(5), pp. 1828-1832.
- Rath, A., Glibowicka, M., Nadeau, V. G., Chen, G. and Deber, C. M. (2009) 'Detergent binding explains anomalous SDS-PAGE migration of membrane proteins', *Proceedings of the National Academy of Sciences*, 106(6), pp. 1760-1765.
- Ritchie, H. and Roser, M. (2019) 'Plastic Pollution', *Published online at OurWorldInData.org*. Available at: <https://ourworldindata.org/plastic-pollution> [Accessed 5 May 2019].

- Roohi, Bano, K., Kuddus, M., Zaheer, M. R., Zia, Q., Khan, M. F., Ashraf, G. M., Gupta, A. and Aliev, G. (2017) 'Microbial enzymatic degradation of biodegradable plastics', *Current Pharmaceutical Biotechnology*, 18(5): pp. 429-440.
- Rosa, D. S., Lotto, N. T., Lopes, D. R. and Guedes, C. G. F. (2004) 'The use of roughness for evaluating the biodegradation of poly- β -(hydroxybutyrate) and poly- β -(hydroxybutyrate-co- β -valerate)', *Polymer Testing*, 23(1), pp. 3-8.
- Rosano, G. L. and Ceccarelli, E. A. (2014) 'Recombinant protein expression in *Escherichia coli*: advances and challenges', *Frontiers in Microbiology*. 5(172), pp. 1-17.
- Saïda, F. (2007) 'Overview on the expression of toxic gene products in *Escherichia coli* ', *Current Protocols in Protein Science*, 50(1), pp. 5.19.1-5.19.13.
- Sardon, H., Dove, A.P. (2018) 'Plastics recycling with a difference', *Science* 360 (8367): pp. 380–381.
- Schlegel, S., Löfblom, J., Lee, C., Hjelm, A., Klepsch, M., Strous, M., Drew, D., Slotboom, D. J. and De Gier, J. W. (2012) 'Optimizing membrane protein overexpression in the *Escherichia coli* strain Lemo21 (DE3)', *Journal of Molecular Biology*, 423(4), pp. 648–659.
- Sezonov, G., Joseleau-Petit, D. and D'Ari, R. (2007) '*Escherichia coli* physiology in Luria-Bertani broth', *Journal of Bacteriology*, 189(23), pp. 8746–8749.
- Shah, A. A., Eguchi, T., Mayumi, D., Kato, S., Shintani, N., Kamini, N. R. and Nakajima-Kambe, T. (2013a) 'Degradation of aliphatic and aliphatic-aromatic co-polyesters by depolymerases from *Roseateles depolymerans* strain TB-87 and analysis of degradation products by LC-MS', *Polymer Degradation and Stability*, 98(12), pp. 2722–2729.
- Shah, A. A., Eguchi, T., Mayumi, D., Kato, S., Shintani, N., Kamini, N. R. and Nakajima-Kambe, T. (2013b) 'Purification and properties of novel aliphatic-aromatic co-polyesters degrading enzymes from newly isolated *Roseateles depolymerans* strain TB-87', *Polymer Degradation and Stability*, 98(2), pp. 609–618.
- Shah, A. A., Kato, S., Shintani, N., Kamini, N. R. and Nakajima-Kambe, T. (2014) 'Microbial degradation of aliphatic and aliphatic-aromatic co-polyesters', *Applied Microbiology and Biotechnology*, 98(8), pp. 3437–3447.

- Singh, N., Hui, D., Singh, R., Ahuja, I. P. S., Feo, L. and Fraternali, F. (2017) 'Recycling of plastic solid waste: A state of art review and future applications', *Composites Part B: Engineering*, 115, pp. 409-422.
- Singh, P., Sharma, L., Kulothungan, S. R., Adkar, B. V., Prajapati, R. S., Ali, P. S. S., Krishnan, B. and Varadarajan, R. (2013) 'Effect of signal peptide on stability and folding of *Escherichia coli* thioredoxin', *PLoS ONE*, 8(5), pp. 63442.
- Song, J. (2009) 'Insight into "insoluble proteins" with pure water', *FEBS Letters*, 583, pp. 953-959
- Su, J. H., Chang, M. C., Lee, Y. S., Tseng, I. C. and Chuang, Y. C. (2004) 'Cloning and characterization of the lipase and lipase activator protein from *Vibrio vulnificus* CKM-1', *Biochimica et Biophysica Acta (BBA) - Gene Structure and Expression*, 1678(1), pp. 7-13.
- Sullivan, E. R., Leahy, J. G. and Colwell, R. R. (1999) 'Cloning and sequence analysis of the lipase and lipase chaperone-encoding genes from *Acinetobacter calcoaceticus* RAG-1, and redefinition of a Proteobacterial lipase family and an analogous lipase chaperone family', *Gene*, 230(2), pp. 277-285.
- Suyama, T., Tokiwa, Y., Ouichanpagdee, P., Kanagawa, T. and Kamagata, Y. (1998) 'Phylogenetic affiliation of soil bacteria that degrade aliphatic polyesters available commercially as biodegradable plastics', *Applied and Environmental Microbiology*, 64(12), pp. 5008-5011.
- Tanaka, R., Mizukami, M., Ishibashi, M., Tokunaga, H. and Tokunaga, M. (2003) 'Cloning and expression of the ccdA-associated thiol-disulfide oxidoreductase (*catA*) gene from *Brevibacillus choshinensis*: Stimulation of human epidermal growth factor production', *Journal of Biotechnology*, 103(1), pp. 1-10.
- Tanio, M., Tanaka, R., Tanaka, T. and Kohno, T. (2009) 'Amino acid-selective isotope labeling of proteins for nuclear magnetic resonance study: Proteins secreted by *Brevibacillus choshinensis*', *Analytical Biochemistry*, 386(2), pp. 156-160.
- Teeraphatpornchai, T., Nakajima-Kambe, T., Shigeno-Akutsu, Y., Nakayama, M., Nomura, N., Nakahara, T. and Uchiyama, H. (2003) 'Isolation and characterization of a bacterium that degrades various polyester-based biodegradable plastics', *Biotechnology Letters*, 25(1),

pp. 23–28.

- Teuten, E. L., Saquing, J. M., Knappe, D. R. U., Barlaz, M. A., Jonsson, S., Björn, A., Rowland, S. J., Thompson, R. C., Galloway, T. S., Yamashita, R., Ochi, D., Watanuki, Y., Moore, C., Viet, P. H., Tana, T. S., Prudente, M., Boonyatumanond, R., Zakaria, M. P., Akkhavong, K., Ogata, Y., Hirai, H., Iwasa, S., Mizukawa, K., Hagino, Y., Imamura, A., Saha, M. and Takada, H. (2009) ‘Transport and release of chemicals from plastics to the environment and to wildlife’, *Philosophical Transactions of the Royal Society B: Biological Sciences*, 364(1526), pp. 2027–2045.
- Thompson, R. C., Olsen, Y., Mitchell, R. P., Davis, A., Rowland, S. J., John, A. W. G., McGonigle, D. and Russell, A. E. (2004) ‘Lost at sea: Where is all the plastic?’, *Science*, 304(5672), pp. 838.
- Thumarat, U., Kawabata, T., Nakajima, M., Nakajima, H., Sugiyama, A., Yazaki, K., Tada, T., Waku, T., Tanaka, N. and Kawai, F. (2015) ‘Comparison of genetic structures and biochemical properties of tandem cutinase-type polyesterases from *Thermobifida alba* AHK119’, *Journal of Bioscience and Bioengineering*, 120(5), pp. 491–497.
- Tjalsma, H., Bolhuis, A., Jongbloed, J. D., Bron, S. and van Dijk, J. M. (2000) ‘Signal peptide-dependent protein transport in *Bacillus subtilis*: a genome-based survey of the secretome’, *Microbiology and Molecular Biology Reviews*, 64(3), pp. 515–547.
- Tokiwa, Y. and Calabia, B. P. (2007) ‘Biodegradability and biodegradation of polyesters’, *Journal of Polymers and the Environment*, 15(4), pp. 259–267.
- Tserki, V., Matzinos, P., Pavlidou, E., Vachliotis, D. and Panayiotou, C. (2006) ‘Biodegradable aliphatic polyesters. Part I. Properties and biodegradation of poly(butylene succinate-co-butylene adipate)’, *Polymer Degradation and Stability*, 91(2), pp. 367–376.
- Uchida, H., Nakajima-Kambe, T., Shigeno-Akutsu, Y., Nomura, N., Tokiwa, Y. and Nakahara, T. (2000) ‘Properties of a bacterium which degrades solid poly(tetramethylene succinate)-co-adipate, a biodegradable plastic’, *FEMS Microbiology Letters*, 189(1), pp. 25–29.
- Uchida, H., Shigeno-Akutsu, Y., Nomura, N., Nakahara, T. and Nakajima-Kambe, T. (2002) ‘Cloning and sequence analysis of poly(tetramethylene succinate) depolymerase from *Acidovorax delafieldii* strain BS-3’, *Journal of Bioscience and Bioengineering*, 93(2), pp.

245–247.

- Udaka, S. and Yamagata, H. (1993) 'High-level secretion of heterologous proteins by *Bacillus brevis*', *Methods in Enzymology*, 217, pp. 23-33.
- Vroman, I. and Tighzert, L. (2009) 'Biodegradable polymers', *Materials*, 2(2), pp. 307-344.
- Wagner, S., Baars, L., Ytterberg, A. J., Klussmeier, A., Wagner, C. S., Nord, O., Nygren, P.-Å., van Wijk, K. J. and de Gier, J.-W. (2007) 'Consequences of membrane protein overexpression in *Escherichia coli*', *Molecular & Cellular Proteomics*, 6(9), pp. 1527-1550.
- Wagner, S., Klepsch, M. M., Schlegel, S., Appel, A., Draheim, R., Tarry, M., Hogbom, M., van Wijk, K. J., Slotboom, D. J., Persson, J. O. and de Gier, J. W. (2008) 'Tuning *Escherichia coli* for membrane protein overexpression', *Proceedings of the National Academy of Sciences*, 105(38), pp.14371-14376.
- Walsh, J. H. (2001) 'Ecological considerations of biodeterioration', *International Biodeterioration and Biodegradation*, 48(1–4), pp. 16-25.
- Werner, M. H., Clore, G. M., Gronenborn, A. M., Kondoh, A. and Fisher, R. J. (1994) 'Refolding proteins by gel filtration chromatography', *FEBS Letters*, 345(2-3), pp. 125-130.
- Whangsuk, W., Sungkeeree, P., Nakasiri, M., Thiengmag, S., Mongkolsuk, S. and Loprasert, S. (2015) 'Two endocrine disrupting dibutyl phthalate degrading esterases and their compensatory gene expression in *Sphingobium* sp. SM42', *International Biodeterioration & Biodegradation*. Elsevier, 99, pp. 45–54.
- Yashiro, K., Lowenthal, J. W., O'Neil, T. E., Ebisu, S., Takagi, H. and Moore, R. J. (2001) 'High-level production of recombinant chicken interferon- γ by *Brevibacillus choshinensis*', *Protein Expression and Purification*, 23(1), pp. 113-120.
- Yazdani, S. S. and Mukherjee, K. J. (1998) 'Overexpression of streptokinase using a fed-batch strategy', *Biotechnology Letters*, 20(10), pp. 923–927.
- Yoshida, S., Hiraga, K., Takehana, T., Taniguchi, I., Yamaji, H., Maeda, Y., Toyohara, K., Miyamoto, K., Kimura, Y. and Oda, K. (2016) 'A bacterium that degrades and assimilates PET', *Science*, 351(6278), pp. 1196-1199.

- Zhao, J. H., Wang, X. Q., Zeng, J., Yang, G., Shi, F. H. and Yan, Q. (2005) 'Biodegradation of poly(butylene succinate-co-butylene adipate) by *Aspergillus versicolor*', *Polymer Degradation and Stability*, 90(1), pp. 173-179.
- Zhu, S., Gong, C., Ren, L., Li, X., Song, D. and Zheng, G. (2013) 'A simple and effective strategy for solving the problem of inclusion bodies in recombinant protein technology: His-tag deletions enhance soluble expression', *Applied Microbiology and Biotechnology*, 97(2), pp. 837–845.
- Zimmermann, W. and Billig, S. (2011) 'Enzymes for the biofunctionalization of poly(ethylene terephthalate)', *Advances in Biochemical Engineering/Biotechnology*, 125, pp. 97-120.
- Louwrier, A. and Van Der Valk, A. (2001) 'Can sucrose affect polymerase chain reaction product formation?', *Biotechnology Letters*, 23(3), pp. 175–178.

ADDENDUM

Some parts of this thesis were published in referred journal and conference under the following title:

Paper published

Ahmad, A., Tsutsui, A., Iijima, S., Suzuki, T., Shah, A. A. and Nakajima-Kambe, T. (2019) ‘Gene structure and comparative study of two different plastic-degrading esterases from *Roseateles depolymerans* strain TB-87’, *Polymer Degradation and Stability* 164, pp. 109-117.

Paper presented

Ahmad, A., Tsutsui, A., Iijima, S., Suzuki, T., Shah, A. A. and Nakajima-Kambe, T. (2019, July). ‘Functional analysis of a gene-encoding region of an aliphatic-aromatic polyester type plastic degrading enzyme from *Roseateles depolymerans* strain TB-87’. The 14th Asian Congress on Biotechnology, Taipei, Taiwan, R.O.C, July 1-4.

ACKNOWLEDGEMENTS

In the name of Allah the Almighty, with His blessings and grace, enabled me to complete this research and subsequently this thesis. In the preparation of this thesis, I encountered many people who have contributed directly or indirectly. Therefore, I would like to express my appreciation to those who had helped me achieve my goals in this research completion.

First and foremost, I wish to express my sincerest appreciation to my advisor, Prof. Toshiaki Nakajima-Kambe for his inspiration, encouragement, ideas, advice and endless guidance and support. I am grateful for the opportunity to join Prof. Nakajima's laboratory and working under his supervision. I would also like to extend my sincerest appreciation to my thesis advisors; Prof. Utsumi, Prof. Nakamura, and Prof. Kitamura, for their useful advice and helpful suggestions during the preparation of this thesis. Utmost appreciation goes to the Ministry of Science, Sport, and Culture (MEXT) for the scholarship that has made my coming to Japan possible. I am indebted to MEXT for the wonderful experiences during my 5 years in Japan that was made possible by this scholarship.

Special thanks are given to Dr. Suzuki Toshihiro and Dr. Keiji Kiyoshi, seniors in the laboratory for their guidance, valuable suggestions, and supports in conducting the experiments. Thanks are extended to all my labmates for their encouragement, companions, advice, assistance, and useful discussion.

Special thanks are forwarded to my best friends, Juliana, Haida, Hazita, and Ainee for their endless encouragement and support. Not to forget my juniors and friends at the University of Tsukuba; Natalia, Azila, Nadirah, Hamizah, Hidayah, Emi Fazlina and Maisarah for the endless encouragements and companionship. Special thanks to all professors, staff, and friends in the Graduate School of Life and Environmental Sciences for their encouragement and help. Heartfelt appreciation to Ms. Furukawa for her kind assistance and helps in research-related documentation.

I would also like to extend my sincerest appreciation to my mentors; Prof. Dr. Noor Aini Abdul Rashid for her help and guidance and Mr. R. Kumaraguru for his advice, endless encouragements, and for always believing in me.

Last but not least, my utmost appreciation to my parents, my in-laws, my brother, and my family, and my husband for their undying love and support.